Master's thesis

NTNU
Norwegian University of Science and Technology
Faculty of Natural Sciences
Department of Materials Science and Engineering

Olav Biørnstad

Decrepitation of Comilog, Assmang and UMK manganese ores during prereduction

Master's thesis in Materials Science and Engineering
Supervisor: Merete Tangstad
July 2020

NTNU
Norwegian University of
Science and Technology

Olav Biørnstad

Decrepitation of Comilog, Assmang and UMK manganese ores during prereduction

Master's thesis in Materials Science and Engineering
Supervisor: Merete Tangstad
July 2020

Norwegian University of Science and Technology
Faculty of Natural Sciences
Department of Materials Science and Engineering

NTNU
Norwegian University of
Science and Technology

Preface

This MSc task is a continuance of the specialisation project[1] where some introductory experiment with Comilog and UMK ores were reduced in CO/CO2. In the MSc project the literature is revised and extended with thermal decomposition of manganese ores. In the experimental part Assmang ore has been reduced in CO/CO_2 as well as air experiments for all ores. The characterisation has been extended with pressure force tests and SEM examination.

I would like to thank my supervisor, Merete Tangstad, and my co-supervisors, Jonas Einan Gjøvik and Nicholas Smith, for guidance and support during my work. Secondly, I would thank Ingeborg Solheim for doing some of my experiments when the lab was closed for students. I would also like to thank the administration and technical staff of the Department of Materials Science and Engineering for making the labs available for students during the extraordinary situation this spring. Lastly, I thank my fellow students for distracting me when I was working on this MSc.

This MSc is funded by Sintef in the PreMa project which is funded by European Union's Horizon 2020 research and innovation programme under grant agreement No 820561.

Olav Biørnstad

Abstract

Production of manganese alloys is a large consumer of electrical energy and carbon material. Prereduction of manganese ores is desired to decrease the energy and carbon usage in production of manganese alloys. Knowing how the manganese ores react to heating in reducing gas atmospheres is therefore necessary to ensure efficient and safe operation. Assmang, UMK and Comilog will be examined and compared after heating to 400°C, 600°C and 800°C in 70/30% CO/CO_2 and air atmosphere.

Firstly, it was found that the Assmang ore was heated in CO/CO_2 is reduced up to MnOx = 1 at 800°C. The ore had more decrepitation than UMK, but less than Comilog which was examined in earlier work. Secondly, all three ores were heated in synthetic air before being tumble-tested. The ore were then tumble-tested, pressure force tested and examined in SEM as well as porosity measurements and chemical analysis done by Sintef.

The manganese oxides were not reduced past Mn_2O_3 (MnOx=1,5) in air atmosphere, which for Assmang (MnOx = 1,45) and UMK (MnOx=1,43) increased the oxygen content of the ore. Comilog (MnOx = 1,94) ore had a decrease in oxygen content due to decomposition of MnO_2. The decrepitation of the three ores were lower than when heated in CO/CO_2, UMK and Comilog having the lowest decrepitation. Assmang had the most decrepitation in air atmosphere, though it was only ∼6% higher than the other ores at 800°C.

Pressure force tests showed that the strength of the ores decreased as the temperature was increased. Comilog was the weakest of the ores, while Assmang and UMK having similar strength. This was probably due to the increased porosity of Comilog which was measured to be from 12 - 36,9% depending on temperature. Assmang and UMK had a most a porosity of 21,8% at higher temperatures, and significantly lower at lower heating temperatures. This difference in porosity was also seen in SEM examination of the cross sections of the ore.

Ores heated in CO/CO_2 show a higher degree of prereduction, but decrepitates more at the same time. This means more fines are produced when reducing manganese ores in CO/CO_2 than in air. Though the decrepitation is lower in air, it is not possible to reduce Mn_2O_3 at the temperatures used in this study. An atmosphere of CO/CO_2 is needed in order to fully reduce manganese ores to MnO.

Sammendrag

Produksjon av manganlegeringer er en industri som forbruker mye elektrisk energi og karbonmaterialer. Prereduksjon av manganmalm er ønsket for å senke forbruket av elektrisk energi og karbonmaterialer. For at dette skal være mulig må man vite hvordan manganmalmen reagerer når den blir varmet opp i forskjellige gassatmosfærer. Assmang, UMK og Comilog vil bli undersøkt etter å ha blitt varmet opp til 400°C, 600°C og 800°C i syntetisk luft og 70/30 % CO/CO_2.

Først ble Assmang varmet opp i CO/CO_2 som resulterte i at alle manganoksidene ble redusert til MnO ved 800°C. Assmang malmen dekrepiterte mer enn UMK, men mindre enn Comilog som har blitt undersøkt i tidligere arbeid. Så ble alle malmene varmet i syntetisk luft. Malmene ble tumbletestet, trykkkraft-testet og undersøkt i SEM, i tillegg til porøsitetsmålinger og kjemisk analyse som ble gjort av Sintef.

Manganoksidene ble kun redusert til Mn_2O_3 (MnOx = 1,5) da de ble varmet i syntetisk luft, som førte til en økning i oksygeninnholdet for Assmang (MnOx = 1,45) og UMK (MnOx = 1,43). Comilog (MnOx = 1,94) fikk en reduksjon av oksygeninnholdet på grunn av dekomponering av MnO_2. Alle malmene dekrepiterte mindre i luft enn i CO/CO_2, hvor UMK og Comilog hadde minst dekrepitering. Assmang dekrepiterte mest i luftatmosfære, men den var bare 6% høyere enn de andre malmene ved 800°C.

Trykktesting viste at styrken til malmene synker når temperaturen stiger. Comilog var den svakeste malmen, mens UMK og Assmang har liknende styrke. Dette er mest sannsynlig på grunn av forskjellen i porøsitet. Porøsiteten til Comilog ble målt opp til 36,9% ved 800°C. Assmang og UMK hadde maks 21,8% porøsitet ved 800°C, og betydelig mindre ved lavere temperaturer. Forskjellen i porøsitet ble videre sett i SEM undersøkelse av tverrsnittet til malmen.

Manganmalm varmet i CO/CO_2 har en høyre grad av prereduksjon, men dekrepiterer også mer enn malm varmet i luft. Dette betyr at mer fines blir produsert under prereduksjon i CO/CO_2. Derimot er det ikke mulig å redusere manganmalm lavere enn Mn_2O_3 i luft ved temperaturene undersøkt i denne studien. En atmosfære av CO/CO_2 er nødvendig for å redusere manganmalm til MnO.

Contents

1 Introduction

Production of manganese alloys is a big consumer of electricity and carbon. A prereduction unit may be used to reduce the ore as much as possible before the furnace which will decrease the demand for electrical energy and carbon consumption when producing manganese alloys. The behaviour of the ores while heated are integral to the safe production of manganese alloys. The goal of this work is to find the possible degree of prereduction and decrepitation of Comilog, Assmang and UMK ores during heating in a prereduction unit.

This MSc task is a continuance of the specialisation project[1] where some introductory experiment with Comilog and UMK ores were reduced in CO/CO2 gas mixtures. In the MSc project the literature is revised and extended with thermal decomposition and thermal prereduction of manganese ores. In the experimental part Assmang ore has been reduced in CO/CO_2 as well as air experiments for all ores. The characterisation has been extended with pressure force tests and SEM examination. Comparison and discussion of the results of the MSc task and the specialisation project will follow in this paper.

The majority of the manganese production in the world are used for ferro-alloys for the steel industry. The manganese is used to improve the strength of the steel and the corrosion resistance. About 6-7 kg of manganese is used for each ton of steel and pure manganese is also used in the chemical industry for batteries, pigments and reactants. About 20 % of the manganese alloys produced goes to the production of pure manganese metal and other chemicals.[2]

Manganese ferroalloys are produced from manganese oxide ores, fluxes and coke by carbothermic reduction. This can be done in a submerged arc furnace (SAF) or in a blast furnace, but the latter has higher consumption of coke and a higher loss of manganese to slag and off-gases. This is the reason why production of manganese is mainly done by reduction in a SAF illustrated in figure 1.

The SAF has two zones with different characteristics, the coke bed zone and the prereduction zone. In the high temperature coke bed zone oxides are melted and travels down through the coke layer and MnO is reduced to Mn metal. This is also where the main heat generation is happening. Most of the electrical energy is supplied by

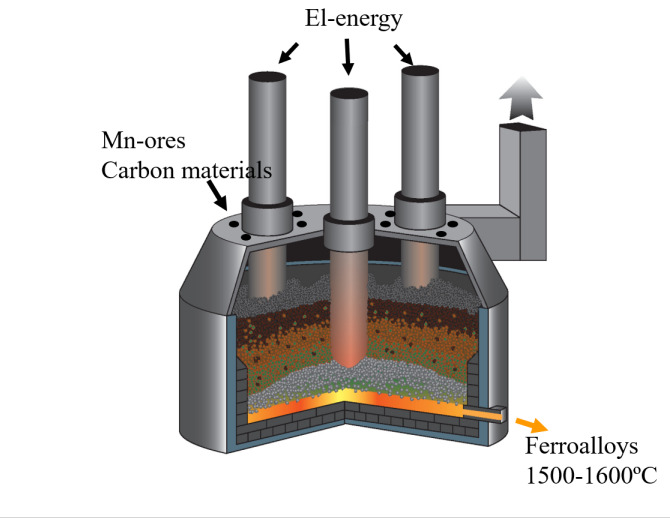

Figure 1: Illustration of a submerged arc furnace used in manganese production[3]

the electrodes. The heat is generated by the electrical resistance of the furnace charge as the current travels through either the coke bed and metal bath or through the prereduction zone. Most of the electrical current travels through the coke bed as it is the path of least resistance. Some of the current travels through the charge, heating the ore in the prereduction zone.[4]

The manganese ore is reduced through several steps while it descends through the prereduction zone. This happens due to a gas-solid reaction between the ore and CO gas produced lower in the furnace. The charge is heated by exothermic reactions, in addition to the heat produced by the current and a heat exchange with the ascending gases. Fluxes added will also decompose in the prereduction zone.

The charge material will melt as it enters the coke bed and form a slag phase. This slag phase consists of SiO_2, Al_2O_3, CaO, MgO and MnO and will descend into the coke bed when the temperature is high enough. The MnO will be reduced at the interface between the slag and the coke or by the carbon dissolved in the metal.

$$MnO(l) + C(s,l) \rightarrow Mn(l) + CO \tag{1}$$

Reaction 1 is strongly endothermic reaction ($\Delta H^o_{298} = 252,3kJ$) and its reaction rate is controlled by the chemical reaction rather than transport mechanisms. The slag tapped have a MnO content of 30-45 % depending on the operating conditions of the furnace and the basicity of the slag. This slag is used as a raw material for the SiMn production due to its high MnO content. The main reactions are the same for production of SiMn with the exception of a higher temperature in the lower zone to reduce the SiO_2 and MnO at the same time. FeMn-slags are added in addition to Mn-ores, fluxes, quartz and coke. Reduction of MnO (equation 1) and SiO_2 happens simultaneously in the coke bed[4]:

$$\mathrm{SiO_2}(l) + 2C \rightarrow Si(l) + 2CO(g) \tag{2}$$

The combined reaction of reaction 1 and 2 is:

$$\mathrm{SiO_2}(l) + 2Mn(l) \rightarrow Si(l) + 2MnO(l) \tag{3}$$

Both of these processes are energy demanding with about 2000-2500 kWh/ton for the FeMn production and even more for the SiMn production. It is desired to lower the consumption of energy and coke by adding a pre-treatment unit to the SAF in order to pre-reduce the ore before it enters the furnace. This will in theory reduce the emissions of CO_2[5] and reduce the production costs. Knowledge on how the raw material decrepitates in different gas atmospheres, time and temperature is needed.

The decrepitation and degree of prereduction of Comilog and UMK heated in a CO/CO_2 have previously been examined in the Specialisation project. This work will extend that with Assmang in the same CO/CO_2 gas mixture, as well as heating for all three ores in synthetic air. SEM examination, porosity measurements and pressure force tests will be done for all samples as part of this MSc work. The results from the experiments performed in the MSc work will be shown in the Result part of the thesis, and these results will be compared to the experiments done in the Specialisation project fall 2019 in the discussion section.

2 Theory

In this section literature related to the pre reduction and decrepitation will be examined. This is to explain what could influence the prereduction and decrepitation.

2.1 Reactions in the prereduction zone during heating

The temperature is about 200-600 °C as the charge enters the furnace. Any water left in the charge will evaporate at this point. Higher water content contributes to an increased power consumption as the process is endothermic, so a lower water content is desired because the an increase in water will result in a higher power consumption.

$$H_2O(l) \rightarrow H_2O(g) \qquad \Delta H^o_{298} = 44,0\ kJ \tag{4}$$

The manganese ores starts to react in presence of CO gas which ascends from the lower parts of the furnace. These reactions are exothermic and will contribute to the heating of the charge. This will accelerate further reactions due to the increased heat and depending on the content of MnO_2 this could be a hazard if the gas evolution is too large.

$$MnO_2 + \frac{1}{2}CO(g) \rightarrow \frac{1}{2}Mn_2O_3 + \frac{1}{2}CO_2 \qquad \Delta H^o_{298} = -99,9\ kJ \tag{5}$$

$$\frac{1}{2}Mn_2O_3 + \frac{1}{6}CO(g) \rightarrow \frac{1}{3}Mn_3O_4 + \frac{1}{6}CO_2 \qquad \Delta H^o_{298} = -31,3\ kJ \tag{6}$$

$$\frac{1}{3}Mn_3O_4 + \frac{1}{3}CO(g) \rightarrow MnO + \frac{1}{3}CO_2 \qquad \Delta H^o_{298} = -16,9\ kJ \tag{7}$$

Reaction 7 may happen in conjunction with the Boudouard reaction at temperatures over 800°C. This reaction is very endothermic and this will result in direct reduction of Mn_3O_4 to MnO. The desired reaction is to use CO(g) to reduce the Mn_3O_4. However it may also happen that the Mn_3O_4 reacts with C[6].

$$\frac{1}{3}Mn_3O_4 + \frac{1}{3}C \rightarrow MnO + \frac{1}{3}CO(g) \qquad \Delta H^o_{298} = 42,7\ kJ \tag{8}$$

The reaction showed in eq. 8 is endothermic with an enthalpy of $\Delta H^o = 42,7$ kJ and will increase power demand and the consumption of carbon material. This is why it is important to make sure all the reduction reactions are happening before the ore reaches an area with high enough temperature for the Boudouard reaction to be significant. Ideally all the manganese oxides should be MnO by

the time the ore reaches the coke bed. The ore must have a high reactivity to be sufficiently reduced at this point. The reactivity of the Comilog ore is one of the highest of the manganese ores used by the industry[7]. Other ores have a lower reactivity due to their chemical composition and porosity. Comilog produces bixbyite when reduced which is faster to reduce than ores producing braunite like Mamatwan, Asman or Wessel [8]. It should also be mentioned that Comilog has a higher porosity compared to the South African ores.

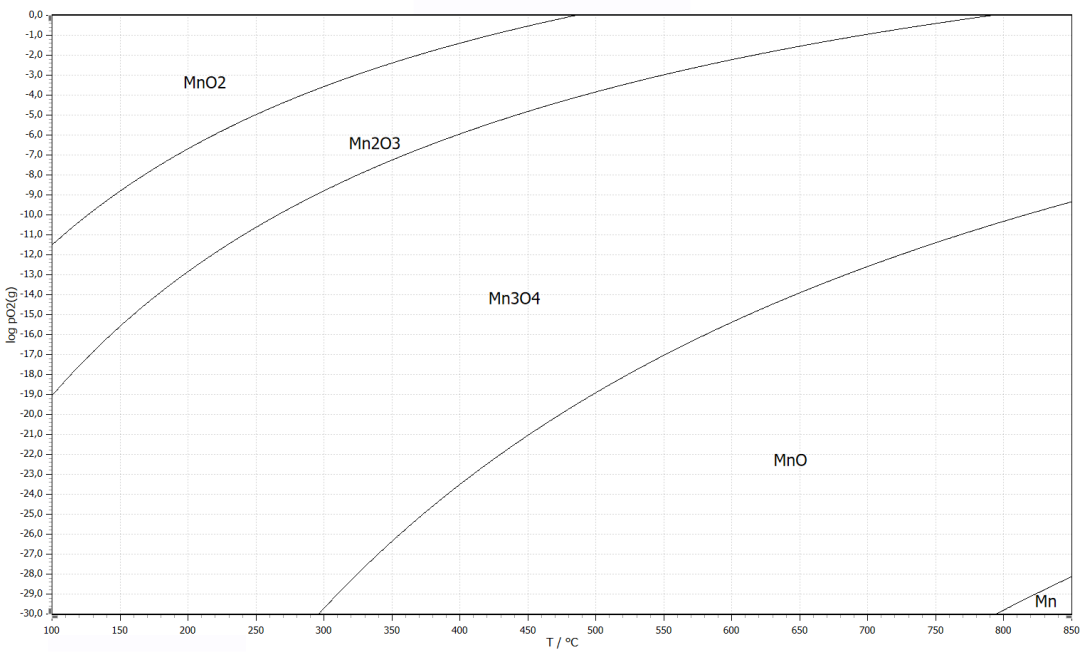

Figure 2: Stability diagram of manganese oxides and Mn created in HSC 9.

Figure 2 show the dominant manganese oxide at a oxygen pressure and temperature. Based on this diagram it is possible to produce manganese metal through heating in CO/CO_2 atmosphere. This is not possible in a manganese furnace[4], though MnO should be produced at higher temperatures. In an air atmosphere the result will most likely be Mn_2O_3 or Mn_3O_4.

The heating temperature has been found to increase the rate of reduction and the degree of prereduction during isothermal studies of other manganese ores . The difference between different ore chemistry is however significant and will heavily influence the reduction of the manganese ores[9].

Decomposition of carbonates will also increase the power usage. $MgCO_3$ will decompose around 300°C, $CaCO_3 \cdot MgCO_3$ at 500°C and $CaCO_3$ at 900°C [4]. This will only be a problem for ores with a high content of carbonates, such as UMK or when fluxes like dolomite or limestone are added.

In addition to the reduction, manganese oxides will at higher temperatures decompose in an air atmosphere[10][11]. Thermal decomposition of MnO_2 in air atmosphere has shown to start at 550°C-600°C and producing Mn_3O_4 at 950°-1050°C. Given oxygen in the reactant gases it was also found that MnO oxygenates after reaching 500°C, increasing the Mn_3O_4 content[12].

$$4MnO_2 \rightarrow 2Mn_2O_3 + O_2(g) \qquad \Delta H^o_{298} = 176\ kJ \tag{9}$$

$$6Mn_2O_3 \rightarrow 4Mn_3O_4 + O_2(g) \qquad \Delta H^o_{298} = 212,4\ kJ \tag{10}$$

Reactions 9 and 10 shows the thermal decomposition of higher manganese ores. Terayama and Ikeda [13] found that reaction 9 proceeds at 483°C and reaction 10 starts at 650°C, suggesting that the reaction starts earlier than what Zaki et al. measured. Some nonstoichiometric compounds also occurs during decomposition of both these manganese oxides, MnO_2 to $MnO_{1,61}$ at ∼560°C and Mn_2O_3 to $MnO_{1.41}$ at ∼780°C. All of these reactions are endothermic and will cool down the sample.

2.2 Shrinking core model

It is assumed that the reaction rate of the manganese reduction is controlled by the chemical reaction until the ore reaches a temperature of 250 - 300°C. Then the reaction is limited by diffusion and is a topochemical gas-solid reaction. This means that the outer layer will be reduced first and the outer layer grows inward. The unreacted core keeps shrinking as the gas is diffusing through the layers of MnO, Mn_2O_3 and Mn_3O_4[4].

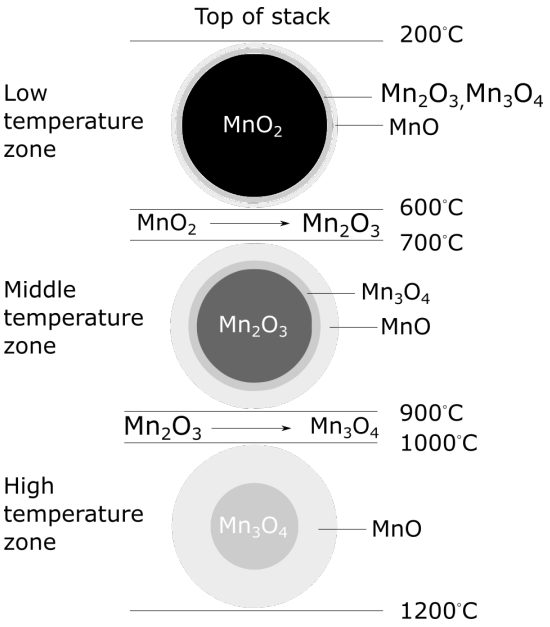

Figure 3: Shrinking core model after [4]

It has also been found that some manganese ores follow the shrinking core as the reactant gas is consumed as soon as it reaches the surface if the temperature is high enough, making the mass transfer the rate limiting process at higher temperatures. However Kumar et al. found that the rate of reduction of lower manganese ores may be controlled by the speed of the chemical reaction[14] at temperatures above 1000°C. This mass transfer is influenced by the porosity of the ore. The higher porosity gives a higher mass transfer as more space available and giving a higher diffusion speed[15]. The core must also be porous after reaction with the gas to be keep reacting until all the reactants are gone, either the gas or the solid. An increase in the

porosity of the ore as it reacts has been observed[16]. The reaction interface recedes towards the centre of the ore lump[17]. This is also influence by the ore size, as smaller size gives a larger chance that the higher oxides are reduced at a lower temperature[18] as well as the availability of CO and CO_2 at higher temperature[19]. This was also observed for Comilog and Assmang ore heated in CO-CO_2 atmosphere where the smaller ore sizes were reduced at a lower temperature and had a larger impact on the reduction rate than increasing the reactant gases[20].

2.3 Influence of porosity on prereduction of manganese ores

The porosity of the ore influences its strength and reactivity, and Comilog has a porosity of 20-30%[21] while UMK has a porosity of 3%[2]. This means the Comilog ore is weaker than UMK and should give a larger amount of fines during heating in the furnace and during tumbling. This does not mean that it does not give good results when used, as furnaces have been operated with up to 100 % Comilog with good results.[7]. The high porosity of the ore gives increased surface area usable for the gas-solid reaction and increases the reduction of manganese oxides, resulting in a higher degree of prereduction[2]. Samples with the highest surface area, the highest porosity will also be the fastest reacting samples due to the availability of possible reaction sites[22]. The UMK ore has a lower permeability, resulting in a lower surface area available for the gas-solid reaction with CO. However the porosity increases as the temperature is increased and at a higher degree of prereduction, thus increasing the porosity for both ores. The difference between the UMK and Comilog will be the same, because the ore with highest initial porosity will still have the highest porosity after heating as seen in figure 4[16].

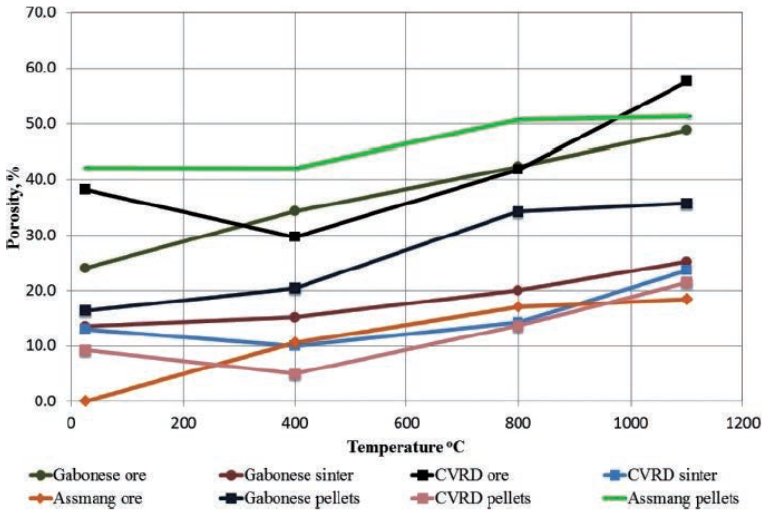

Figure 4: Measure porosity by Turkova et al.[16]

According to Gao et al. the size of the ore lumps may not have a large influence on the rate of reduction due to cracks formed during the reduction reactions[23]. Cracks were formed as the ores were reduced, thus increasing the rate of reduction due to the decrease in effective size caused by the cracks. Though a high initial porosity gives good permeability which is optimal for further reduction of the manganese oxides[24].

2.4 Decrepitation of manganese ores during prereduction

Mechanical strength is another important parameter for the ore in the manganese industry as fine material will decrease the permeability of the prereduction zone in the furnace. This will stop the uniform gas flow which reduces the ore higher up in the furnace. It is important to have ore which do not decrepitate too much as it is transported and charged in the furnace. Tests done on ore heated in a reducing atmosphere has shown that the mechanical strength of the ore is significantly lower than ore heated in other atmospheres.[7]

The thermal properties such as heat transfer coefficient and thermal expansion, as well as density changes due to the reduction reactions, will all increase the internal stress in the ore. This will increase the likelihood of failure at weak points in the ore. Thermal expansion is the increase in volume as the material is heated and is express by

$$\frac{\Delta V}{\mathrm{V}_0} = \alpha_v \cdot \Delta T \tag{11}$$

Where α_v is the volume coefficient of thermal expansion. Oxides do generally have a low coefficient of expansion and a low expansion during heating. If the oxide has a nonuniform expansion and is subjected to heating, then failure is likely due to thermal shock.

The thermal conductivity is a materials ability to transfer heat from a high temperature zone to a low temperature zone. This is described by

$$q = -k\frac{dT}{dx} \tag{12}$$

where q is the heat flux and k is the thermal conductivity. Oxide materials are thermal insulators and the thermal conductivity is decreasing as the temperature increases[25]. This has been shown for the Comilog ore, which has decreasing thermal conductivity as the ore is heated and a large drop in thermal conductivity between 500 and 600 °C [26] as shown in figure 5.

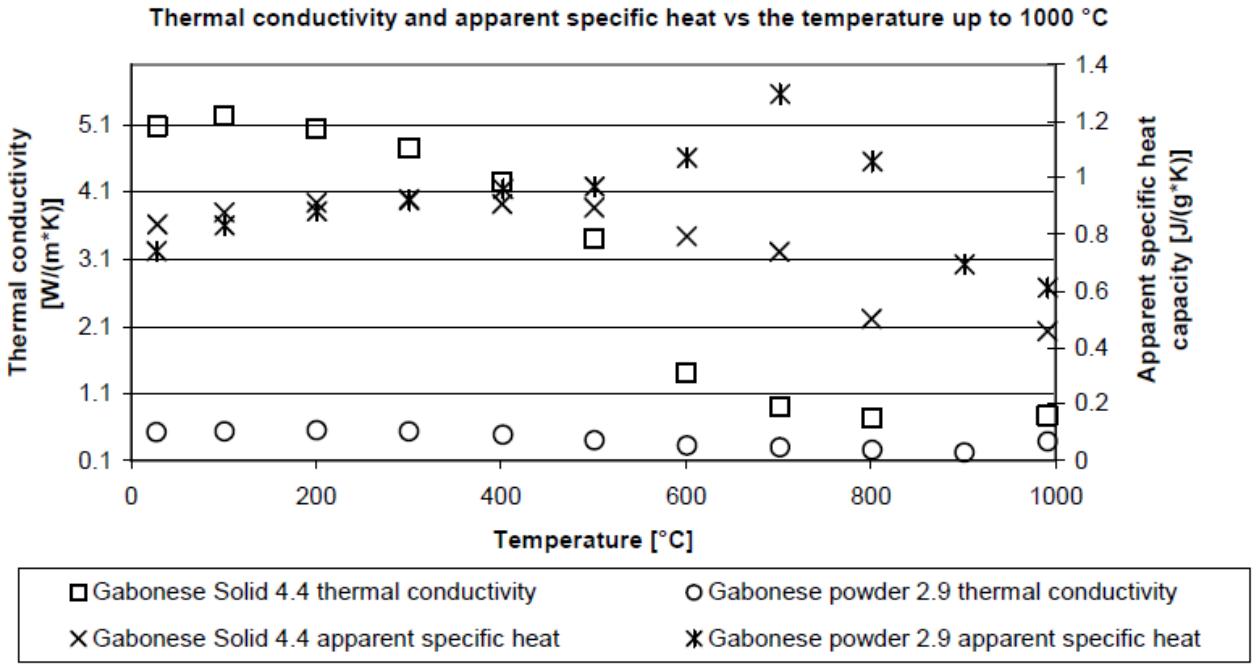

Figure 5: Thermal conductivity and specific heat of Comilog ore during heating [26]

Thermal stresses are induced as the materials are heated due to expansion and temperature gradients. The outer layer of the material will be heated faster and have a different temperature than the core of the material. This leads to different expansion of the different areas in the material, which increases the internal stresses.

Phase transformations in the ore also induces stress by creating an anisotropy which in turn leads to propagation of cracks and eventually fracture.[28] Different densities of the pure manganese oxides can be seen in table 1, however the ore is a complex system consisting of many different minerals and will never have the same density as the pure oxides. The ore is susceptible to thermal shock because it is an oxide material. This can result in brittle fracture from thermal stresses when the temperature gradient in the material is too steep. The resistance to thermal stresses also decreases when the porosity increases, due to the decrease in thermal conductivity for porous materials[29].

Table 1: Density of the manganese oxides taken from SI Chemical data[27] calculated to $[\frac{cm^3}{mol\ Mn}]$

Oxide	Density
MnO_2	23,79
Mn_2O_3	17,54
Mn_3O_4	16,23
MnO	13,14
Mn	7,42

Other mechanisms that may promote decrepitation is entrapment of fluid inclusions. These inclu-

sions may expand as the ore is heated and these fluid inclusions lose water. This induces strain on the ores, increases the probability of fracture when heated[30][31]. Small amount of water trapped in the crystal structure have a huge influence on stresses in quartz and similar mechanisms in the manganese ore, due to it being an oxide and containing small amounts of quartz[32]. Fluid inclusions have been observed in other manganese ores, like Wessel[33]. Structural water has been observed to increase the decrepitation in manganese ores, due to the vapour pressure of the water gathered in the ore pores[28] as well as decomposition of carbonates present in the ore[34].

2.5 Results from specialisation project

The experiments done for the Comilog and UMK ores in CO/CO_2 was done in the fall 2019. These experiments showed that the Comilog ore did overall decrepitate more than the UMK. The UMK however will need more time than the Comilog ore to achieve the same degree of prereduction. The Comilog ore, both the 10-13,2 mm and 3,35-6,7 mm, reached close to MnOx = 1 values at 600°C while the UMK must be heated to up to 800°C to reach similar values.

The heating curves for Comilog and UMK have one big difference, where the temperature of the sample increases rapidly to about 850°C after reaching ca. 100°C due to the exothermic reduction of the higher manganese ores. The UMK ore samples follows the temperature of the furnace during the entire experiment. [1] The smaller ore is heated faster than the large ore for both UMK and Comilog, though the shape of the curve was consistent for all the experiments.

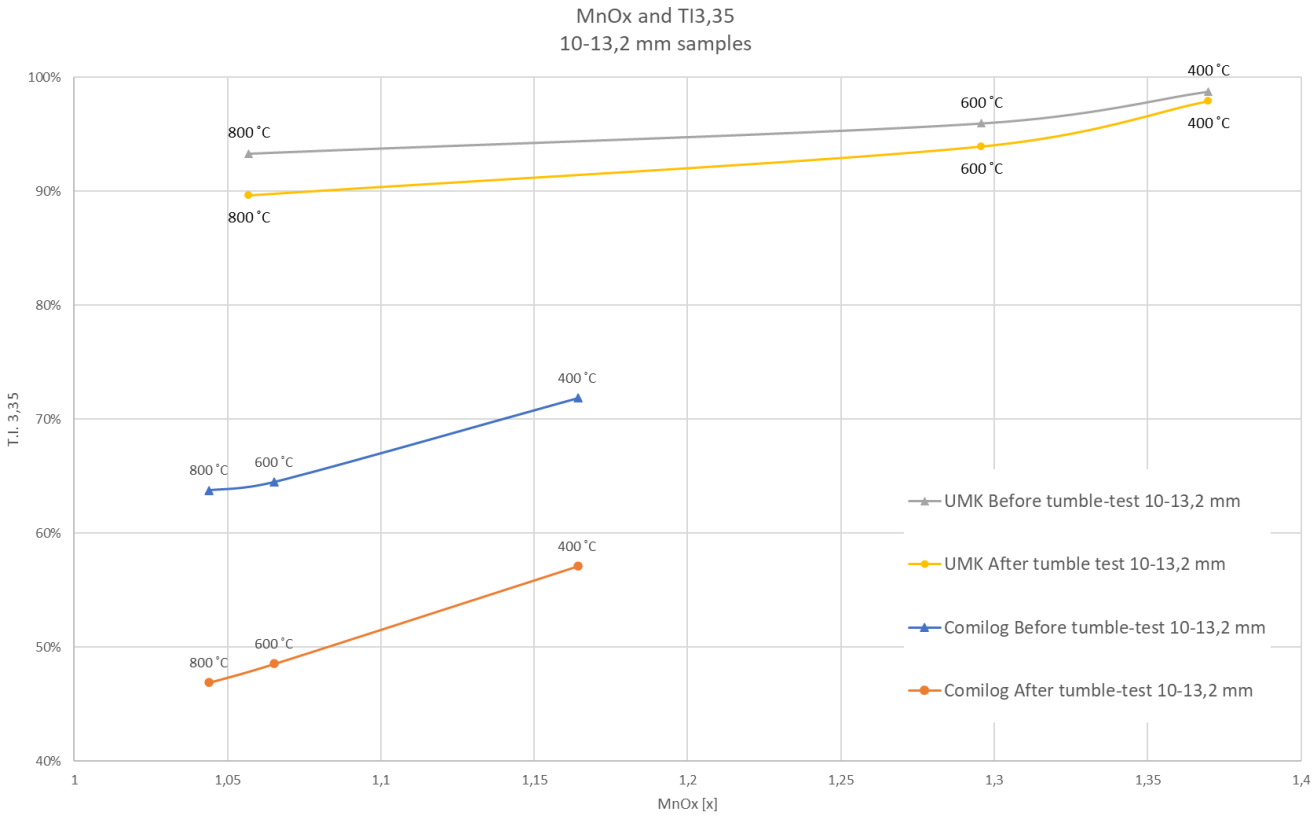

Figure 6: TI3,35 plotted against MnOx for the 10-13,2 mm ore used in the specialisation project [1].

Decrepitation tests showed that the Comilog ore is more susceptible to decrepitation than the UMK ore. The Comilog ore had at most 30 % of the sample in its original size fraction after heating and 20 % after the tumble testing while the UMK kept at most 80 %. The decrepitation increased with the temperature, 800°C had the most and 400°C had least. Comparing the degree and prereduction (MnOx values) and the TI3,35 it is seen that the Comilog ore is reduced more at temperatures below 600°C, but has more decrepitation than the UMK ore. At 800°C the MnOx is similar for both ores, but the UMK ore has decrepitated less than the Comilog [1]. All of this is seen in figure 6.

3 Experimental method

The experimental setup and procedure will be explained in this section. All experiments was done at NTNU in Trondheim if not otherwise stated.

3.1 Raw materials

Table 2: Raw material composition analysed by Sintef NorLab.[35] The Assmang ore was analyse by the same methods at a later time. The Mn and Fe are representet as total amount, but is present as oxides in the ore. The Mn will be present as MnO, Mn_2O_3 or Mn_3O_4 depending on the oxygen content of the ore. The CO_2 or C is the CO_2 in the carbonates and LOI are volatiles which evaporates during heating to 950°C

	Comilog	**UMK**	**Assmang**
Mn	51,15	38,22	51,31
Fe	2,86	4,67	6,43
SiO2	3,54	6,54	8,54
Al2O3	5,75	0,74	0,43
CaO	0,11	13,29	5,51
MgO	0,09	3,17	0,06
P	0,14	0,02	0,013
S	0,012	0,01	0,026
TiO2	0,14	0,01	0,00
K2O	0,79	0,08	0,00
BaO	0,25	0,07	0,11
MnO2	75,90	26,52	36,70
H2O	6,75	0,22	0,05
LOI 950	13,11	15,67	3,06
CO2	-	-	3,0
C	0,13	3,83	-

The ore used in the experiments are Comilog, Assmang and UMK. Comilog is an ore from Gábon and is rich in MnO_2. It is porous compared to the UMK and Assmang ore from South Africa, but it is higher in MnO_2 content. This means that more reactions will happen with the Comilog ore than the UMK and Assmang during heating. The Assmang ore does not have as much carbonates as the UMK, but is otherwise similar in composition. See table 2 for the chemical composition of both ores. The raw UMK had a measured apparent density of $3.44\,g/cm^3$ and an absolute density of $3.55\,g/cm^3$ which gives a porosity of 3,22 %. The Comilog ore had a measured apparent and absolute density of $3.11\,g/cm^3$ and $4.15\,g/cm^3$, respectively. This gives a porosity of 25,43%. No such data was available for the raw Assmang ore. The Comilog ore was damp and unsuitable for sieving and was dried at 105 °C for 20 hours, while the UMK and Assmang could be sieved without any further preparation.

The calculated MnOx value for the raw material is for UMK 1,43, for Comilog 1,93 and for Assmang 1,45. These values are calculated from table 2 using the method described in section 3.3.2 and are used to see how much oxygen that is left in the manganese oxides after the experiments.

3.2 Furnace setup and procedure

The furnace that was used is seen from the outside in figure 10 and the inside in figure 7b. Carbon rods were used as heating elements in the furnace. The furnace was extended in height to accommodate the size of the crucible by using refractory bricks and further insulated to ensure minimal heat loss. The hole in the bottom of the furnace was to attach the gas tube and was clogged with insulation before the furnace was started. Figure 7a shows the crucible ready for charging of the sample

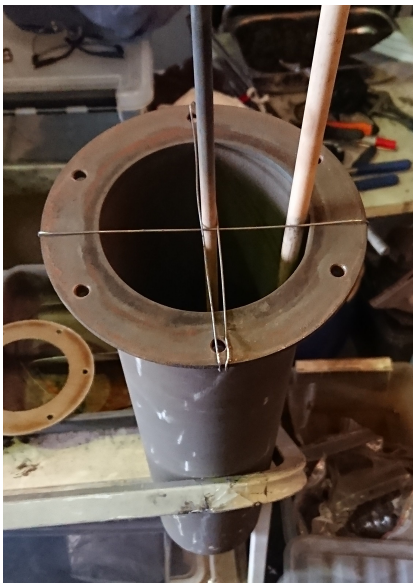

(a) Crucible ready for charging. The steep wire were removed before the crucible was closed after charging.

(b) The inside of the furnace. Carbon rods were used at heating elements,

Figure 7

The kanthal steel crucible with gas flowing in from underneath and exiting on the top was used for the experiments. See figure 8 for a schematic picture of the crucible setup.

Two thermocouples were placed in the crucible, one at the edge and one in the core of the sample to log the temperature in the sample as it was heated. The thermocouples were protected from the heat by two alumina tubes and one was placed as close to the middle of the charge as possible, while the other was place at the edge of the crucible. The alumina tubes were held in place by some steel wires while charging the crucible. The steel wires were removed after charging. A thermocouple was

built in the furnace in addition to the two thermocouples in the crucible. This way the temperature inside and outside the crucible was monitored simultaneously.

The tube for the exhaust gas was directly connected to the ventilation system to dispose of any toxic gases during the heating, and the operator was wearing a CO detector alarm due to the danger this gas posed.

Sample size was 2 kg and the ore in each sample were all within a predetermined size interval. Two different size distributions were used for the CO/CO_2 experiments, 3,35-6,7 mm and 10-13,2 mm in diameter for each ore. Only 10-13,2 mm was used for the synthetic air experiments. These sizes were obtained by sieving dry ore for 1 minute in a sieving machine seen in figure 11.

The samples were carefully placed in the crucible, making sure that the alumina tubes did not shift during charging. The crucible was placed in the furnace after the lid was attached, with a gasket to ensure that the crucible was air tight. Three hoses were attached to the crucible, one in the bottom and two on the lid. These hoses were for the gas used in the experiment, making sure the gas enters at the bottom of the crucible and exiting on the top. One of the top hoses were for the safety valve and one as normal exhaust.

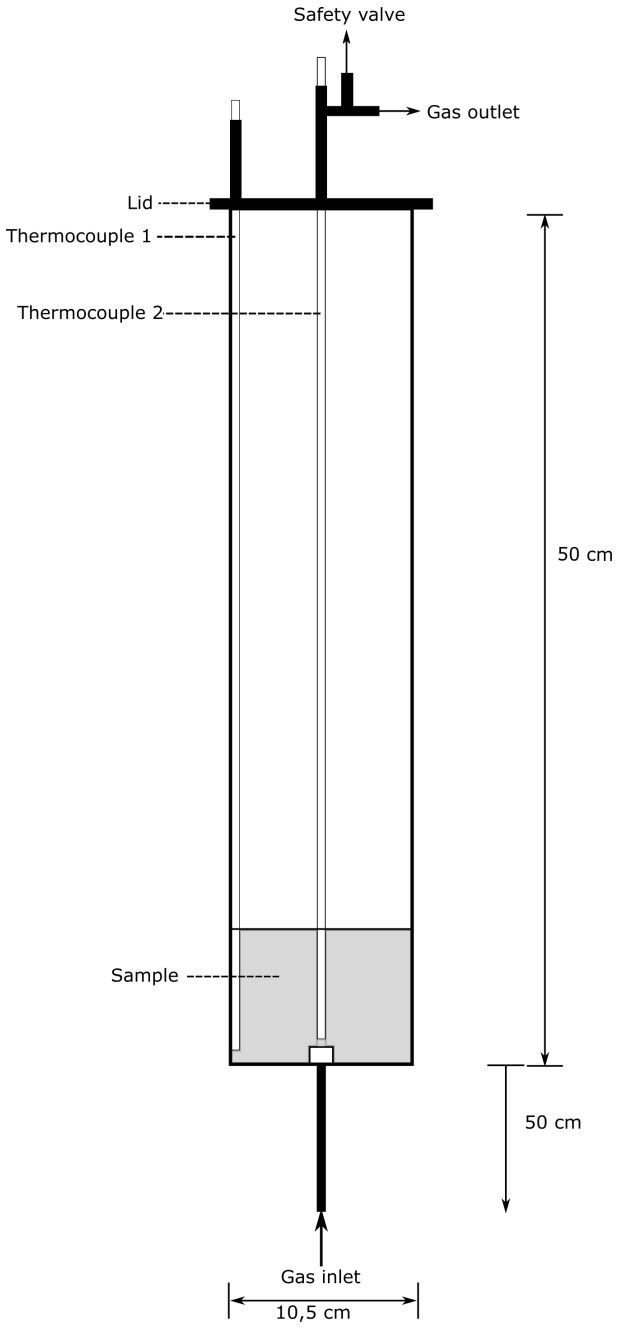

Figure 8: Schematic of the crucible

(a) Thermocouples and off-gas collection for the exhaust.

(b) Entech 1400 furnace used for the heating of the ore.

Figure 10: Furnace setup for the experiments with the crucible inside the furnace.

The furnace was heated to 200 °C in about 15 minutes, before the heating rate was set to 3 °C/min and kept constant until the sample reached target temperature. The furnace was kept at max temperature for a couple of minutes to ensure that the temperature difference between the core and the edge was as small as possible. The crucible was cooled as soon as the sample was at the target temperature using argon to prevent further reactions. It was left to cool in room temperature after about 1 hour of purging with argon. Then sample was collected after the crucible had reached room temperature. Figure 9 shows an example of a generic temperature profile.

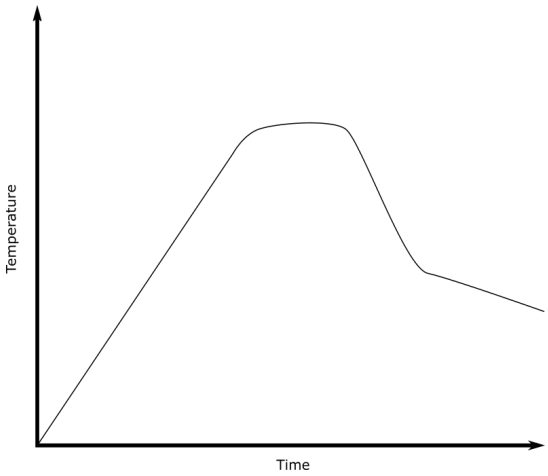

Figure 9: Example of a general temperature profile for a heating experiment.

Two experiments with Comilog ore and quartz in CO/CO_2 were done by careful mixing during charging. This was done to reduce the excess temperature by exothermic reactions. This time the charge was 1:1 mix of Comilog and

quartz, with a total weight of 2 kg. The sample were sorted before further analysis of the manganese ore after the heating program.

Table 3: A complete list over all experiments done in this MSc. Most of the experiments were in air, but the CO/CO_2 experiments were done to complement the experiments done in fall 2019[1].

Ore	**Temperature [°C]**	**Gas**	**Size [mm]**
Comilog	800	Syn. Air	10-13,2
Comilog	600	Syn. Air	10-13,2
Comilog	400	Syn. Air	10-13,2
Comilog/Quartz	800	Syn. Air	10-13,2
Comilog/Quartz	800	Syn. Air	10-13,2
UMK	800	Syn. Air	10-13,2
UMK	600	Syn. Air	10-13,2
UMK	400	Syn. Air	10-13,2
Assmang	800	Syn. Air	10-13,2
Assmang	600	Syn. Air	10-13,2
Assmang	400	Syn. Air	10-13,2
Assmang	800	CO/CO_2	10-13,2
Assmang	600	CO/CO_2	10-13,2
Assmang	400	CO/CO_2	10-13,2
Assmang	800	CO/CO_2	3,35-6,7
Assmang	600	CO/CO_2	3,35-6,7
Assmang	400	CO/CO_2	3,35-6,7

Table 3 shows all experiments done. As the Assmang ore was introduced as one of the raw materials, experiments in CO/CO_2 were also done to be comparable to the work done in the fall 2019[1]. The rest were examined in synthetic air to compare the decrepitation and reduction to the CO/CO_2 experiments. Both of these gases were selected as possible prereduction gases for use industrially.

3.3 Characterisation

The samples were examined using tumble-testing, sieving, and chemical analysis. The chemical analysis was done by Sintef Norlab using a titrimetric method for MnO_2, thermogravimetry for LOI950, an internal method for CO_2 and XRF for the rest. The porosity measurements were done by Sintef using gas pycnometry.

3.3.1 Tumble-testing

Tumble-testing was done to examine the decrepitation of the manganese ores. The tumbling was done to simulate transport and handling of the ore before it is put in the furnace. This was done

to see if the different methods of prereduction and degrees of prereduction would influence the formation of fines. Determining the size distribution after heating was done by sieving in a sieving machine. Firstly the samples were sieved using sieves with mesh sizes 13.2 mm, 10 mm, 6.7 mm, 4.75 mm, 3.35 mm, 1.6 mm and 0.5 mm, as well as a pan to collect the finest particles. The sieves were stacked on top of each other and placed for 1 minute in a sieving machine as seen in figure 11.

(a) Sieves stacked as they were placed in the sieving machine

(b) The sieving machine used to find the size distribution

Figure 11: Sieving setup

Secondly the ore was placed in a Hannover drum and tumbled for 30 minutes at 40 rpm. The drum had a inner diameter at 21 cm and a height of 10 cm. Finally the samples were sieved once more to get the final size distribution. This data was then used for the calculation of the tumbler index to quantify the decrepitation and compare the samples.

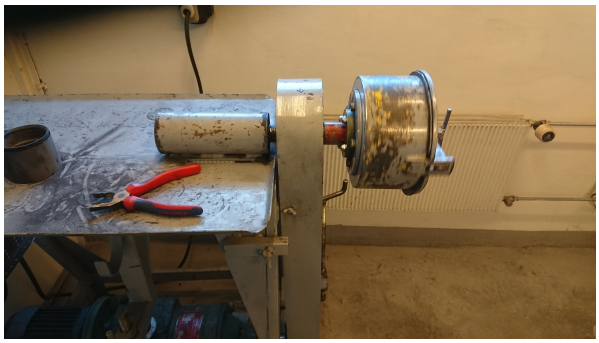

(a) Hannoverdrum mounted on the tumble-machine

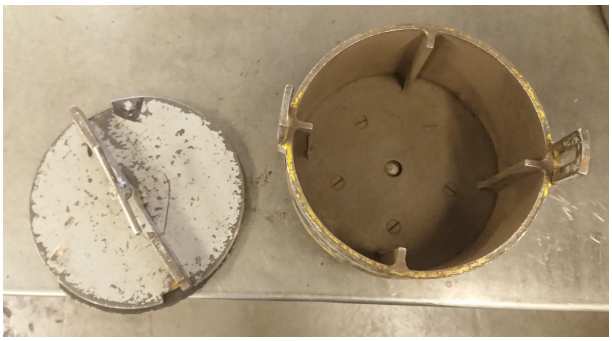

(b) The hannoverdrum used in the experiments, with an inner diameter of 21 cm and a height of 10 cm

Figure 12: Setup for the tumble-testing

3.3.2 Calculations of decrepitation and degree of prereduction

The Decrepitation Index (D.I.) and Tumbler index (T.I.) is used to measure how much the ore decrepitates when heated and transported.

$$DI = \frac{weight\ of\ ore\ < [\mathrm{d_0}]}{weight\ of\ sample} \tag{13}$$

T.I.$\mathrm{d_0}$ is the fraction of the ore larger than $\mathrm{d_0}$ after reduction and tumble-testing[36].

$$TI = \frac{weight\ of\ ore\ > [\mathrm{d_0}]}{weight\ of\ sample} \tag{14}$$

Where $\mathrm{d_0}$ is the mesh size of the sieves in mm. This means that for the same $\mathrm{d_0}$

$$T.I. = 1 - D.I. \tag{15}$$

The O/Mn ratio or the MnOx tells how much the ore has been reduced. This is calculated from chemical analysis where $\mathrm{MnO_2}$ gives MnOx where x = 2, $\mathrm{Mn_2O_3}$ gives x = 1,5 an so forth.[6]

$$x = \frac{\mathrm{O}}{\mathrm{Mn}} = \frac{2 \cdot mol\ \mathrm{MnO_2} + mol\ \mathrm{MnO}}{mol\ \mathrm{Mn}} \tag{16}$$

$$mol\ \mathrm{MnO} = mol\ \mathrm{Mn} - mol\ \mathrm{MnO_2} \tag{17}$$

3.3.3 Calculation of the theoretical weight loss

The weight loss (WL) is used to measure how much of the ore has reacted as varoius gases will escape the sample during the heating. This is done by assuming that all the manganese is reacting to MnO, all Fe starts as Fe_2O_3 and reacts to FeO and all carbon present in the raw material are carbonates which decomposes to CO_2. Water and other volatiles does also influence the weight loss. According to equation 5 to 7 only oxygen will leave the charge in addition to the CO_2 from the carbonates.

Loss from MnOx→ MnO

$$WL = (mol\ Mn \cdot x - mol\ Mn) \cdot molar\ mass\ O \tag{18}$$

Loss from $Fe_2O_3 \rightarrow$ FeO

$$WL = (mol\ Fe \cdot 1,5 - mol\ Fe) \cdot molar\ mass\ O \tag{19}$$

Loss from carbonates

$$WL = mol\ C \cdot molar\ mass\ CO_2 \tag{20}$$

This theoretical mass loss is calculated from the chemical analysis of the raw material[37]

3.3.4 SEM preparation

Before the examination of the cross section of a ore lump, some preparation needs to be done. One ore lump of decent size (1-2 mm in diameter, roughly equiaxial) was selected from each sample after the tumble-testing. This lump was cast in epoxy to make it easier to handle in the subsequent steps, using epoxy resin and a hardener. The epoxy hardened overnight and was ready for grinding the next day. Using a Struers Tegramin 30 the samples were ground to about half its thickness to expose the cross section. The cross section was finely ground using grinding plates of decreasing grain sizes, and polished to be able to easily examine the sample in a SEM.

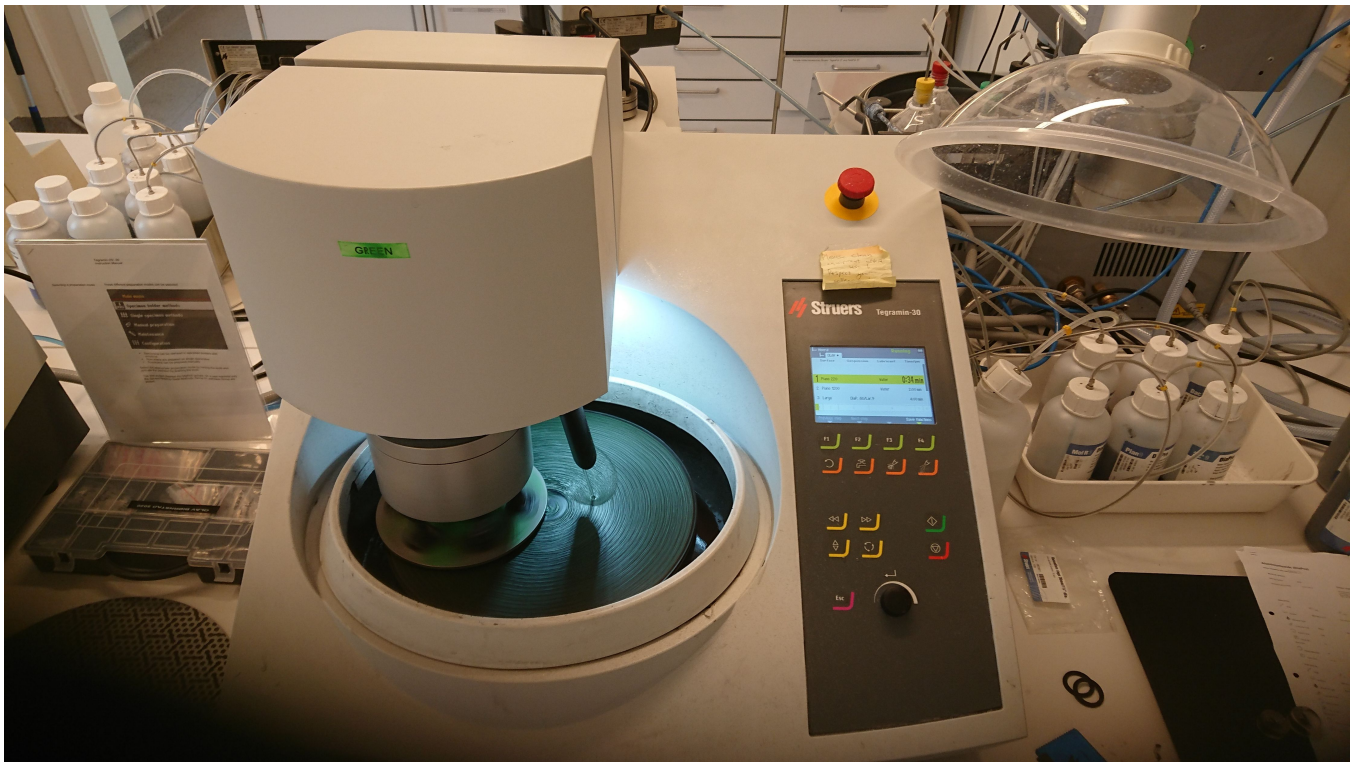

Figure 13: Struers Tegramin 30 machine used in the sample preparation for the SEM examination.

Before the SEM examination the samples were wrapped in aluminium foil and a conductive bridge was made using carbon tape due to the insulating nature of the epoxy. This was to avoid charging of the sample during SEM examination which would inhibit the ability to get a clear image. See figure 14.

Several pictures of each sample was taken from the core of the cross section and from the edge. This was to compare the structure of the pores and cracks present in the sample after the prereduction.

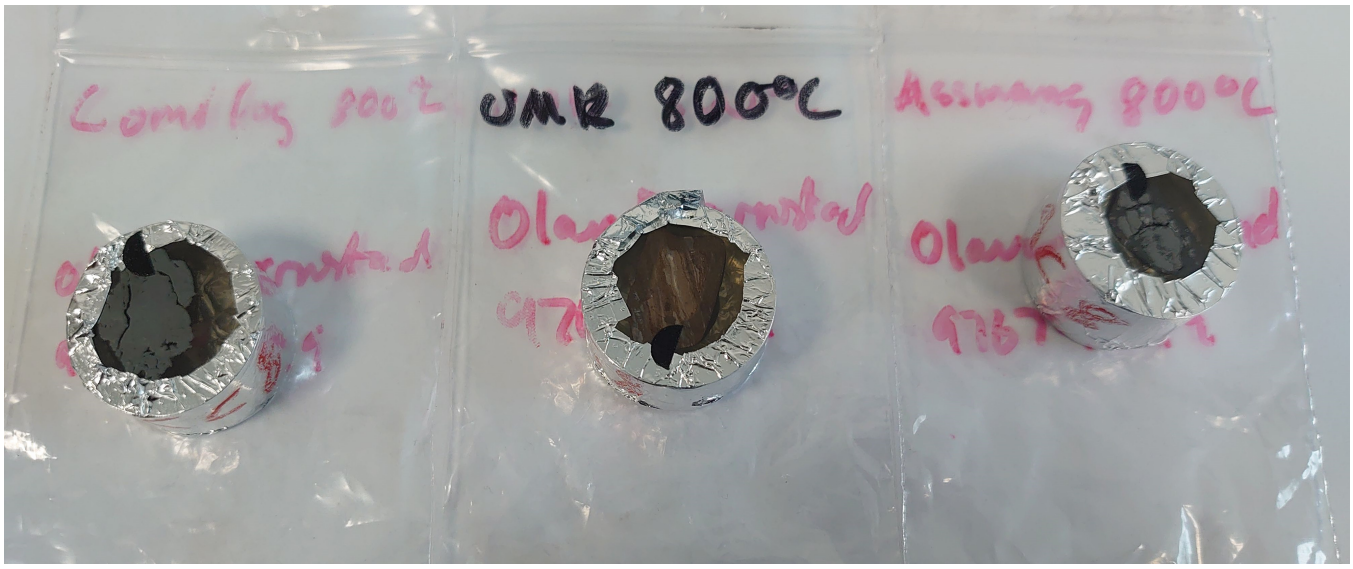

Figure 14: Ore samples prepared for SEM examination, wrapped in aluminium foil to avoid charging of the non-conductive epoxy. A small semi-circle of carbon tape connects the sample and the aluminium foil.

The SEM works by firing electrons at the surface of the sample. This instrument have a high resolution due to the wavelength of an electron which enables a high magnification examination of the surface. The cross section of the ore lump was examined using secondary electron contrast. This mode is used to examine the topography of a sample, which gives a good view of the pores and cracks. The electrons from the electron gun is focused using electromagnetic lenses and is scanning the surface of the sample, knocking loose electrons (secondary electrons) which are collected by a collector. The emission of secondary electrons are a function of the topography, and thus an image is created of the surface sample.[38]

A SEM sample has to be conductive to avoid buildup of electrons (charging) in non-conductive parts of the sample. Carbon tape and aluminium foil is used to conduct electrons away from the non-conductive sample. This is also necessary because the epoxy does not conduct electricity to the sample holder.

3.3.5 Pressure force measurements

The pressure strength of the ore was measured to compare the apparent strength of the ore. To do this, the sample was placed in a holder. This holder was a small, metal cylinder with a bottom. The pressure force of the ore was recorded as the piston was moved down, compressing the sample. The cylindrical sample holder was to avoid shards of ore flying around as the sample cracked. 10 samples were examined for each ore, temperature and gas atmosphere.

(a) The machine used for the pressure strength test. Here is the piston and the sample holder ready for a test. The ore sample is located in the middle of the steel cylinder below the piston.

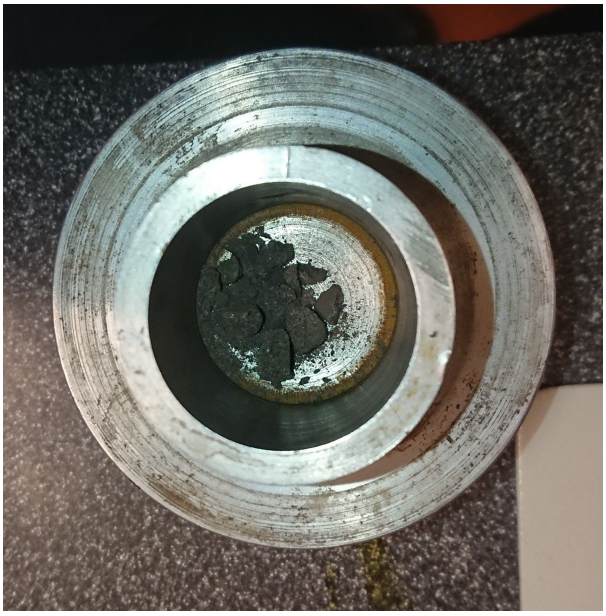

(b) Inside of the sample holder after a test, with the crushed sample still in the holder.

Figure 15: Setup for the pressure strength testing.

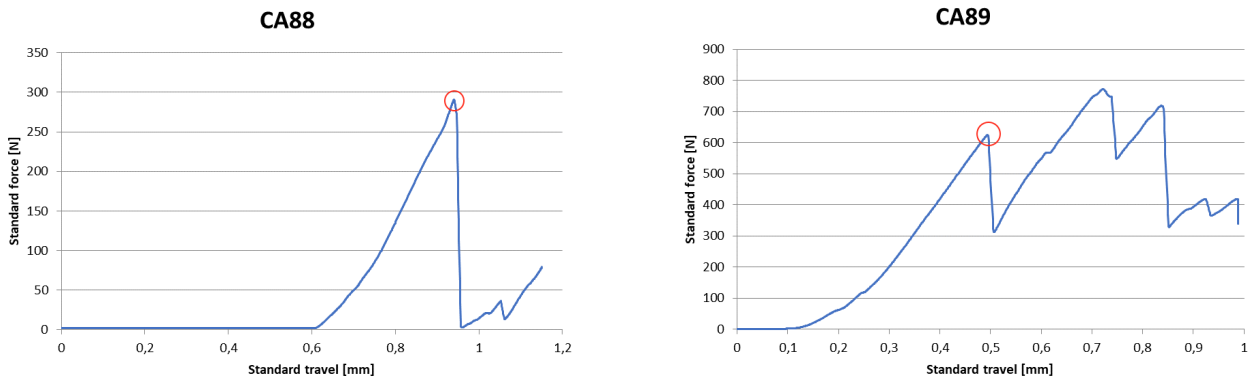

(a) (b)

Figure 16: Examples of two pressure force measurements. The red circle represents the point chosen as the pressure force.

The pressure force at the first major crack was used to compare the different ore samples. Figure 16 show how the graphs were interpreted by the operator to chose the pressure force. The first major decrease in force was chosen as the pressure force as it represents when the ore lump cracks for the first time.

4 Results

This section will contain the results of the experimental work done in the spring 2020. This work is a continuation of the experimental work done in the specialisation project done in the fall 2019[1]. Further discussion of all the result will follow in later sections.

4.1 Degree of prereduction

The degree of prereduction is used to measure how much the ores have been reduced. This is calculated from the chemical analysis done by Sintef Norlab using the method described in section 3.3.2. The chemical analyses can be found in the Appendix.

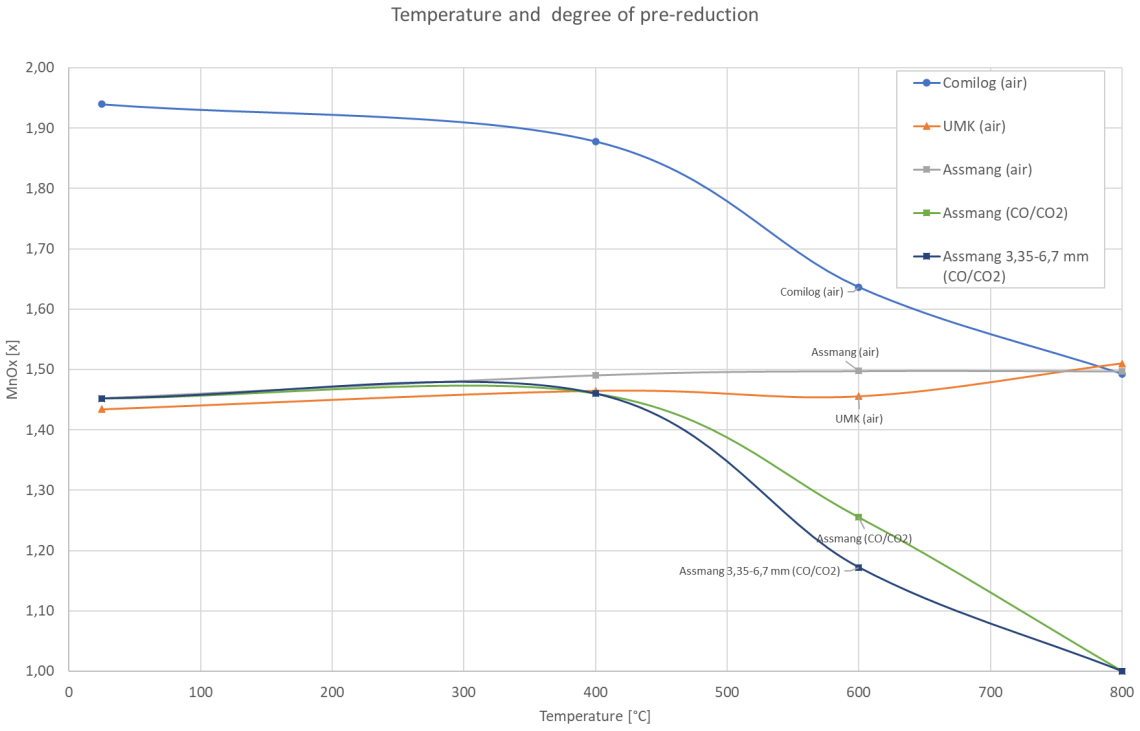

Figure 17: The MnOx values plotted against the temperature for all experiments. All of the ore was in the size interval 10-13,2 mm at the start of the experiments unless otherwise is stated.

Looking at the air experiments in figure 17, all of the ores approach a MnOx value of 1,5, signifying that the majority of manganese is in the form of Mn_2O_3. This increases the MnOx value for Assmang and UMK which are at a slightly lower value for the raw ore. The Comilog ore does however start at a higher MnOx value of 1,94, thus it has a significant decrease in oxygen content as a result of

the heating. In air, there is hardly no decrepitation of Comilog and UMK, where Assmang has a slight increase in the degree of decrepitation.

The Assmang ore heated in CO/CO_2 starts at x = 1,45, but is not reduced before reaching 400°C as the MnOx value is similar to the samples heated in air. Increasing the temperature does however increase the reduction, the smaller ore is reduced faster than the larger, reaching x = 1,17 for the 3,35-6,7 mm ore and x = 1,26 for the 10-13,2 mm ore. Both sizes reaches x = 1 at 800°C, meaning that the only manganese oxide left is MnO.

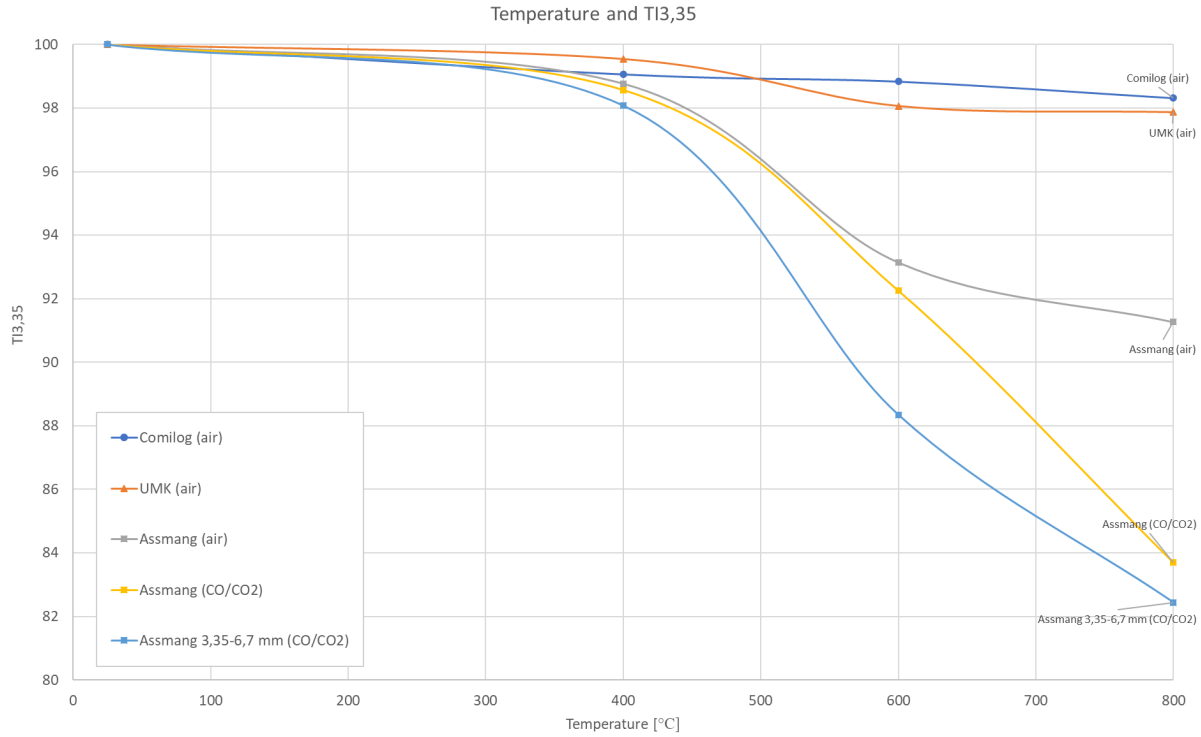

Figure 18: The TI3,35 values before tumble testing plotted against the temperature for all experiments conducted.

All of the ore keeps more than 80% of its ore at a larger size than 3,35 mm as shown in figure 18. The UMK is marginally strongest in air until 600°C is reached and Comilog has the lowest decrepitation in air. The Assmang ore decrepitates the most of the ores in air, but is still above a TI3,35 larger than 90%.

Assmang in CO/CO_2 decrepitates more than all of the air experiments and the ore which initially was at 3,35-6,7 mm has the lowest TI3,35 value.

Table 4: MnOx values for all samples.

Sample	**MnOx**	**Sample**	**MnOx**
Assmang 10-13,2 mm 800°C CO/CO_2	1,00	Assmang 10-13,2 mm 800°C AIR	1,51
Assmang 10-13,2 mm 600°C CO/CO_2	1,26	Assmang 10-13,2 mm 600°C AIR	1,46
Assmang 10-13,2 mm 400°C CO/CO_2	1,46	Assmang 10-13,2 mm 400°C AIR	1,46
Assmang 3,35-6,7 mm 800°C CO/CO_2	1,00	UMK 10-13,2 mm 800°C AIR	1,50
Assmang 3,35-6,7 mm 600°C CO/CO_2	1,17	UMK 10-13,2 mm 600°C AIR	1,50
Assmang 3,35-6,7 mm 400°C CO/CO_2	1,46	UMK 10-13,2 mm 400°C AIR	1,49
Comilog/Quartz CO/CO_2 1	1,06	Comilog 10-13,2 mm 800°C AIR	1,49
Comilog/Quartz CO/CO_2 2	1,07	Comilog 10-13,2 mm 600°C AIR	1,58
		Comilog 10-13,2 mm 400°C AIR	1,88

Table 5: MnOx values of fines. Only some of the experiments yielded enough fines to perform an analysis. BFT is before tumble-test while AFT is after tumble-test.

Sample	**MnOx**	**Sample**	**MnOx**
Assmang fines 800°C CO/CO_2 BFT	1,00	Assmang fines 800°C AIR BFT	1,51
Assmang fines 800°C CO/CO_2 AFT	1,00	Assmang fines 800°C AIR AFT	1,52
Assmang fines 600°C CO/CO_2 BFT	1,09	Assmang fines 600°C AIR AFT	1,54
Assmang fines 600°C CO/CO_2 AFT	1,05	Comilog fines 800°C AIR AFT	1,48
Comilog/Quartz CO/CO_2 1 Fines	1,07	Comilog fines 600°C AIR AFT	1,58
Comilog/Quartz CO/CO_2 2 Fines	1,06	Comilog fines 400°C AIR AFT	1,89

Tables 4 and 5 is a collection of the calculated MnOx values for all samples analyse by Sintef Norlab. Table 5 shows values for fines produced during the experiments. However not all of the experiments produced enough fines for analysis, which is why only some fines were examined. All of the fines produced had similar value as the rest of the sample, with the exception of the Assmang fines from the CO/CO_2 at 600°C. The Assmang sample is at x = 1,26, while the fines is reduced to x $\approx$ 1.

4.2 Decrepitation

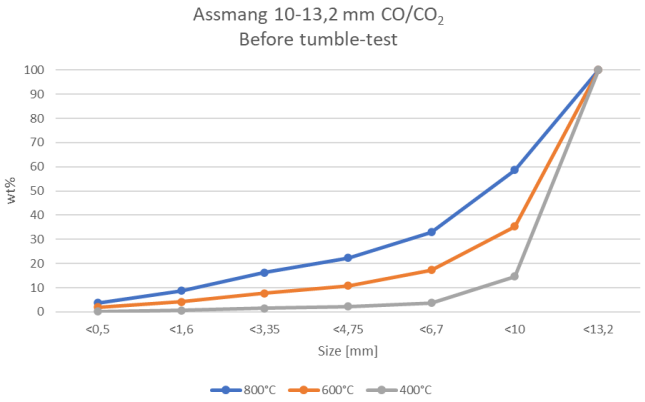

(a) Cumulative size distribution of the Assmang heated in CO/CO_2 atmosphere, before the tumble-testing

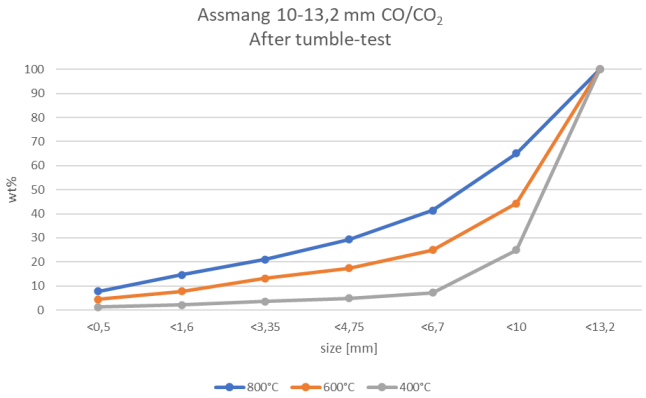

(b) Cumulative size distribution of the Assmang heated in CO/CO_2 atmosphere, after tumble-testing

Figure 19

Figure 19a show the size distribution of the ore sample before the tumble test. The decrepitation increases with increasing temperature (and time) in the furnace. Over 85% of the ore are in its original size interval at 400°C and the amount declines to just above 40 % at 800°C. The same trend is seen in figure 19b showing the size distribution after the tumble-testing. The original size fraction has decreased to about 75 % and 35 % for 400°C and 800°C, respectively.

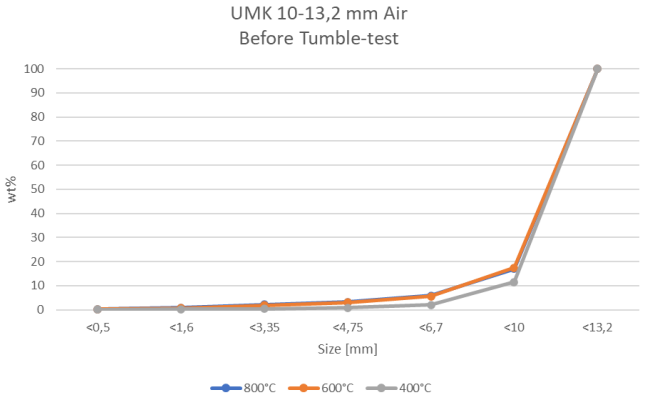

(a) Cumulative size distribution of the UMK heated in air atmosphere, before tumble-testing

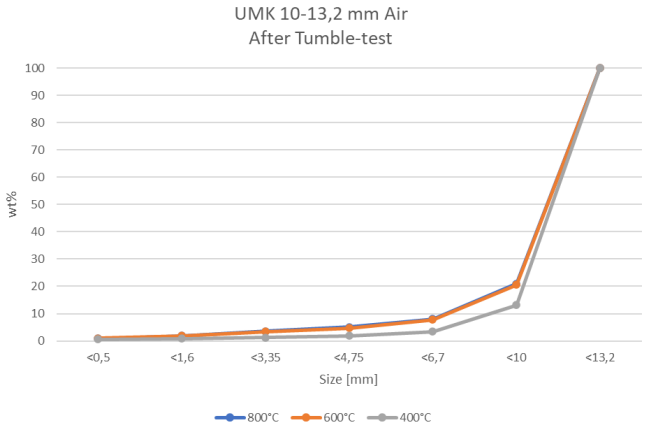

(b) Cumulative size distribution of the UMK heated in air atmosphere, after tumble-testing

Figure 20

Figure 20a and 20b shows the size distribution of the UMK ore at 13,2-10 mm heated in an air atmosphere. Most of the ore is still at its original size. Regardless of the temperature, more than 80% of the ore is still at its original size and even after tumble-testing it decreases to only slightly below 80%.

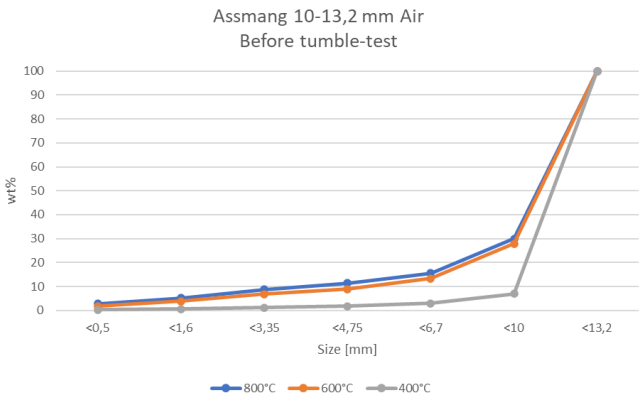

(a) Cumulative size distribution of the Assmang heated in air atmosphere, before tumble-testing

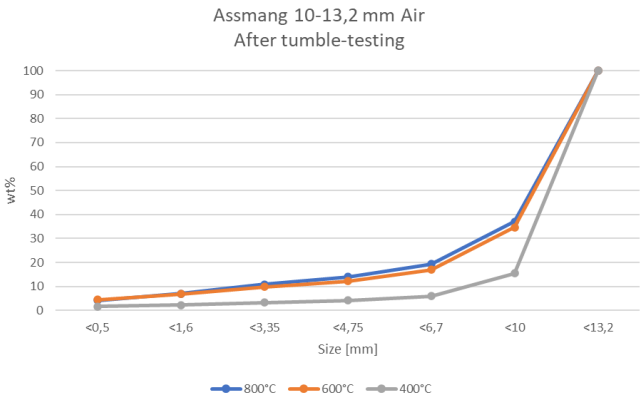

(b) Cumulative size distribution of the Assmang heated in air atmosphere, after tumble-testing

Figure 21

Figures 21a and 21b shows the cumulative size distribution of Assmang ore at 10-13,2 mm original size heated in air atmosphere before and after tumble testing. There is a slight decrease of the ore in the original size after tumble testing. The decrepitation is also increasing as the temperature is increased

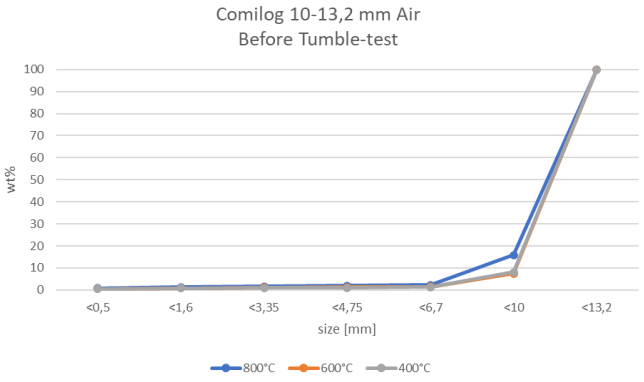

(a) Cumulative size distribution of the Comilog heated in air atmosphere, before tumble-testing

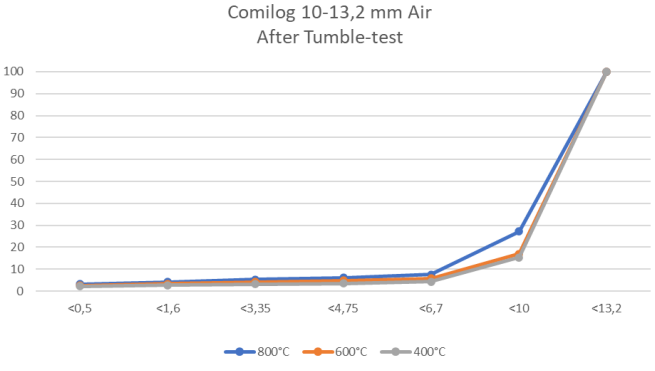

(b) Cumulative size distribution of the Comilog heated in air atmosphere, after tumble-testing

Figure 22

The Comilog ore does not decrepitate a lot when heated in synthetic air. Figure 22 shows that most of the ore remains larger than 10 mm, with 80% of the ore is larger than 10 mm before tumble test. After tumble-testing the fraction has decreased to 70%. Decrepitation is increasing as the temperaure is increaseing. Both 400°C and 600°C seems to have the same amount of decrepitation.

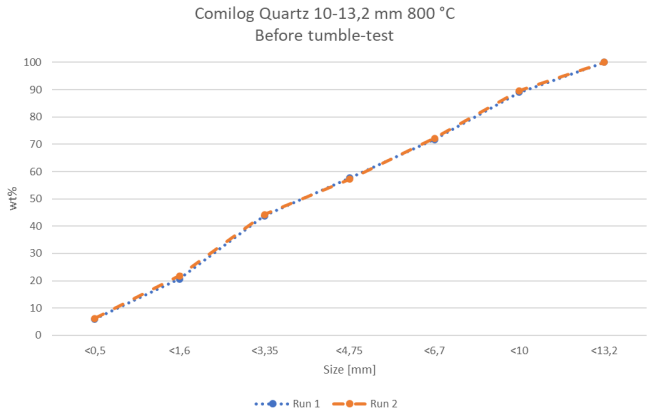

(a) Cumulative size distribution of the Comilog ore heated together with quartz in a CO/CO_2 atmosphere before tumble-testing.

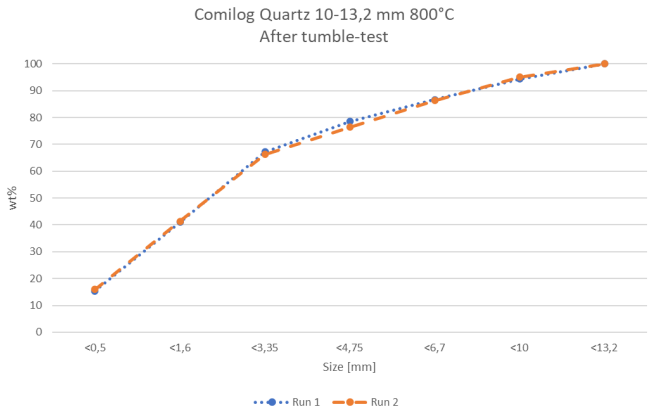

(b) Cumulative size distribution of the Comilog ore heated together with quartz in a CO/CO_2 atmosphere after tumble-testing

Figure 23

Figure 23 Shows the decrepitation of the two Comilog/Quartz experiments in CO/CO_2. The Comilog was separated from the quartz before the sieving and tumble testing. The quartz is quite stable and do not disintegrate in this temperature area, with the exception of some fine quartz particles. This does however give an increased content of SiO_2 in the smaller size fractions, as complete separation of manganese ore and quartz was impossible.

4.3 Pressure strength

After the tumbletesting some of the ore lumps were selected for pressure strength testing. this was done by selecting ore lumps of a similar size, about 1-2 cm in size an a equiaxial shape. The procedure is described in section 3.3.5.

Most of the measurements vary widely, but after 10 tests for each ore temperature and gas atmosphere a pattern emerges. The blue line in each of the plots represents the average value, and if present to help see the general pattern of the measurements. The value at 25°C is the same for both reactant gases.

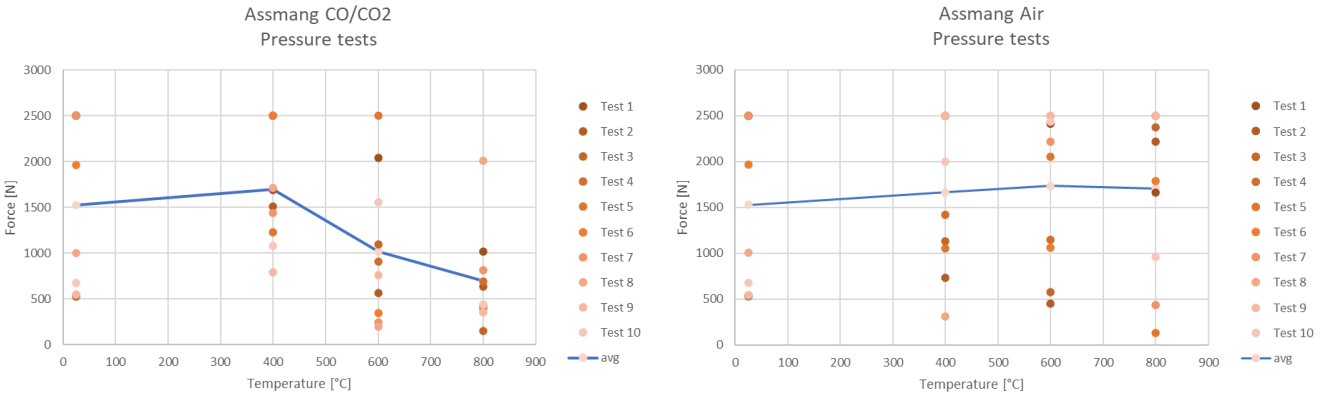

(a) **(b)**

Figure 24: Pressure strength test results for Assmang ore heated in CO/CO_2 (a) and synthetic air (b)

Figure 24 shows the biggest change between the two different gas atmospheres. The air heated ore has little to no decrease in the force needed to crack the ore, while the CO/CO_2 heated ore is decreasing in strength as the temperature is increasing.

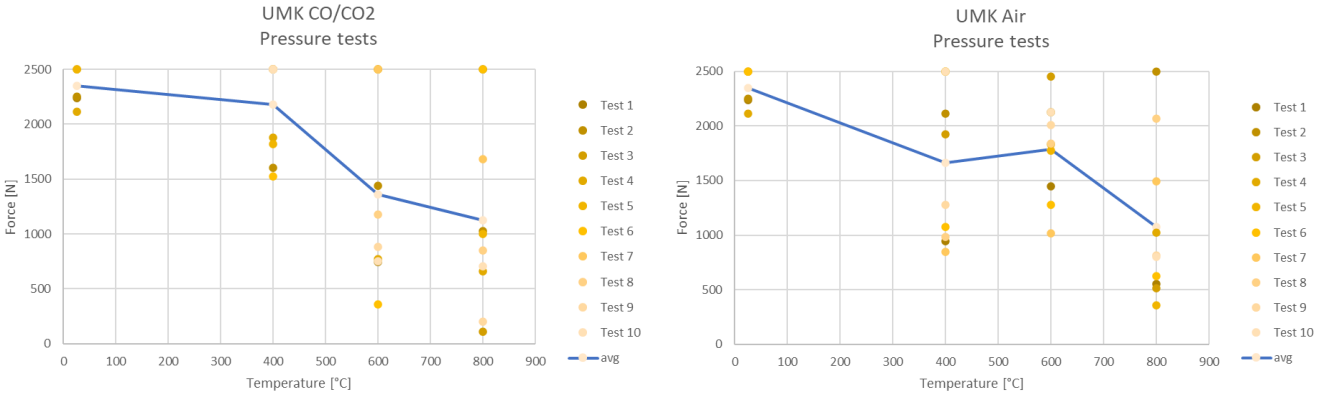

(a) **(b)**

Figure 25: Pressure strength test results for UMK ore heated in CO/CO_2 (a) and synthetic air (b)

The UMK ore keeps a similar behaviour in both gas atmospheres seen in figure 25, showing a decreasing strength as the temperature increases. There is a slight difference between the 400°C and 600°C experiments, but this could be due to the large variation of the measured values. Though the strength of the CO/CO_2 heated ore seems to have the fastest decline in strength.

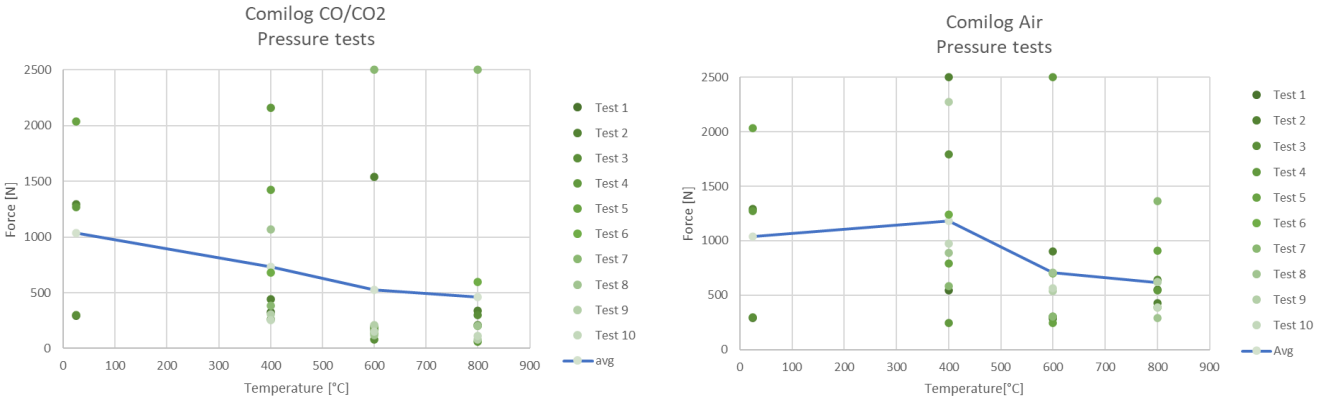

(a) **(b)**

Figure 26: Pressure strength test results for Comilog ore heated in CO/CO_2 (a) and synthetic air (b)

The Comilog ore is generally weaker than the other ores and shows a decrease in strength as the ore is heated in both gases, similar to the UMK ore. The strength of the initial raw ore is significantly lower than the other ores as can be seen in figure 26.

4.4 Heating curves

Heating curves for the experiments are presented here. Due to the similarities of the curves only the 400°C and 800°C curves are presented here. See appendix for the remaining temperature curves.

The Assmang ore keeps a temperature similar to the furnace during the entire heating program, though the sample temperature increases above the furnace temperature at around 500°C as seen in figure 27. This is most likely due to exothermic reduction of manganese oxides increasing the temperature of the sample, as the sample temperature is reduced to the furnace temperature in the end of the heating program when most of the manganese oxides are reduced as much as possible.

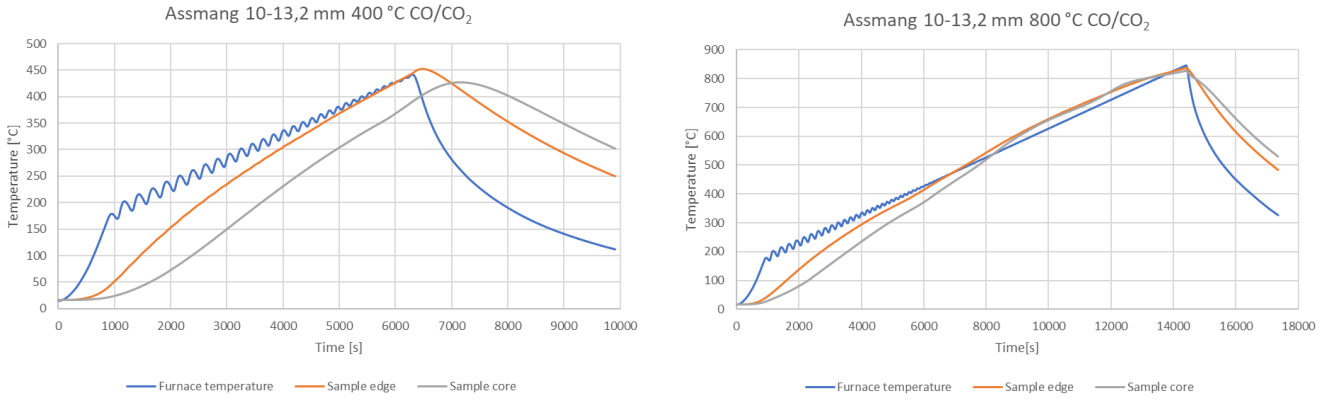

(a) **(b)**

Figure 27: Heating curves of Assmang ore, 10-13,2 mm, heated in CO/CO_2

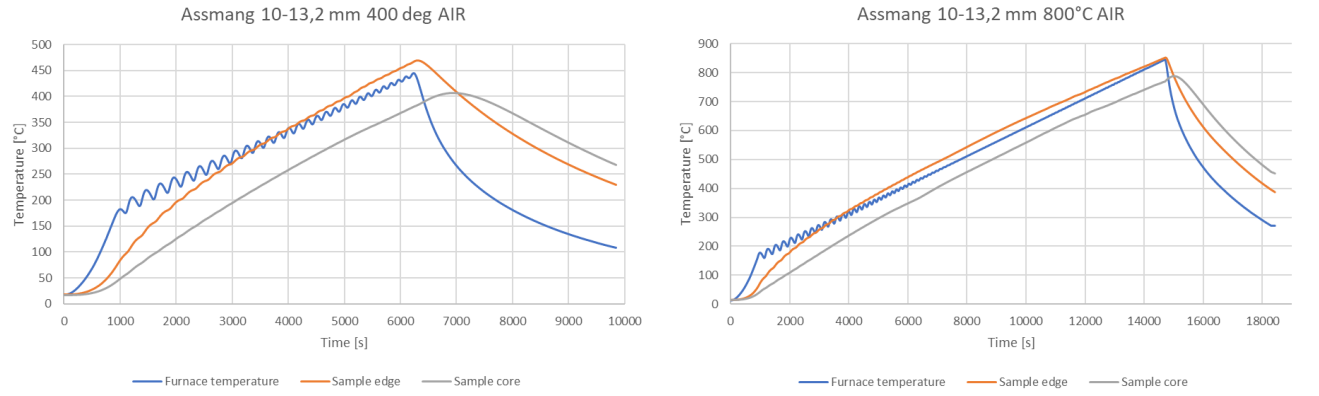

(a) **(b)**

Figure 28: Heating curves of Assmang ore, 10-13,2 mm, heated in synthetic air

Figure 28 and 29 shows the heating of Assmang and UMK ore. Both have similar heating curves, following the furnace temperature while the edge of the sample is slightly warmer than the furnace after the furnace reaches ~300°C. In all cases the temperature at the edge of the sample is increasing and decreasing faster than the core temperature.

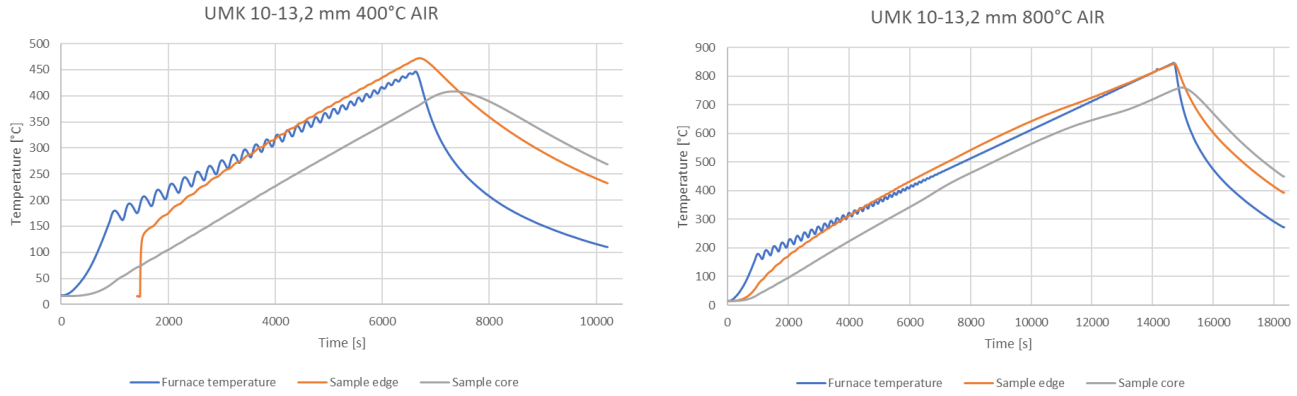

(a) **(b)**

Figure 29: Heating curves of UMK ore, 10-13,2 mm, heated in synthetic air

Only difference seen in while heating the Comilog in synthetic air compared to the two other ores are a decrease in the core temperature at the end of theheating program. This is visible in figure 30b where the sample is reaching ∼550°C before the change is significant.

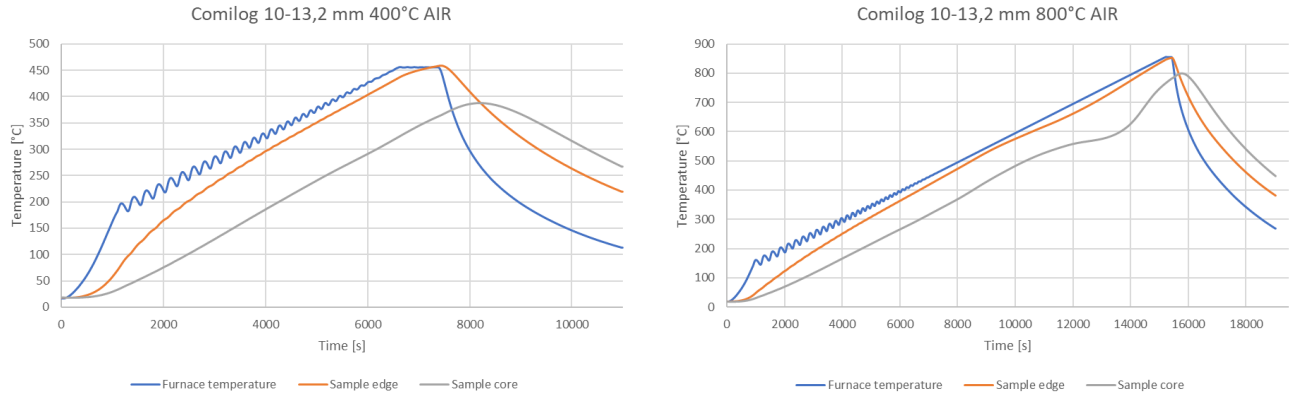

(a) **(b)**

Figure 30: Heating curves of Comilog ore, 10-13,2 mm, heated in synthetic air

The last experiments were Comilog and quartz in a mixture heated in CO/CO_2, to see if this would influence the results. As the ore is heated the temperature in the sample rises due to the exothermic reduction of manganese oxides. Figure 31 show an increase in the edge and core temperature of the sample after reaching ∼200°C, which almost reaches 500°C before returning to the furnace temperature.

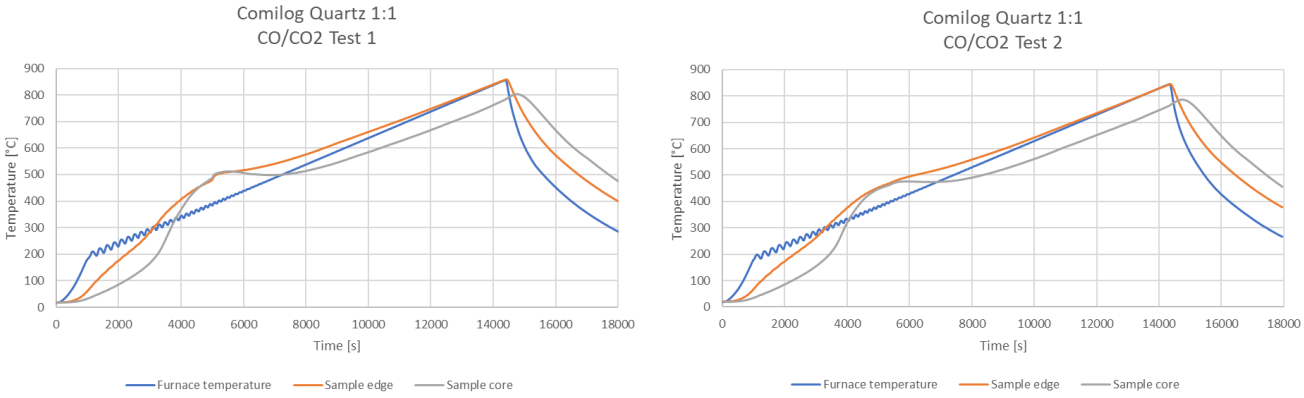

(a) **(b)**

Figure 31: Comilog heated together with quartz to help absorb the heat from the reduction of MnO_2.

4.5 SEM examination

The SEM examination was done to find if the pore structure changed during the heating of the sample. Examination of the cross section of ore lumps from all samples focused on the pores and cracks in the ore, rather than phase composition. Secondary electron imaging was selected to easily see the topography of the pores and cracks in the flat sample surface. Charging of the sample surface happened because of the insulating properties of the epoxy resin stuck in pores during sample preparation, however this did not decrease the presence of pores. These areas are the shiny patches seen in many of the figures.

4.5.1 CO/CO_2 experiments

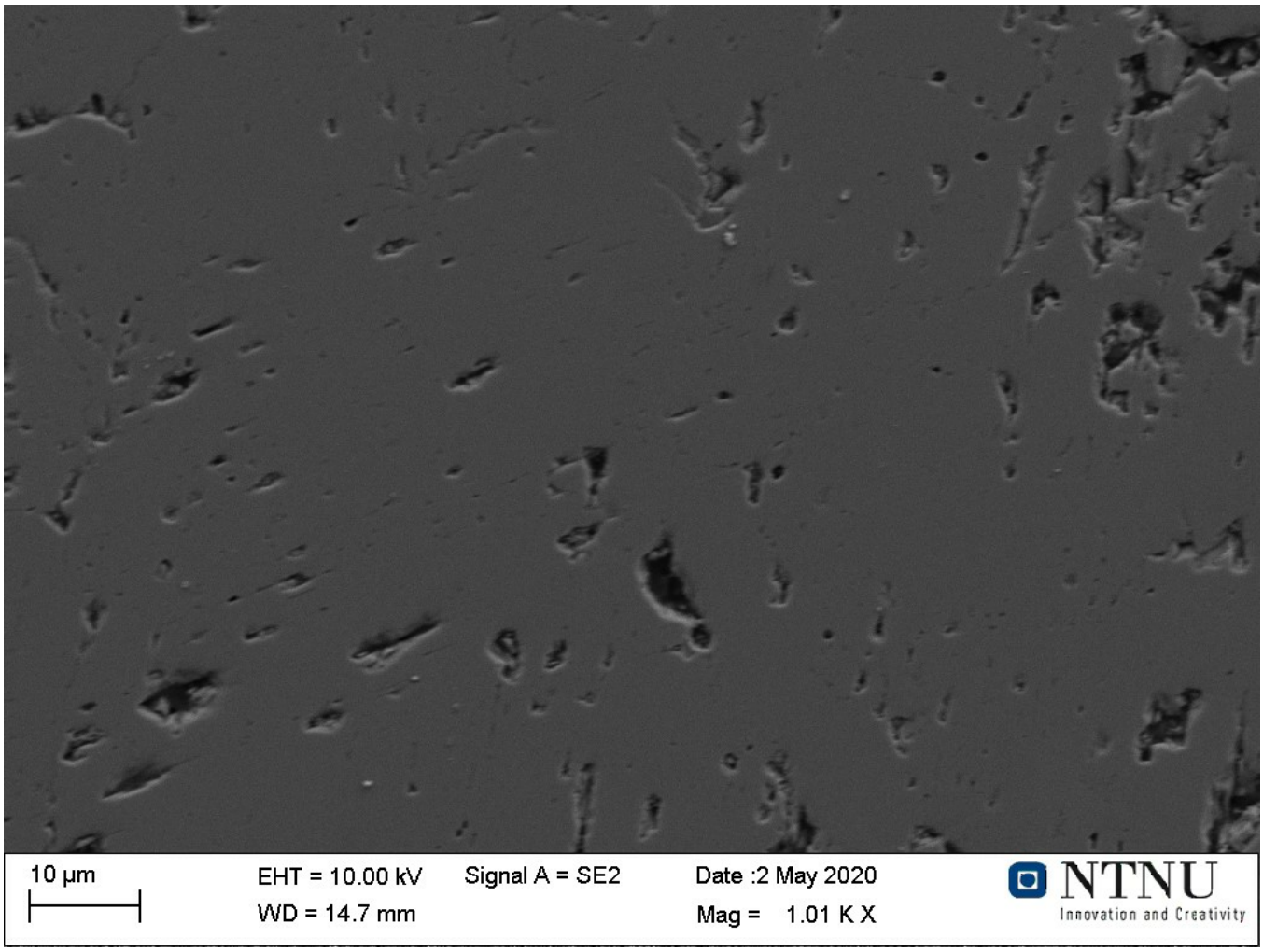

Figure 32: Cross section of raw, untreated Assmang ore

The untreated Assmang does not have a lot of large pores, as seen in figure 32. Pores visible in this figure is all smaller than 10 µm and no cracks are present.

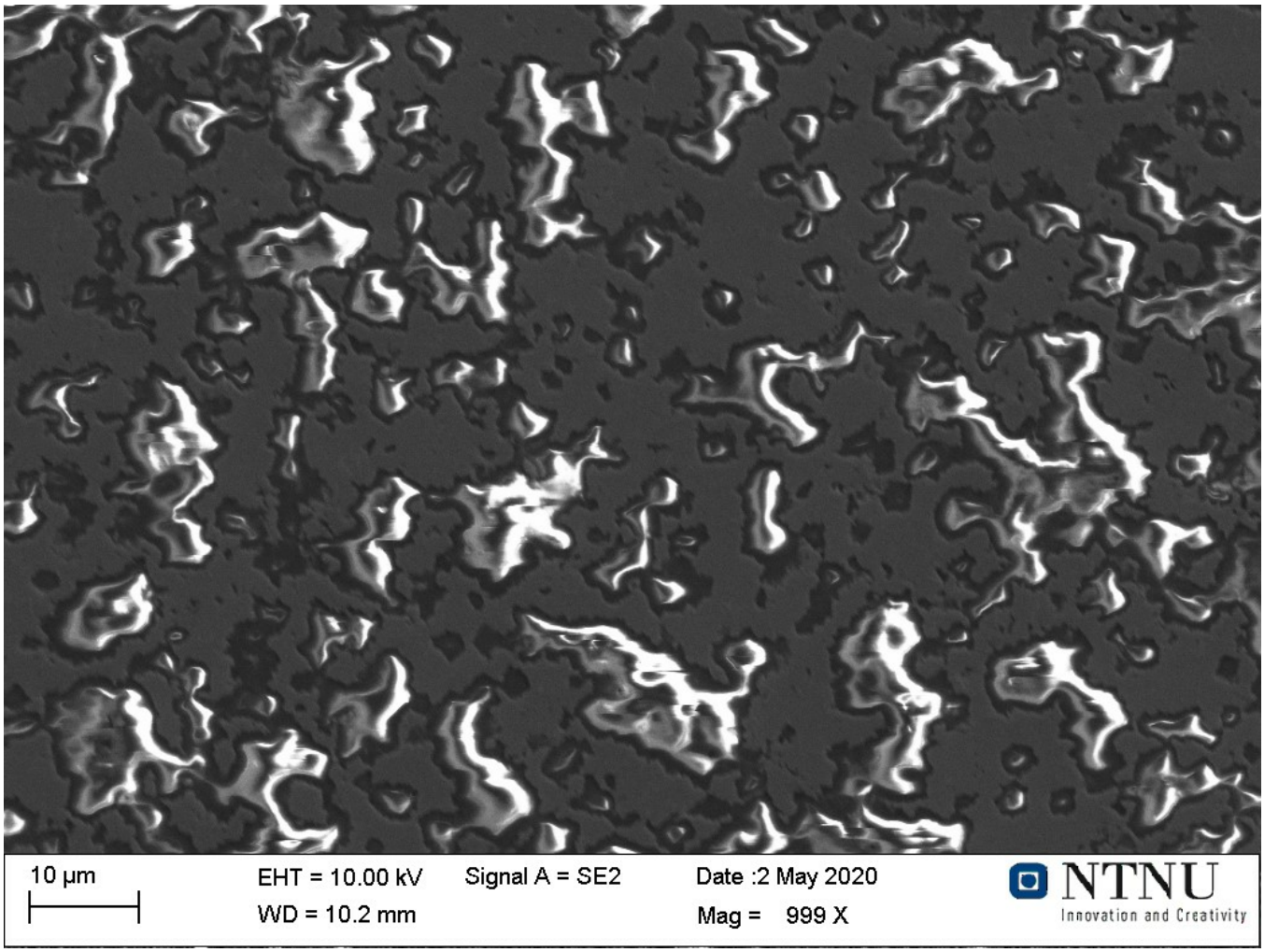

Figure 33: Cross section of Assmang ore heated in CO/CO_2 to 400°C.

Figure 33 is showing a cross section of the Assmang ore with epoxy filling many of the cavities. This results in charging of the epoxy which gives a lighter colour of the pores. Most of the pores in the sample are smaller than 10 µm, similar to figure 34 which is the same ore, only at a higher temperature.

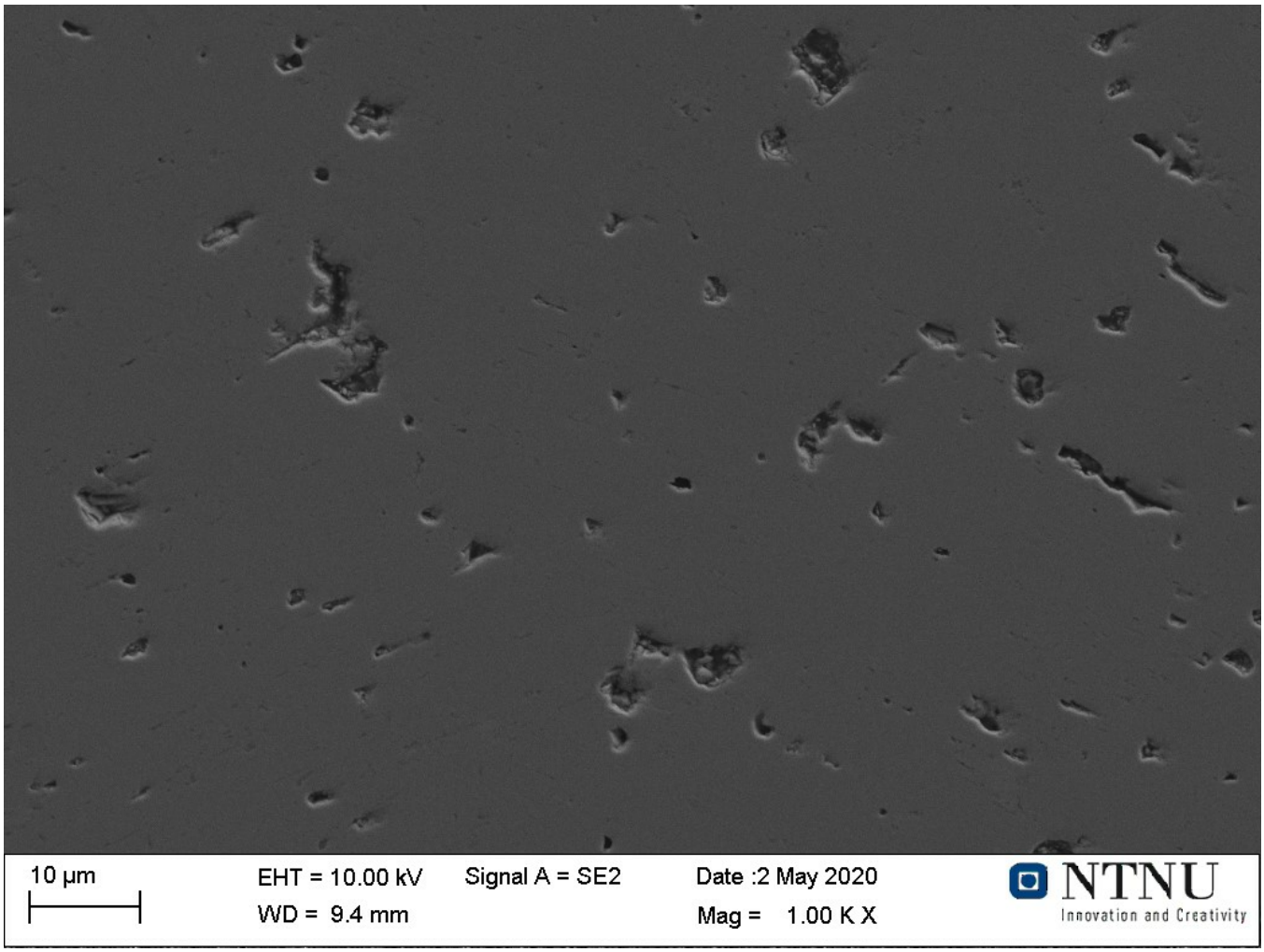

Figure 34: Cross section of Assmang ore heated in CO/CO_2 to 600°C.

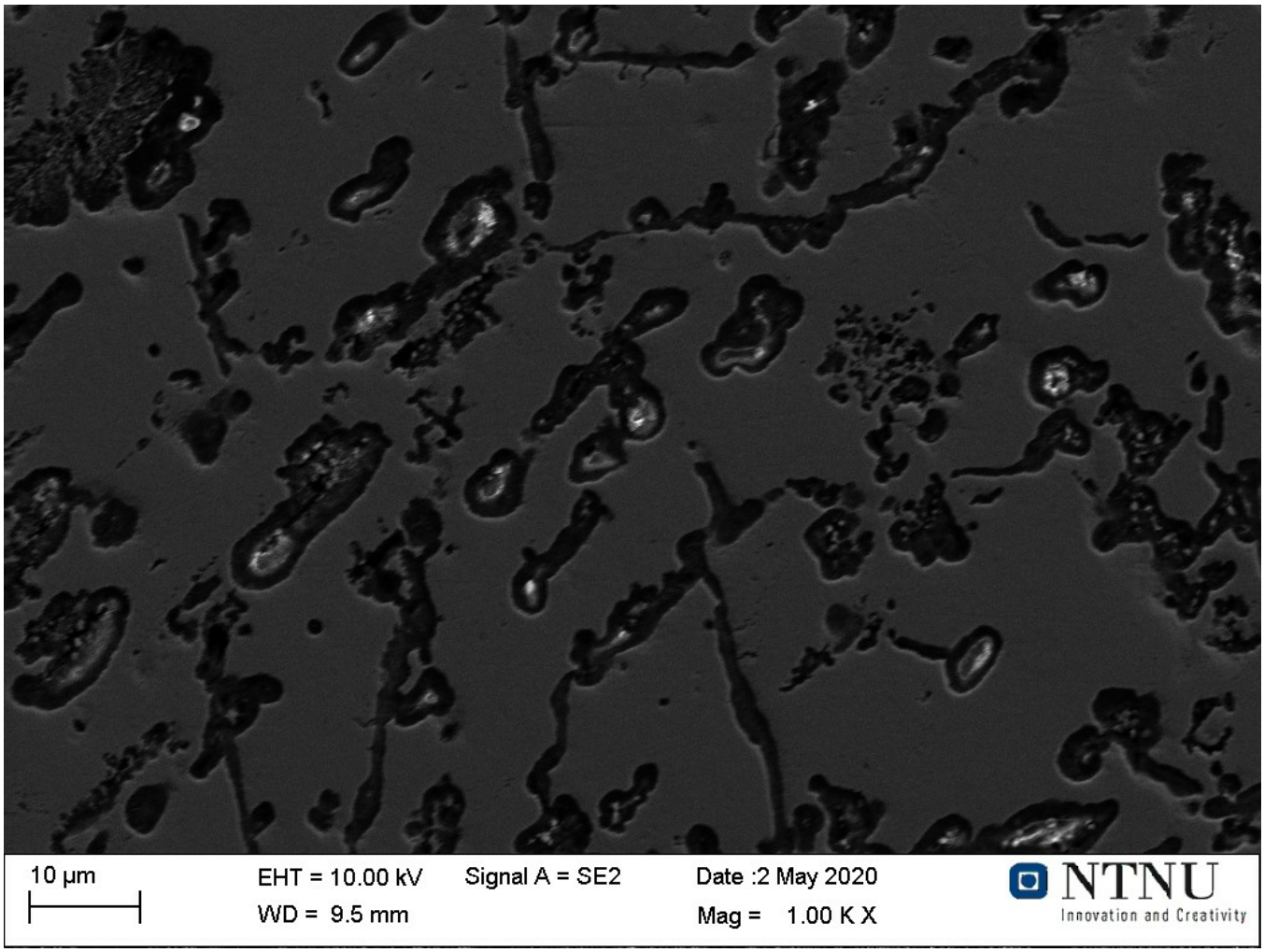

Figure 35: Cross section of Assmang ore heated in CO/CO_2 to 800°C.

Figure 35 shows the Assmang ore at 800°C, but has a slightly different structure. Most of the pores are elongated, while those which are equiaxial still remain under 10 µm in diameter. No significant cracks were found in these samples.

Comilog and UMK were heated as part of earlier project work[1], though the examination of the ores in SEM were not done at the time. These ores were examined together with the Assmang ore, spring 2020.

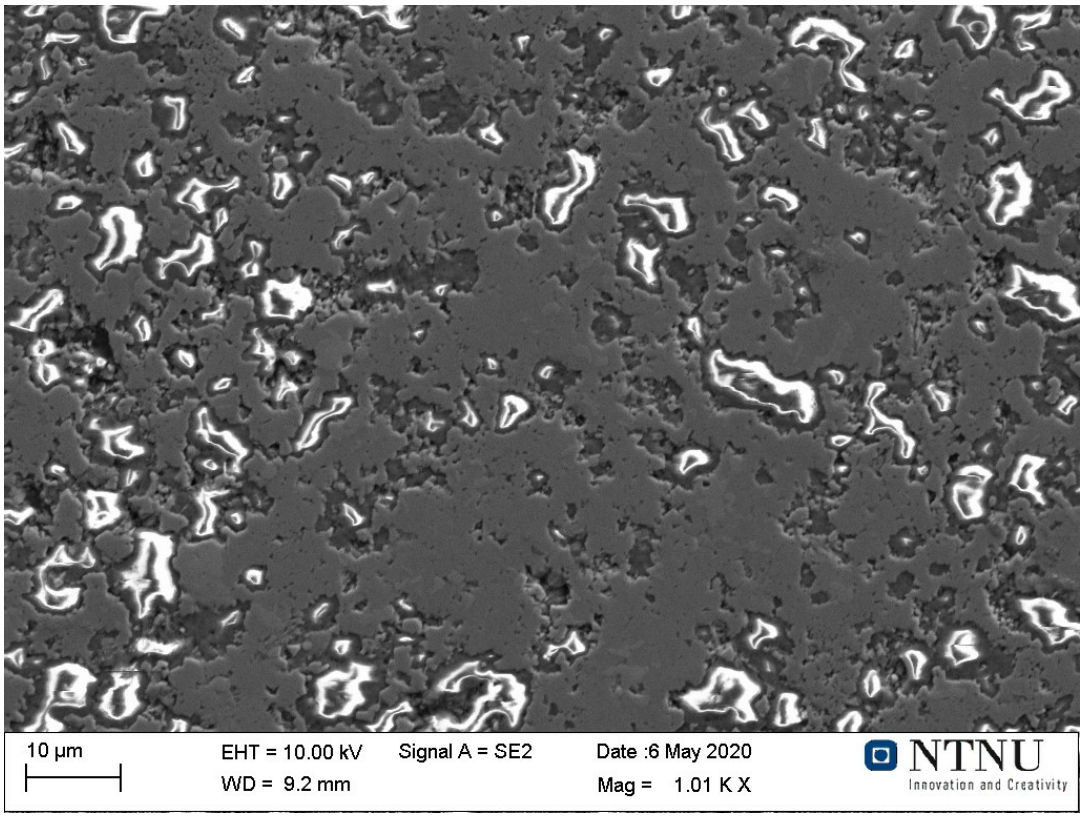

Figure 36: Cross section of UMK ore heated in CO/CO_2 to 400°C.

The lower temperature UMK show in figure 36 similar structure to the Assmang regarding pores and cracks. The pore size seems a bit smaller than 10 µm. Epoxy is caught in many of the pores similarly to the Assmang ore in figure 33.

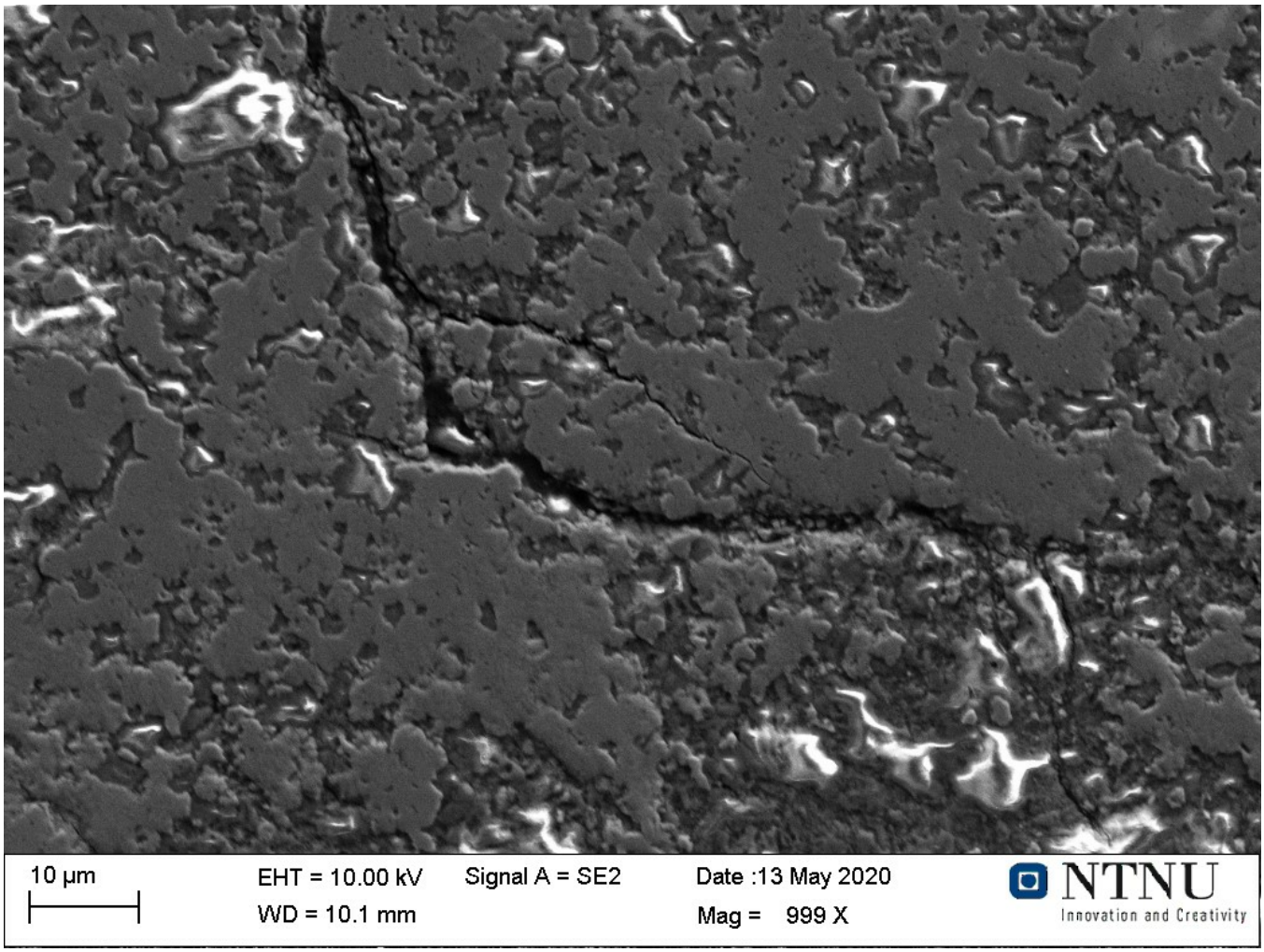

Figure 37: Cross section of UMK ore heated in CO/CO_2 to 600°C.

Figure 37 shows small pores and some cracks in the ore. The structure is similar to figure 36 showing no big change as the temperature is increased from 400°C to 600°C. The structure changes more as the temperature is increased to 800°C as seen in figure 38. This sample seems to have a rougher surface, showing many small pores as well as some cracks in figure 38b.

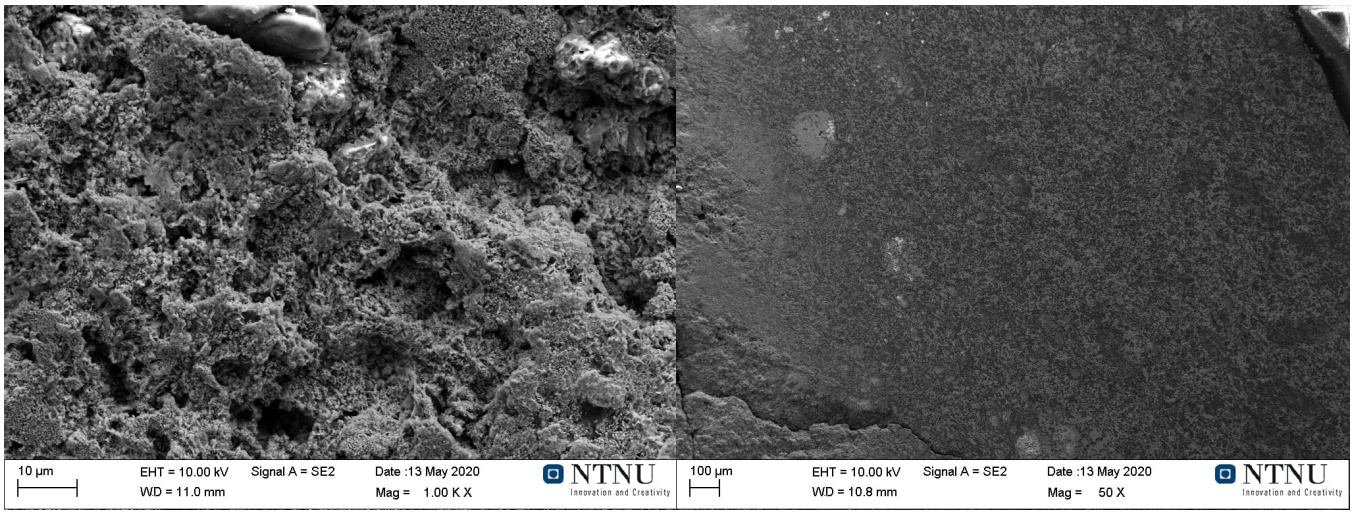

(a) **(b)**

Figure 38: UMK heated to 800°C in CO/CO_2 atmosphere. (a) is a close up image showing an irregular structure differing from the structure in the lower temperatures. (b) is a lower magnification image showing the outer to inner section of the ore lump.

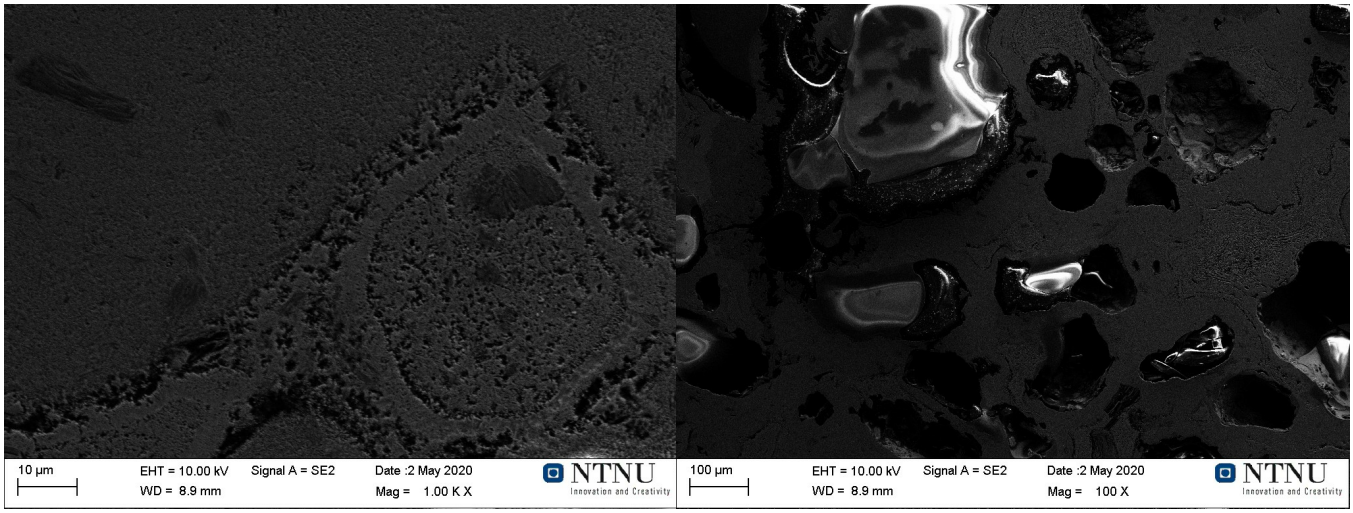

(a) **(b)**

Figure 39: Unheated Comilog ore, used in the Comilog experiments. (b) Shows the large pores in the Comilog ore at a low magnification.

Comilog ore is in theory the most porous ore and figure 39 shows the raw Comilog ore. Figure 39b is a low magnification picture showing large pores, some which are filled with epoxy due to the

sample preparation, in the the ore lumps. Smaller pores are present in the higher magnification shown in figure 39a.

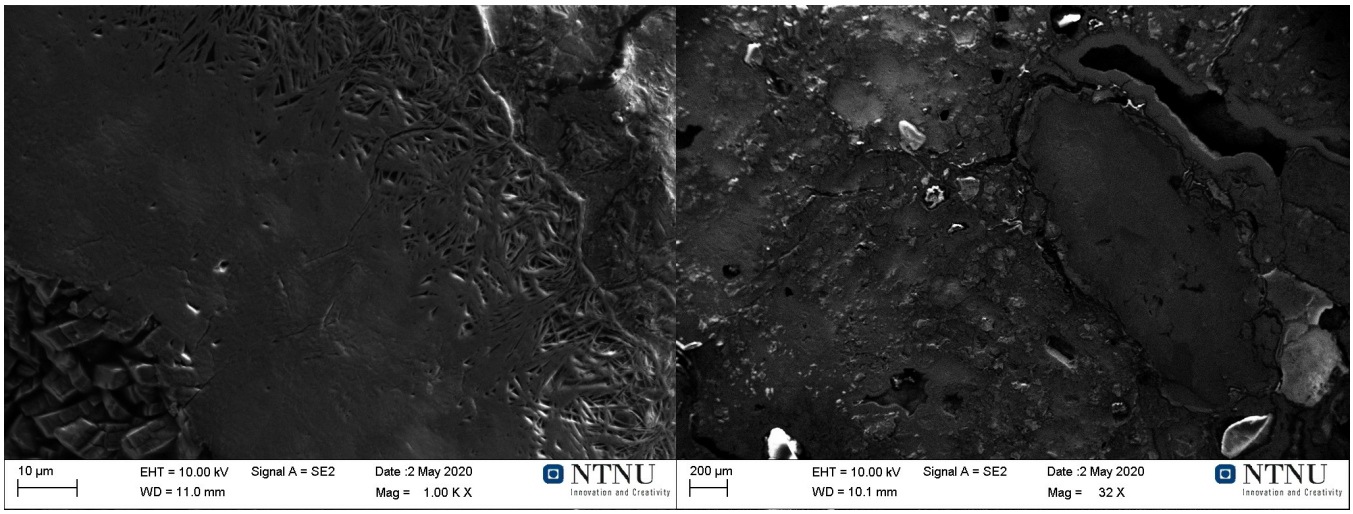

(a) **(b)**

Figure 40: Comilog heated to 400°C in CO/CO_2

Heated to 400°C the structure of the Comilog is changing, though the large pores are still present in figure 40b and a lot of smaller pores are present in the high magnification.

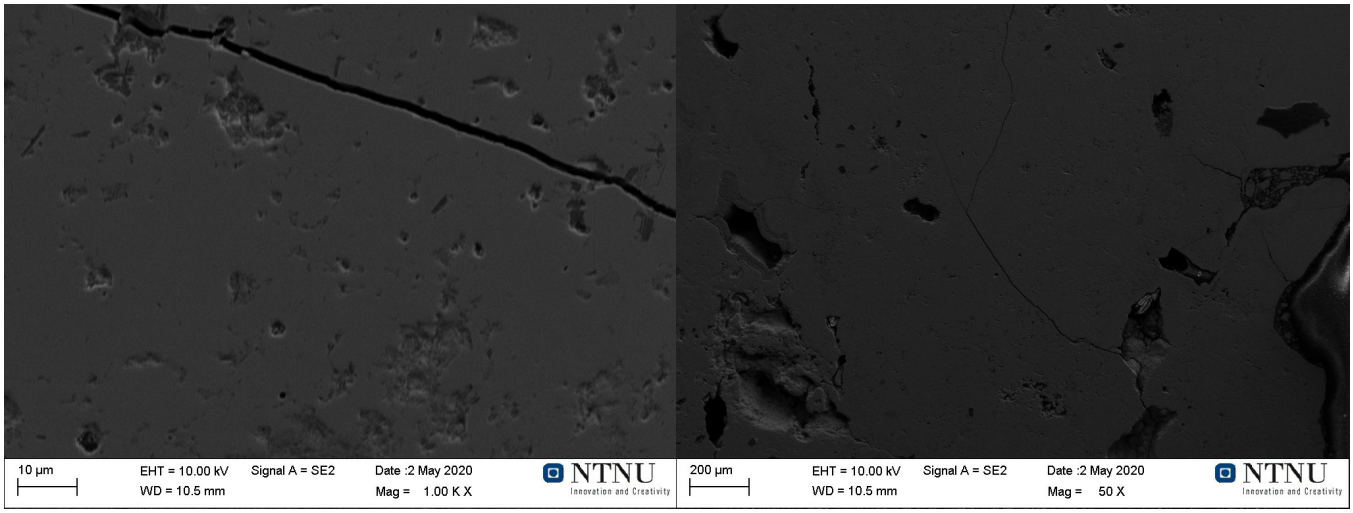

(a) **(b)**

Figure 41: Comilog heated to 600°C in CO/CO_2

Cracks are present at 600°C, shown in figure 41a, as well as the larger pores shown in figure 41b.

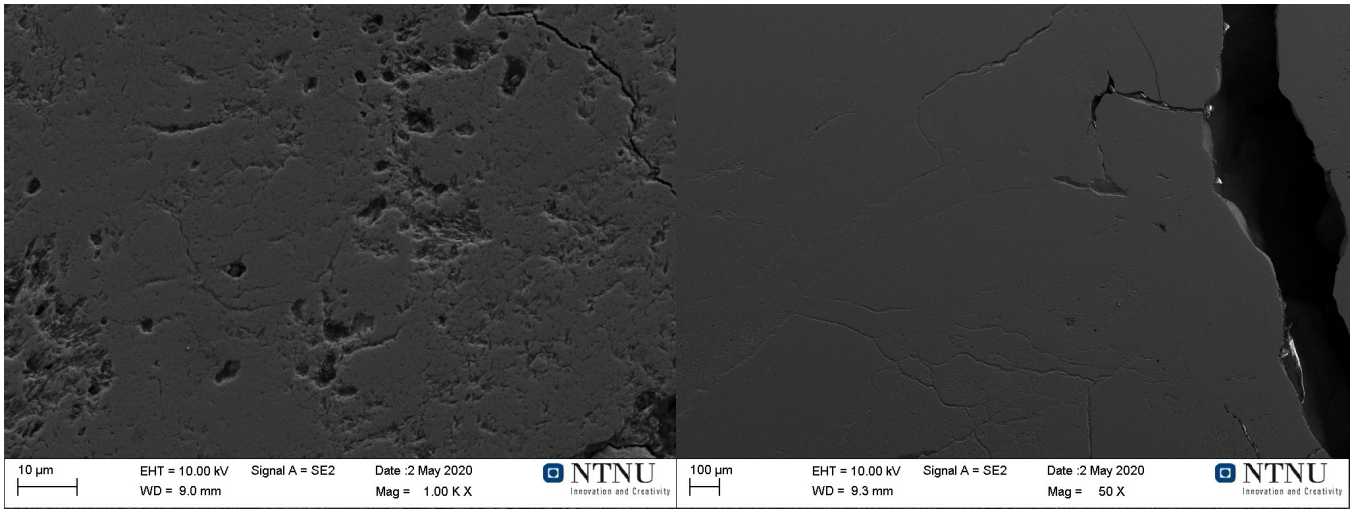

(a) **(b)**

Figure 42: Comilog heated to 800°C in CO/CO_2

Comilog ore is still porous as the temperature is increased to 800°C, and more cracks are present at higher magnification seen in figure 42a. However there is larger cracks present at lower magnification, while the smaller pores are not visible.

4.5.2 Air experiments

All the air experiments were done in the spring 2020 and was also examined using SEM with secondary electron imaging. The Assmang ore in figure 43 shows small pores and cracks present after heating to 400°C. Some pores are large enough to be present at low magnification, in an otherwise dense structure.

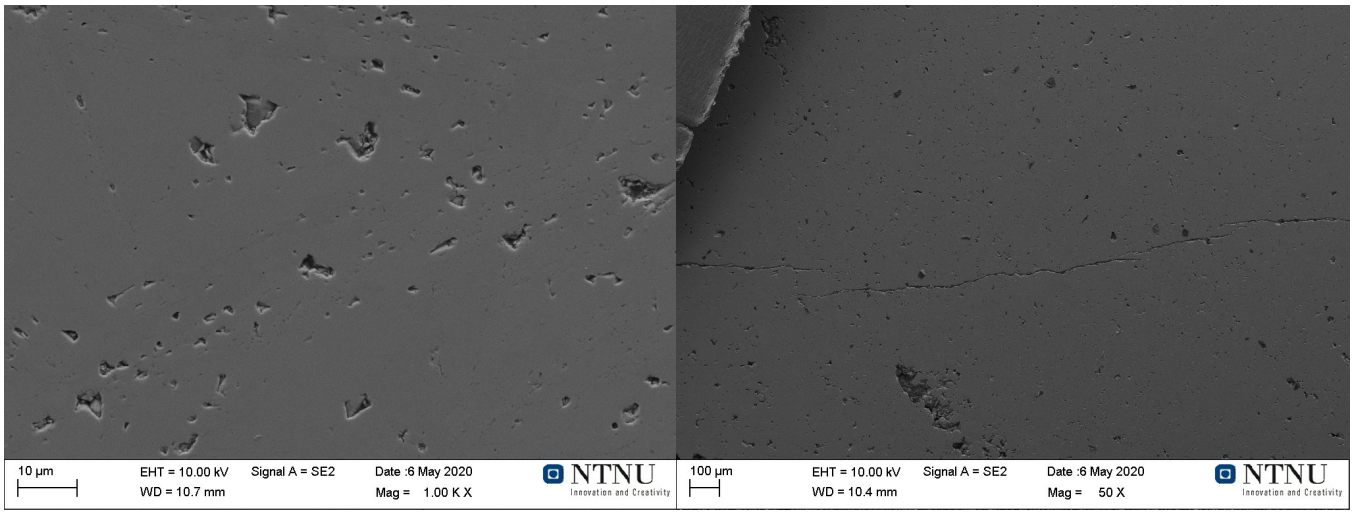

(a) **(b)**

Figure 43: Assmang ore heated to 400°C in synthetic air atmosphere.

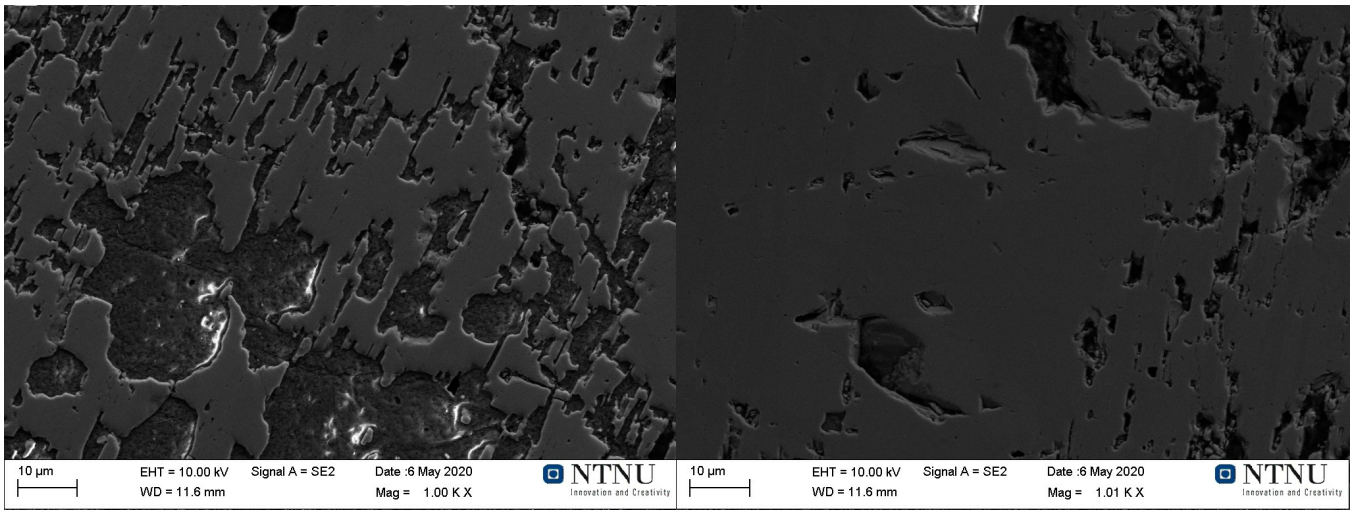

(a) **(b)**

Figure 44: Assmang heated to 600°C in synthetic air atmosphere

The amount of pores and cracks are increasing as the Assmang ore is heated to higher temperatures. Figure 44 shows two different areas of the cross section of the ore, giving a good view of the difference inside the ore lump. Some of the pores in figure 44a have a diameter of more than 30 µm.

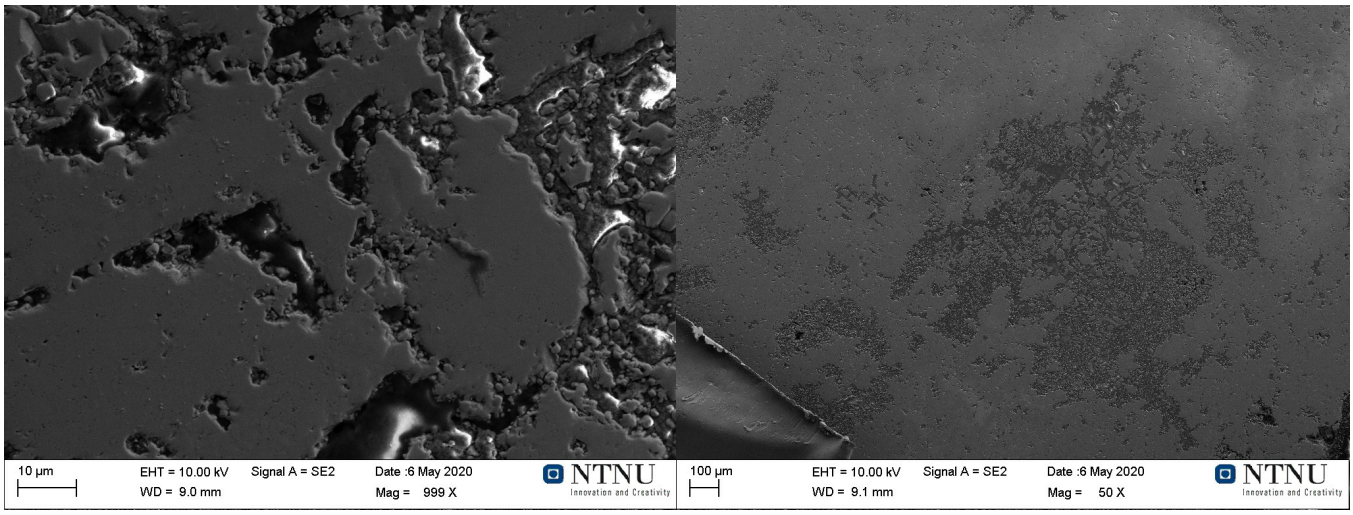

(a) **(b)**

Figure 45: Assmang heated to 800°C in synthetic air atmosphere. Some aluminium foil is present in the lower left corner of 45.

The pores increases in size as the temperature is elevated to 800°C. As seen in the low magnification picture, figure 45b, there are large areas of the cross section with different structure. Some areas have a rougher structure, while others are denser with less pores.

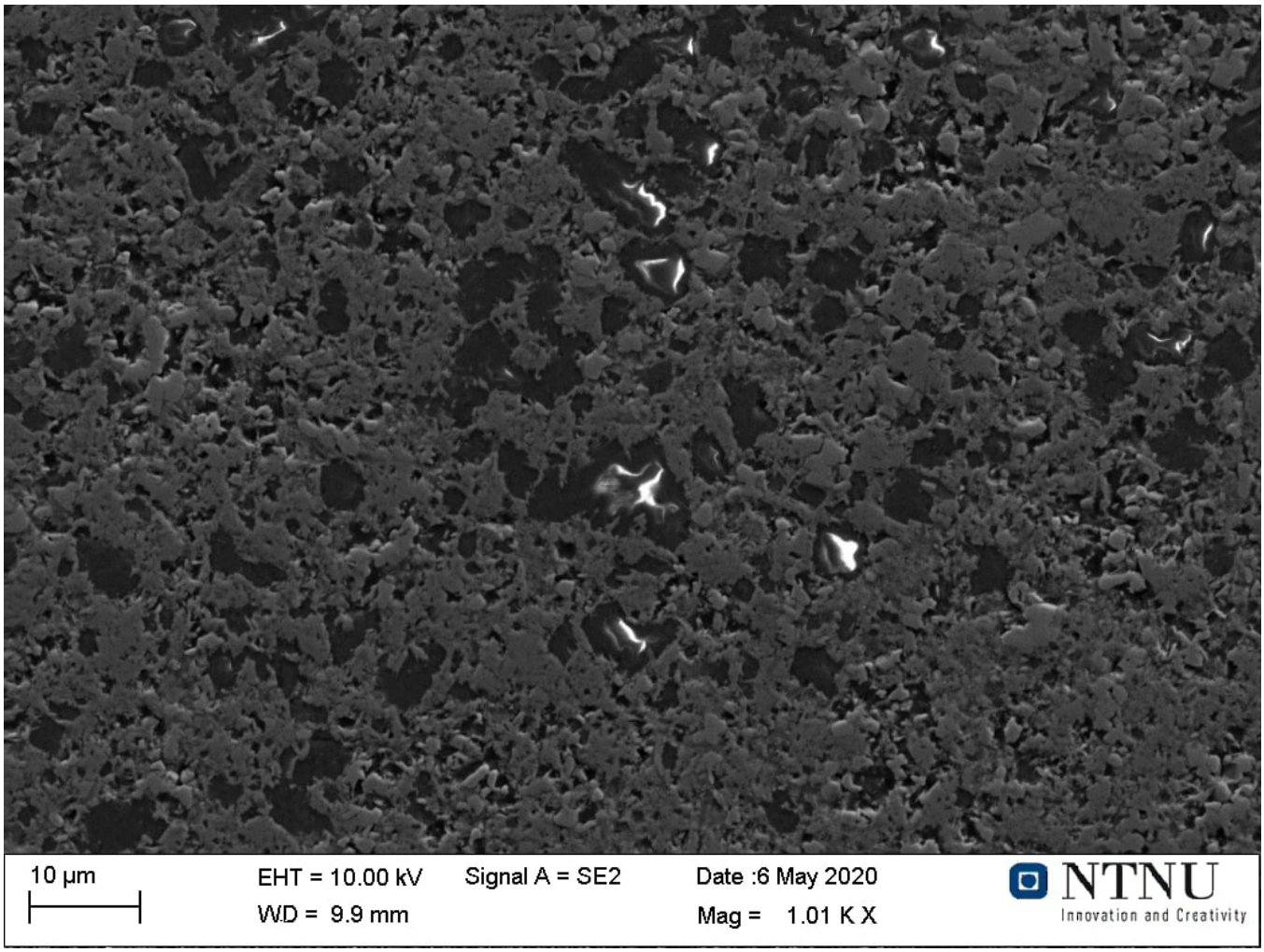

Figure 46: UMK heated to 400°in a synthetic air atmosphere

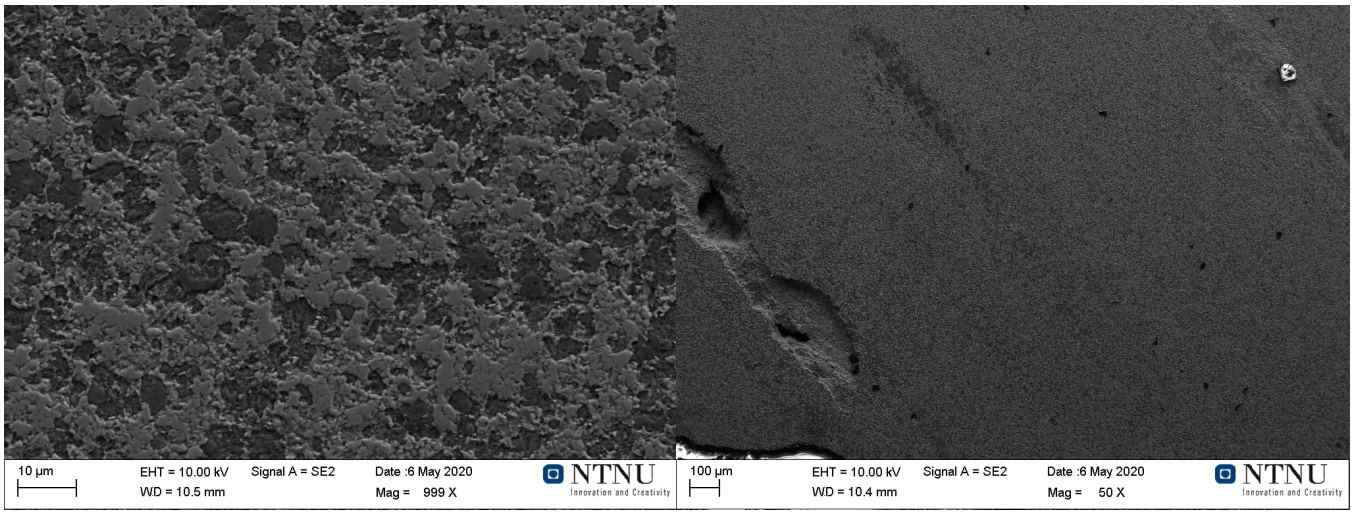

(a) **(b)**

Figure 47: UMK heated to 600°C in a synthetic air atmosphere

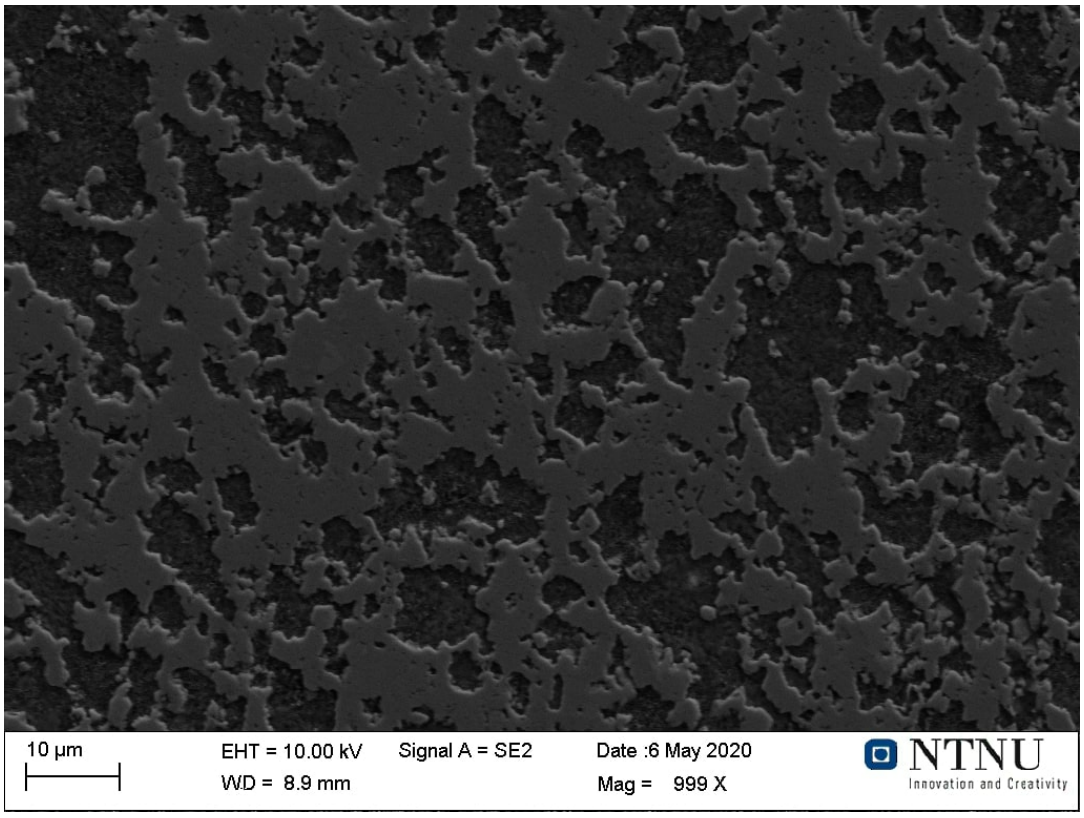

Figure 48: UMK heated to 800°C in a synthetic air atmosphere

Figures 46, 47 and 48 shows a similar structure for all temperatures of the UMK in synthetic air. Slightly larger pores are observed in the larger temperatures. Most pores are smaller than 10 µm and no cracks are visible in any of the pictures.

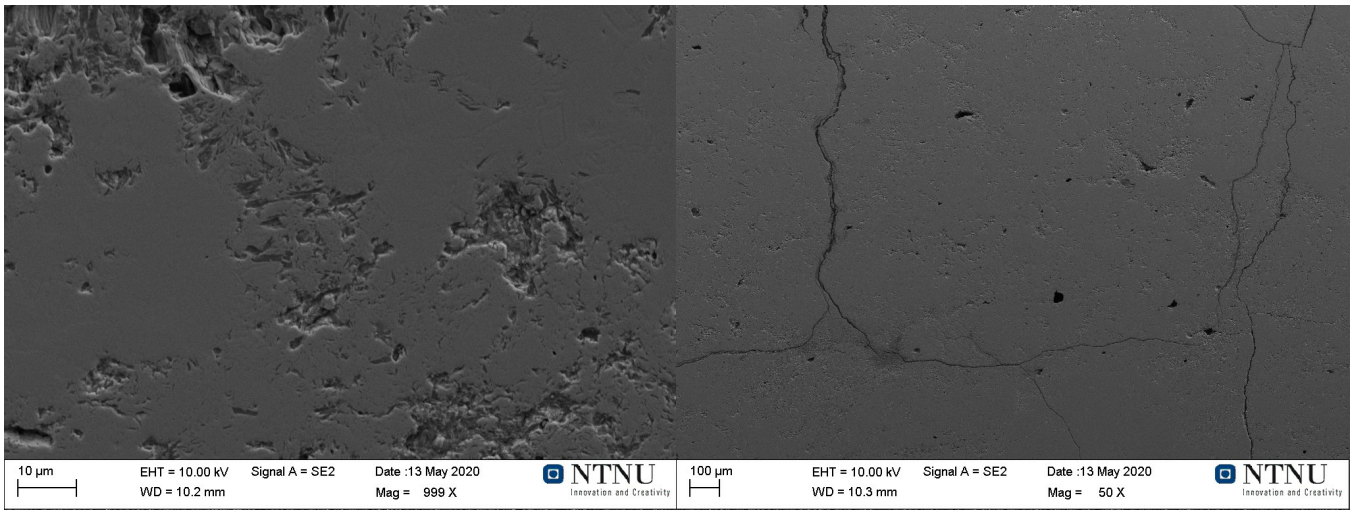

(a) **(b)**

Figure 49: Comilog ore heated to 400°C in synthetic air atmosphere

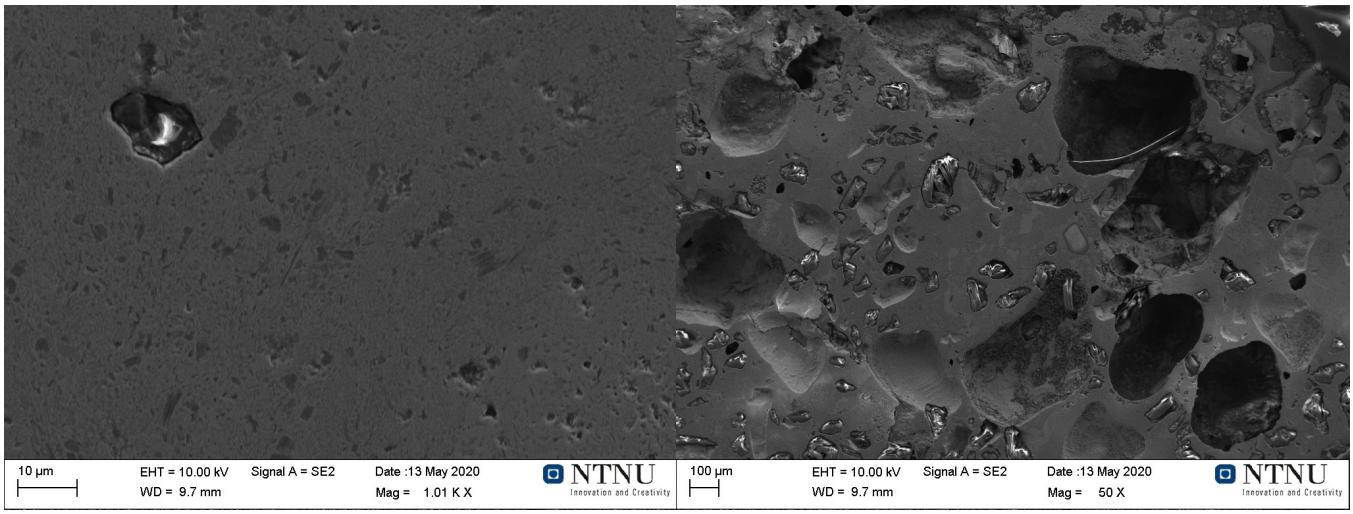

(a) **(b)**

Figure 50: Comilog ore heated to 600°C in synthetic air atmosphere

The Comilog ore heated in air also keeps its structure through the different temperatures. At low magnification the large pores are visible, while the higher magnification shows some, but not a lot of

smaller pores. Smaller than pores are mostly present at higher temperatures, while the larger pores are present at all temperatures. Figure 49b shows a part of the Comilog ore which is cracked. Figures 50 and 51 shows no significant difference at higher magnification, but has a different structure at lower magnification. This is probably just difference due to the inhomogeneity in the ores.

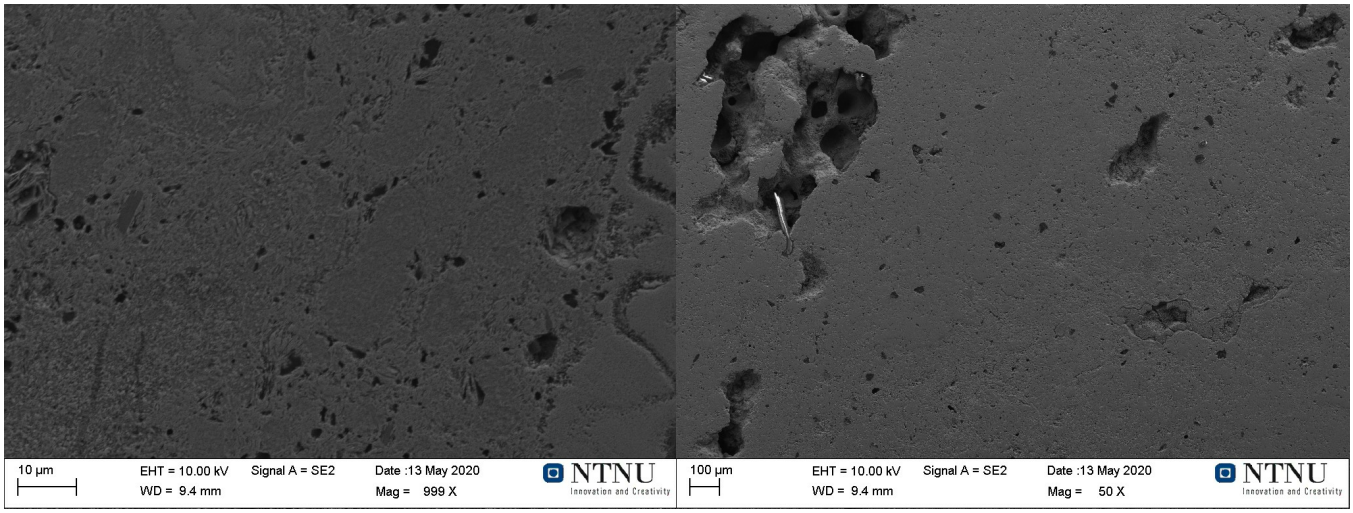

(a) **(b)**

Figure 51: Comilog ore heated to 800°C in synthetic air atmosphere

4.6 Porosity measurements

The density and porosity of the ore was measured by gas pycnometry by Sintef. The results are in table 6. Some of the measurements vary a lot, suggesting that the density of the ores vary a lot for each ore lump.

Table 6: Measured densities and porosity of the ore samples heated in CO/CO_2. Some of the measurements had large deviation in value, so both values are visible in the table

	Absolute density	**Apparent density**	**Porosity**
Assmang raw	4,21	4,21	0,1
Assmang 400°C	4,33	4,33	0,1
Assmang 800°C	4,47	3,96	21,8/1
UMK raw	3,7	3,345	16,4/2,6
UMK 400°C	3,45	3,445	0,25
UMK 800°C	3,25	3,02	5,15
Comilog raw	4,56	4,185	3,6/12,9
Comilog 400°C	4,61	2,675	30,4/53,6
Comilog 800°C	5	3,155	36,95

The Comilog ore is the most porous ore when heated. Both the samples tested have similar porosity regardless of temperature. The Assmang and UMK have similar porosity, though the Assmang seems to be a little bit denser. Assmang increases in porosity as the temperature is increased, while it is difficult to see a trend for UMK and Comilig due to the large deviations of the measurements. The most porous ore is Comilog with up to 53,6% at higher temperature.

4.7 Weight loss

The weight of the ore was measured before and after the heating program. In table 7 is the measured weight loss after heating of the ores.

Table 7: The measured weight loss for Assmang in CO/CO_2 and all the ores in air.

	WL (g)
Comilog 10-13,2 mm 800°C AIR	243,39
Comilog 10-13,2 mm 600°C AIR	197,41
Comilog 10-13,2 mm 400°C AIR	96,93
UMK 10-13,2 mm 800°C AIR	269,18
UMK 10-13,2 mm 600°C AIR	85,65
UMK 10-13,2 mm 400°C AIR	42,14
Assmang 10-13,2 mm 800°C AIR	68,3
Assmang 10-13,2 mm 600°C AIR	31,64
Assmang 10-13,2 mm 400°C AIR	2,77
Assmang 10-13,2 mm 800°C CO/CO_2	217,39
Assmang 10-13,2 mm 600°C CO/CO_2	84,62
Assmang 10-13,2 mm 400°C CO/CO_2	22,01

The theoretical weight loss was calculated to 389,84 g for UMK, 309,25 g for Comilog and 212,89 g for Assmang.

5 Discussion

The degree of prereduction was calculated from the chemical analysis done by Sintef Norlab and the TI3,35 from the size fractions of the ore using the procedure described in section 3.3.2. The summary of the results are shown in figure 17 and 18. Here the results from the MSc will be compared to the results obtained in the specialisation project and shown i figure 52. From this is was found that Assmang heated in CO/CO_2 decrepitates less than Comilog and more than the UMK ore. The smallest size fraction ore (3,35-6,7 mm) is reduced faster than the larger size fraction (10-13,2 mm) as the smallest ore reaches a lower MnOx value at lower temperatures, which was common for all the ores. This can be seen in figure 52 and is most likely due to that a smaller diameter means the reaction interface reaches the core of the lump, according to the shrinking core model[4]. The entire ore lump will have reacted at an earlier point due to the smaller diameter as the reaction interface moves towards the centre of the lump. However, both Assmang ore size intervals is fully reduced to MnO at 800°C, meaning that the time and temperature was enough for the reduction to be completed.

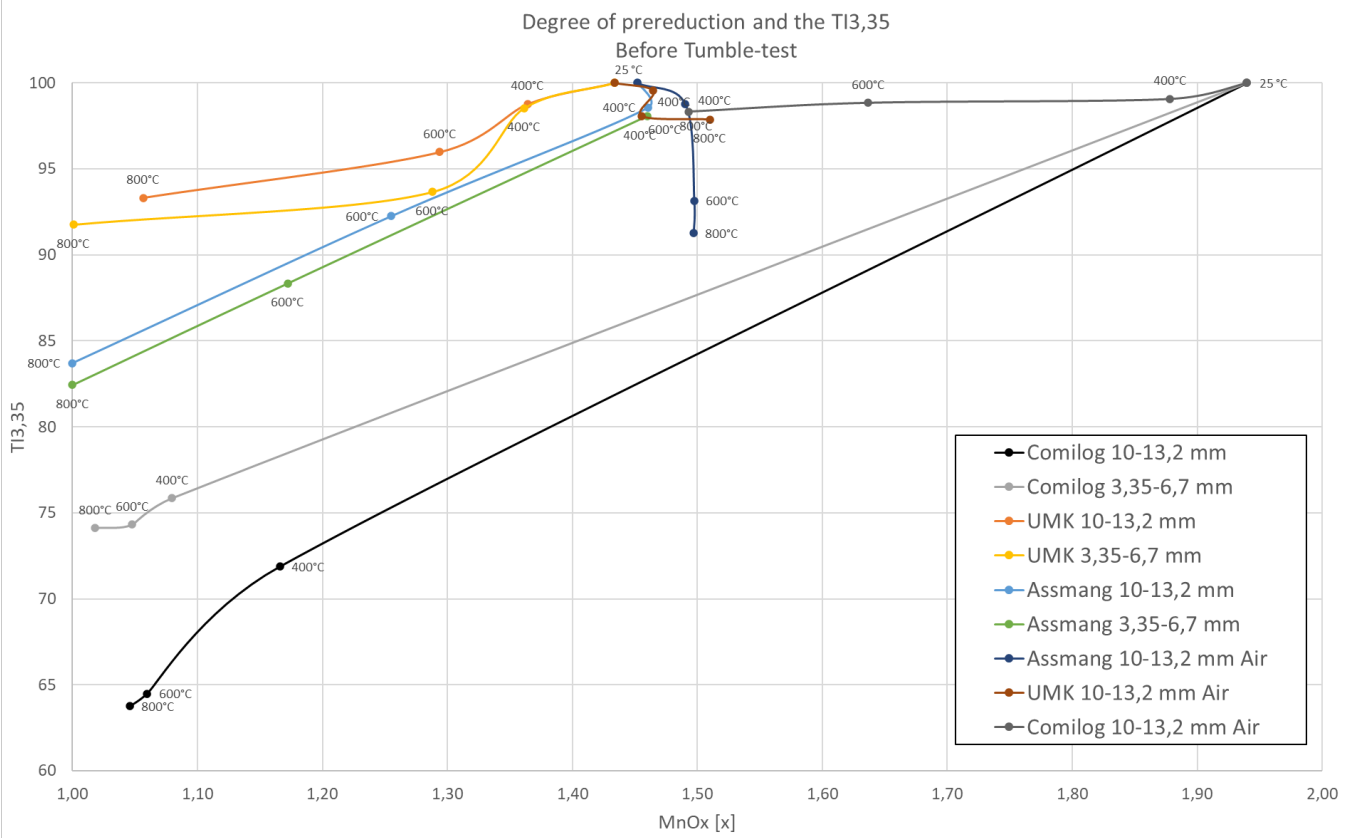

Figure 52: The degree of prereduction for the ore heated in plotted against the TI3,35 value of the ore before tumble-testing [1].

Additionally the TI3,35 is similar for both Assmang size fractions at 800°C showing that the decrepitation is not significantly larger in either size fraction. The Assmang ore has larger decrepitation than UMK, but less than Comilog. It is reduced faster than UMK at lower temperatures, while being slower than Comilog ore.

Decrepitation of air heated samples were less than the CO/CO_2 heated samples. All of the ores have a TI3,35 above 90% as seen in figure 52 and the figures in section 4.2, suggesting that the transformation of higher manganese oxides to MnO heavily influences the decrepitation. Based on these re sults it seems like UMK is the strongest ore when heated in both cases, as the Assmang ore decrepitates the most in air and Comilog decrepitates the most in CO/CO_2.

It is clear that pre-reducing manganese ores in air atmosphere is possible, though the ore will not be reduced lower than to Mn_2O_3 at the tested temperatures as suggested by Sorensen et al.[10].This will increase the oxygen content in UMK and Assmang ore based on their chemical composition. Comilog ore starts at mostly MnO_2 and will be reduced to Mn_2O_3 when heated to 800°C. The MnOx value of Comilog is at this point about the same as Assmang and UMK. The increase in oxygen is seen in figure 52 as the MnOx value of the two ores is increasing with temperature, stopping at about x = 1,5 as expected from the stability diagram (figure 2).

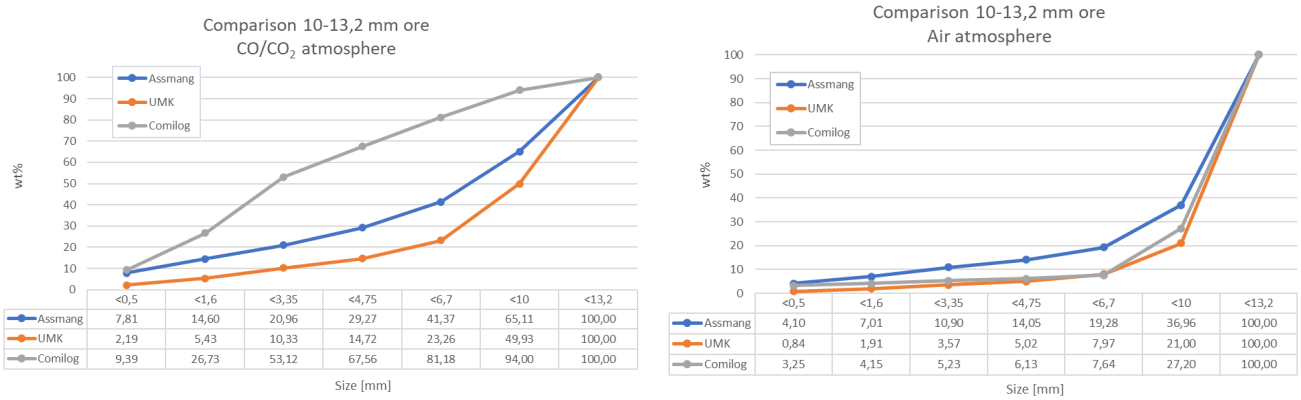

(a) **(b)**

Figure 53: The cumulative size distribution of the different ores in air and CO/CO_2. Comparison of the samples heated to 800°C. This does also include results from the Specialisation project [1].

Figure 53 show a comparison of the size distribution of the ores after tumble-testing for both gas mixtures. The Assmang ore curve has a similar shape as the UMK ore compared to the Comilog ore curve when heated in CO/CO_2. Unlike the Comilog, Assmang keeps ~35% of the ore in the initial size interval, which is slightly lower than UMK and higher than the Comilog ore. It is different in air where Assmang decrepitates the most of the three ores. The difference is not large as seen in figure 53b, as the Comilog and UMK ores both have a similar size distribution in this case.

Based on this it seems that the reduction of the higher manganese oxides to MnO heavily increases the decrepitation. There is significant differences in the size distribution for all three ores in CO/CO_2 and the air heated samples. The only ore which is reduced in air is the Comilog ore, and while the ore is reduced from mostly MnO_2 to Mn_2O_3 it does not decrepitate much. The ore is reduced further in CO/CO_2 and the decrepitation is significantly larger suggesting that the increase in decrepitation across all ores is due to the reduction reactions. The large temperature peak present in heating of Comilog ore in CO/CO_2 is not present in air and this rapid heating may increase the decrepitation further because of thermal shock. This peak is due to the reduction reactions of MnO_2 (eq.5), Mn_2O_3 (eq. 6) and Mn_3O_4 (eq. 7). All of these reactions are exothermic and will contribute to the heating of the ore sample. The difference between Comilog heated in air and CO/CO_2 suggests that the reduction reaction is a major influence on the ores resistance to decrepitation. These differences are less prominent in Assmang and UMK ore, but there is still an increase in the decrepitation for all ores.

The porosity should increase as the temperature and reduction increases according to Turkova et al. (2014). If an ore had an initial high porosity, then the heated ore would also have a higher porosity. The porosity measurements of the Comilog, UMK and Assmang ore shows that Comilog ore has the highest porosity, seen in table 1 as well as in the SEM pictures. Some of the measurements had a large deviation in porosity, which could be due to the inhomogeneity of the ore lumps. It should be noted that only two ore lumps were measured for each temperature and ore, so the results of the measurements only serve to indicate the general trend.

The difference between Comilog and the other ores is clear at the low magnification SEM picture where the largest pores are present. Most of the pores in UMK and Assmang are smaller and only seen in the 1000x magnification pictures. These small pores are also present in Comilog in addition to the large pores which is backed up by the porosity measurements, showing the difference in porosity despite the large deviation in some of the measurements.

This is also reflected in the pressure force tests where the Comilog ore crumbles on average on a significantly lower pressure force as seen in section 4.3. This is probably due to the increased porosity, which would give a lower strength[29].

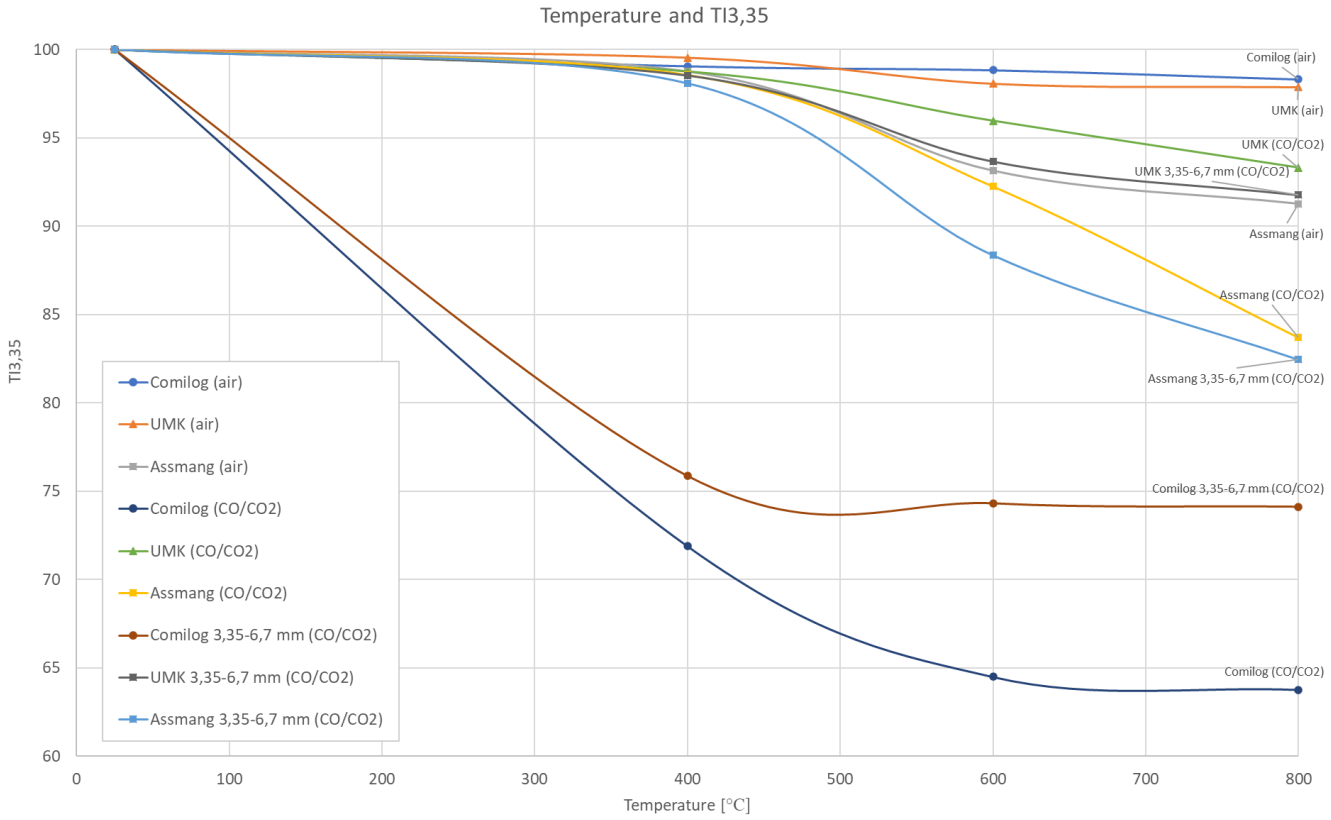

Figure 54: All TI3,35 before tumble testing at all temperatures for all the ores examined[1].

Figure 54 shows a comparison of the TI3,35 values of all the ores at the different temperatures. Overall the UMK is the strongest at higher temperatures and both of the gas mixtures. Only Comilog in air has less decrepitation at higher temperatures, while the Assmang in CO/CO_2 follows the same trend as other ores having the most decrepitation overall. It is still less than Comilog in CO/CO_2 which decrepitates much more than the other ores. It seems like the reduction past x = 1,5 (Mn_2O_3) is responsible for most of the decrepitation for all the ore. The difference i particularly visible for the Comilog ore.

It is clear that it is impossible to reduce any of the ores below x = 1,5 in air at the temperatures used in these experiments. The decomposition of Mn_2O_3 to Mn_3O_4 will only happen after 1000°C according to Zaki et al.[12]. All of the ores stops reacting at x = 1,5 at 800°C. The UMK and Assmang ores are oxidised as they start with a MnOx value of 1,43 and 1,45 respectively. The Comilog is decomposed due to its MnOx value of 1,94. Both Assmang and UMK follow a similar route considering their original starting value, though UMK shows a slightly larger increase in the oxygen content when going from 600°C to 800°C, ending at a slightly higher x value than the two

other ores.

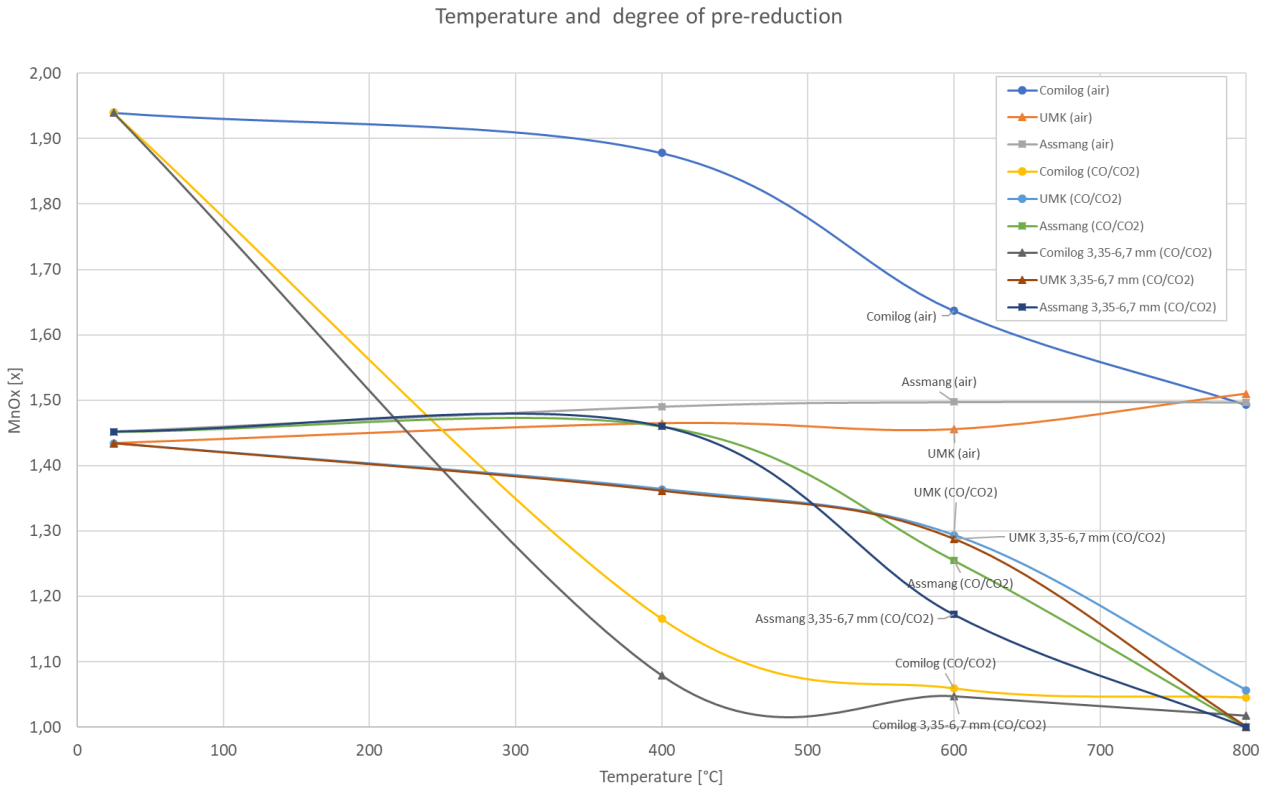

Figure 55: The degree of prereduction for all experiments plotted against the temperatures used.[1].

Comilog is still fastest to reduce after having tested Assmang ore in CO/CO_2. UMK and Assmang has a similar route, though UMK is more reduced at 400°C while the Assmang is more reduced than UMK at 600°C as seen in figure 55. Both ores end at approximately the same point, at $x \approx 1$.

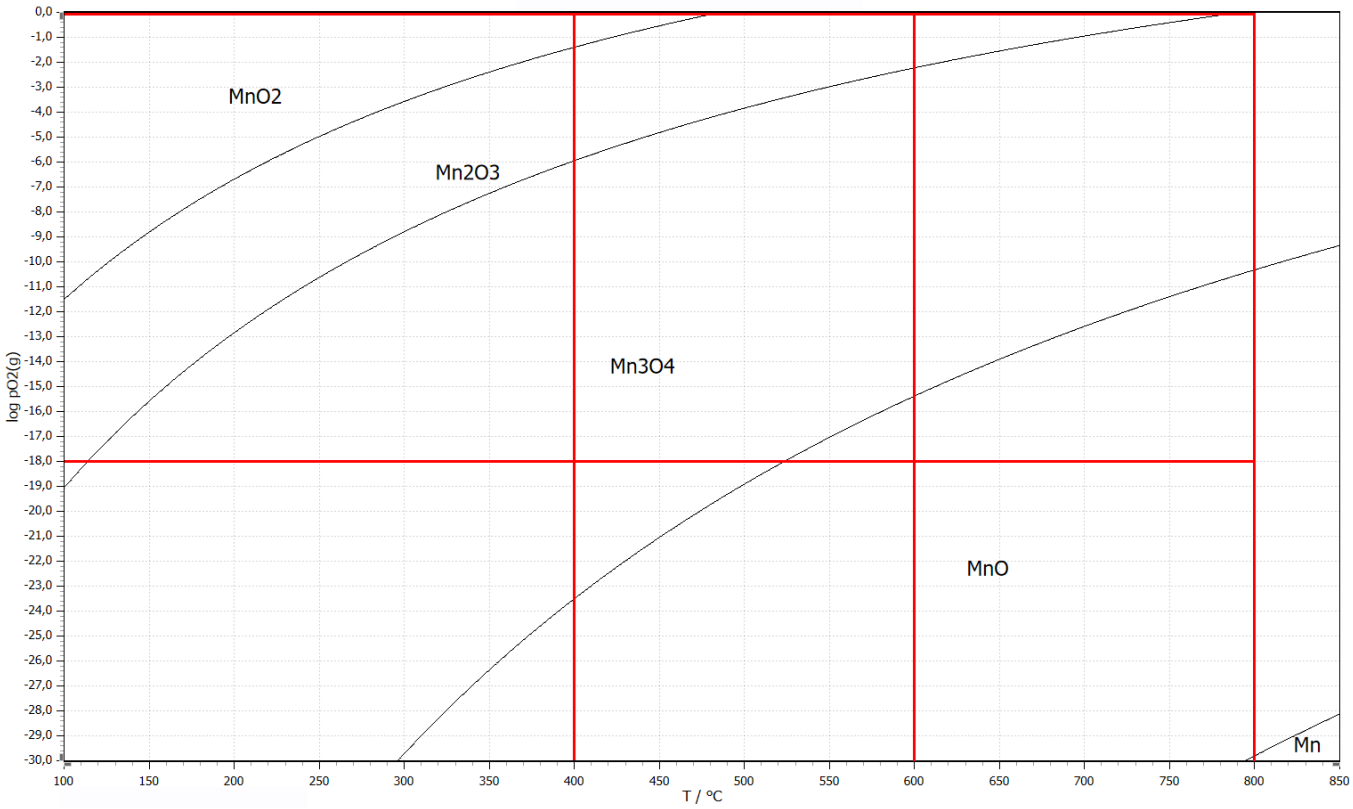

Figure 56: Stability of manganese oxides diagram, made in HSC 9. The red lines represents the temperatures which were used in the experiments. Partial pressure of oxygen was calculated using equilibrium constant at 800°C, found in HSC 9.

Comparing figure 56 with the calculated MnOx values shows that in CO/CO_2 the most likely oxide is MnO or Mn_3O_4 above 400°C. Following the bottom red line in figure 56 shows that Mn_3O_4 should dominate at 400°C, while MnO should be present at 600°C and 800°C in the CO/CO_2 experiments. The MnOx values tells that higher manganese oxides are still present at all of these temperatures. This is due to kinetics and the time needed for all the manganese oxides to react. At 600°C more of the oxides are reduced to MnO and at 800°C almost all the manganese in the ore is present as MnO.

Mn_2O_3 is the dominating manganese oxide in the ores heated in synthetic air. Both Assmang and UMK starts at MnOx $\approx$ 1,5 and remain around the same value up at up to 800°C. The only ore showing a large change in the oxygen content is Comilog starting at MnO_2. Comilog goes from x = 1,94 to x $\approx$ 1,5 at 800°C, which what one should expect according to the stability diagram. Mn_3O_4 is the stable manganese oxide at 800°C, but the intersection of the red lines at that temperature is so close to the border to Mn_2O_3 so most of the manganese oxides will not have reached equilibrium

at that time.

Lastly, two samples of Comilog was mixed with quartz to see if this would influence the decrepitation when heated in CO/CO_2. Figure 57 is a comparison of the heating curves from the Comilog in CO/CO_2 done in the Specialisation project and the Comilog/quartz in CO/CO_2. There is a large difference in the peak temperature during the heating, 850°C without and 450°C with. The increase from the sample temperature is lessened from ~600°C to ~200°C. This is partly due to that the Comilog/quartz experiments had less Comilog ore, 1 kg, while the other experiments was 2 kg Comilog ore. Thus less heat could the produced due to less material reacting. The rest of the temperature reduction is due to quartz absorbing heat from the reduction reactions of manganese oxides. The peaks happen at the same point in the heating program and seems to last the same time despite their difference in height.

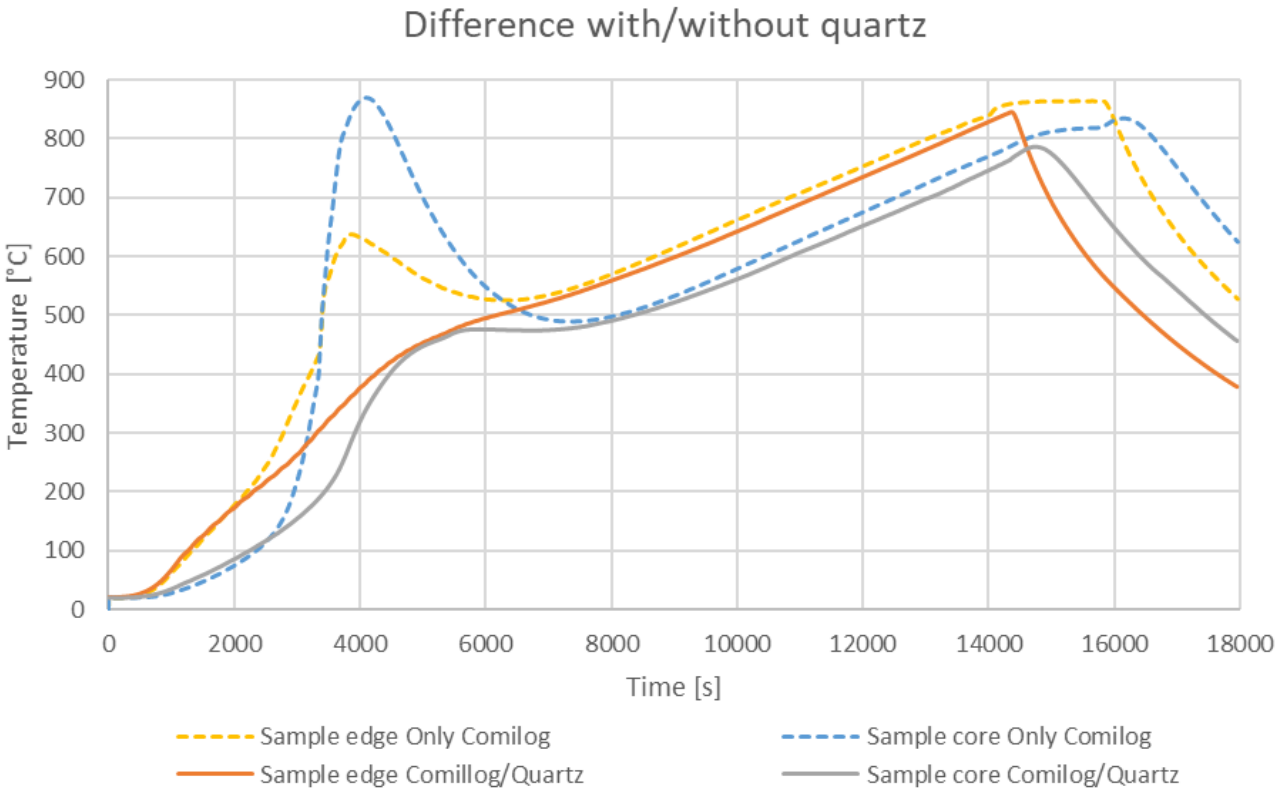

Figure 57: Difference between 2kg Comilog[1] and a mixture of 1kg Comilog and quartz.

The ore was separated from the quartz before the tumble testing so not to increase the decrepitation as the quartz is harder than the heated manganese ore. A comparison of the ore heated with and without quartz is shown in figure 58.

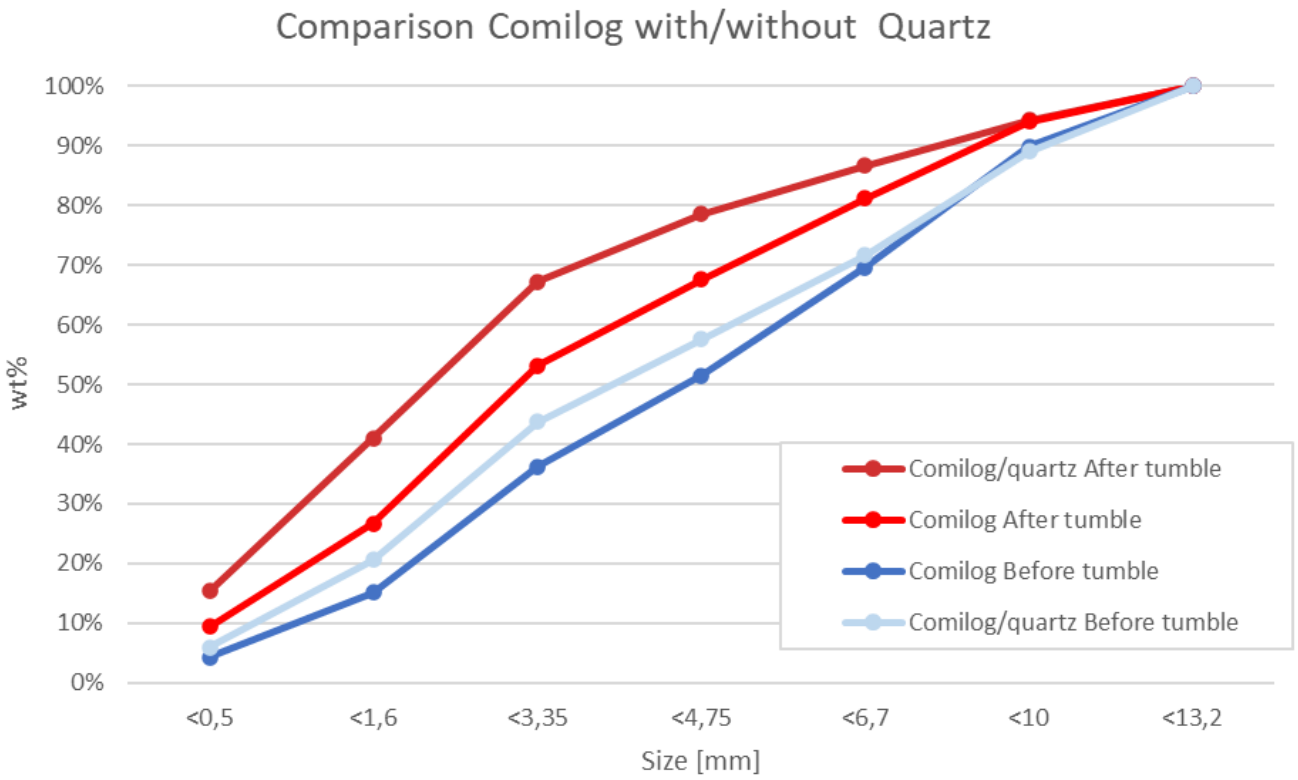

Figure 58: Comilog in CO/CO_2 with and without quartz, before and after tumble testing[1]

The ore that was heated with quartz has a larger decrepitation than the ore heated without. At most it has a ≈10% increase in the ore below 3,35 mm size after tumble-testing. The ore heated with quartz is reduced to the same degree as the other Comilog ore at the same temperature, suggesting that the reduction of manganese oxides are the main reason for decrepitation.

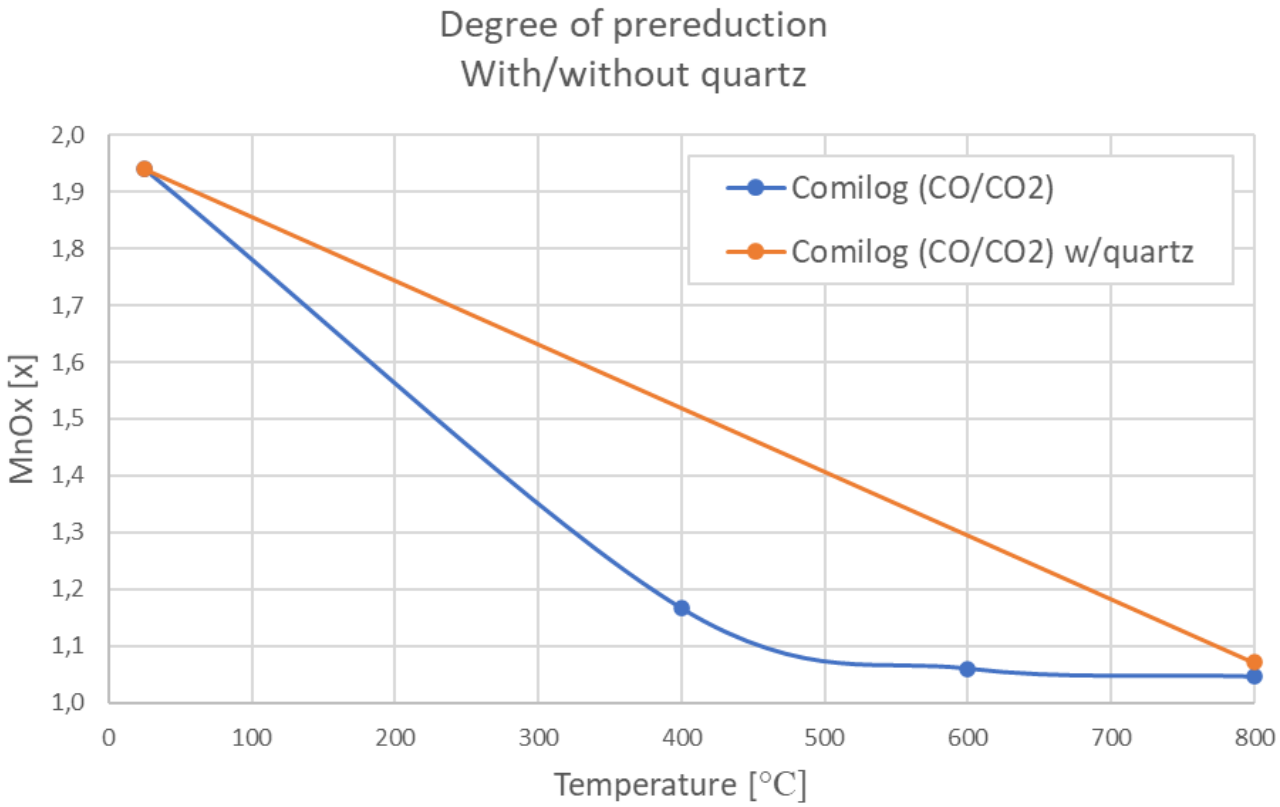

Figure 59: Comilog in CO/CO_2 with and without quartz, MnOx values at the different temperatures. Only 800°C was tested for Comilog quartz.

Figure 59 shows a comparison of the degree of prereduction for the Comilog ore heated with and without quartz. The line for Comilog/quartz is linear due to only being tested at 800°C, but is probably similar to the other Comilog line. This is based on the similarities in decrepitation as well as reaching a similar value after the same amount of time, as well as the predicted result based on the stability of manganese oxides in figure 56.

The weight loss increases with temperature as expected. Assmang in 800°C CO/CO_2 has a similar weight loss to its theoretical weight loss. The 5 g difference could be due to water or other volatiles not included in the theoretical calculations. This suggests that all of the iron oxides, manganese oxides and all of the carbonates have reacted or decomposed at 800°C. The majority of the mass loss was after reacting 600°C, when carbonates decomposes, as well as the reduction of the last manganese oxides.

The weight loss in the air experiments are significantly lower than the theoretical weight loss due

to that the manganese oxides stops reacting at Mn_2O_3 rather than to MnO. Most of the carbonates should still have decomposed 800°C. Comilog and UMK has a rather large weight loss compared to the Assmang because of their chemical composition, Comilog due to the decomposition of MnO_2 to Mn_2O_3 and UMK has a large amount of carbonates which decomposes at higher temperatures. Assmang however has little carbonates and mostly Mn_2O_3, so it has the lowest weight loss of the three ores in air atmosphere as seen in table 7.

As a summary, Comilog heated in CO/CO_2 is the fastest to be reduced to MnO. It also has the most decrepitation with a TI3,35 value of 63,76% after heating. When heated in air it decomposes to Mn_2O_3, while having little to no decrepitation, TI3,35 = 98,31%. Assmang is reduced slower than Comilog, but ends at only MnO at 800°C in CO/CO_2. The ore has less decrepitation than Comilog at TI3,35 = 83,70% at 800°C. However Assmang is not reduced in air and remains at mostly Mn_2O_3, while having some decrepitation, ending at TI3,35=91,27%. UMK is the strongest of the ores ending at MnO and TI3,35 = 93,31% in CO/CO_2. The UMK is not reduced past Mn_2O_3 in air, but has similar decrepitation to Comilog at TI3,35 = 97,87%.

6 Conclusion

The goal for this MSc was to examine the behaviour of manganese ores as they are heated. This is done because it is desired to have a prereduction unit for the manganese production. Prereduction of the manganese ore would reduce the consumption of electrical energy and carbon material by using either heated air or CO/CO_2 from the manganese furnace.

It was found that manganese ore heated in CO/CO_2 decrepitates more than in air, but is at the same time reduced to MnO at 800°C. Air heated ores is not reduced past Mn_2O_3, but shows little decrepitation suggesting that the reduction of manganese oxides is a major influence on the decrepitation. Comilog had the biggest difference between the two gas atmospheres, having the most decrepitation in CO/CO_2 and almost no decrepitation in air. UMK decrepitated the least of the ores in both atmospheres, while Assmang was in the middle in CO/CO_2 and had the most decrepitation in air.

Assmang did reach a similar degree of prereduction as the other ores in CO/CO_2, ending at x = 1 at 800°C. Similarly to UMK ore it did not show any significant reduction before reaching a temperature higher than 600°C. All of the ores ends at MnOx $\approx$ 1,5 when heated in synthetic air, Comilog being the only ore which was reduced as MnO_2 was decomposing at higher temperatures. Assmang and UMK ore had an increase in the oxygen content, as was expected from the stability diagram of the manganese oxides. This suggest that if only Comilog is used, then a prereduction unit using air would be sufficient for some reduction of the manganese ore. If lower oxides are desired, for example MnO, then CO/CO_2 is needed to reduce the ore as much as possible.

The strength of the ores are reduced as they are heated according to the pressure force measurements. This could be due to cracking from thermal shock or an increase in the porosity from reactions with the gases. An increase in porosity as the ore is heated is indicated by the porosity measurements, but some of the results deviates a lot and does not give a clear answer. This is however shown to happen in other work (Turkova et al.). SEM examination of the ores shows larger pores in the Comilog ore, while all of the ores have smaller pores at $\sim$10 µm in their cross section at magnification of 1000x.

Lastly, the Comilog ore heated with quartz showed more decrepitation than the ore heated without, despite avoiding the high temperature peak during heating. It should be noted that this lower peak could be due that the sample was 1 kg Comilog, half of what was heated without quartz. The increased decrepitation was measured before and after tumble-test, suggesting again that the reduction of manganese oxides are the most important factor for the decrepitation.

References

[1] Olav Biørnstad. *Decrepitation of Comilog and UMK manganese ores during pre-reduction*. Specialization project. Trondheim: Norwegian University of Science and Technology, 2019.

[2] G Pochart et al. "Metallurgical benefit of reactive high grade ore in manganese alloys manufacturing". In: *World* 800.1000 (2007), p. 1200.

[3] Merete Tangstad. *Introduction to manganese ferroalloy production*. Manganese course. 2017.

[4] Sverre E. . Olsen and Merete Tangstad. *Production of manganese ferroalloys*. eng. Trondheim: Tapir akademisk forl, 2007. ISBN: 978-82-519-2191-6.

[5] dpicampaigns. *About the Sustainable Development Goals*. en-US. URL: `https://www.un.org/sustainabledevelopment/sustainable-development-goals/` (visited on 11/04/2019).

[6] Rodney Ishak and Merete Tangstad. "Degree of prereduction without coke consumption in industrial furnaces". In: *INFACON XI* (2007), pp. 268–279.

[7] M Tangstad et al. "Use of Comilog ore in ferromanganese production". In: *Proceedings: Tenth International Ferroalloys Congress*. Vol. 1. 2004, p. 4.

[8] Merete Tangstad et al. "Kinetics of the prereduction of manganese ores". In: *Conference proceedings, Infacon IX (Quebec)*. 2001, pp. 202–207.

[9] Ring Kononov, Oleg Ostrovski, and Samir Ganguly. "Carbothermal solid state reduction of manganese ores: 1. Manganese ore characterisation". In: *ISIJ international* 49.8 (2009), pp. 1099–1106.

[10] Bjørn Sorensen et al. "Phase compositions of manganese ores and their change in the process of calcination". In: *International Journal of Mineral Processing* 94.3-4 (2010), pp. 101–110.

[11] Ring Kononov, Oleg Ostrovski, and Samir Ganguly. "Carbothermal solid state reduction of manganese ores: 2. Non-isothermal and isothermal reduction in different gas atmospheres". In: *ISIJ international* 49.8 (2009), pp. 1107–1114.

[12] M. I. Zaki et al. "Thermochemistry of manganese oxides in reactive gas atmospheres: probing redox compositions in the decomposition course MnO2 to MnO". In: *Thermochimica Acta* 303.2 (1997), pp. 171–181.

[13] Kiyoshi Terayama and Masao Ikeda. "Study on thermal decomposition of MnO2 and Mn2O3 by thermal analysis". In: *Transactions of the Japan institute of metals* 24.11 (1983). Publisher: The Japan Institute of Metals, pp. 754–758.

[14] Manoj Kumar, S. Ranganathan, and S. N. Sinha. "Kinetics of reduction of different manganese ores". In: *INFANCON XI-International Ferro-Alloys Congress. New Delhi:[sn]*. 2007, pp. 241–246.

[15] Julian Szekely, James W. Evans, and Hong Yong Sohn. *Gas-solid reactions*. Elsevier, 1976.

[16] Kira Turkova, Dmitry Slizovskiy, and Merete Tangstad. "CO Reactivity and Porosity of Manganese Materials". eng. In: *ISIJ International* 54.6 (2014), pp. 1204–1208.

[17] R. King and C. Brown. "The rate of movement of the topochemical interface during gas-solid reactions". eng. In: *Metallurgical Transactions B* 11.4 (1980), pp. 585–592.

[18] K. Berg and S. Olsen. "Kinetics of manganese ore reduction by carbon monoxide". eng. In: *Metallurgical and Materials Transactions B* 31.3 (2000), pp. 477–490.

[19] G. J. W. Kor. "The thermal decomposition of Mn2O3 and the reduction of Mn3O4 by C and CO". eng. In: *Metallurgical Transactions B* 9.3 (1978), pp. 307–311.

[20] Trine Asklund Larssen, Merete Tangstad, and IT Kero. "Gaseous Reduction of Mn Ores in CO-CO 2 Atmosphere". In: *Extraction 2018*. Springer, 2018, pp. 1093–1101.

[21] L.S. Todd. "High Temperature Reactivity of Manganese Charge Materials". In: New York, May 1979.

[22] LS Todd, BW Webb, and SD Martin. "Solid-state reactivity of manganese ores (Job No. 528-50534)". In: *Union Carbide, Progress Report June* 30 (1979).

[23] Y. B. Gao, H. G. Kim, and H. Y. Sohn. "Kinetics of pre-reduction of manganese ore by CO". In: *Mineral Processing and Extractive Metallurgy* 121.2 (2012), pp. 109–116.

[24] Mohammed Salah Fahim et al. "Characterization of Egyptian manganese ores for production of high carbon ferromanganese". In: *Journal of Minerals and materials characterization and engineering* 1.02 (2013), p. 68.

[25] William D Callister. *Materials science and engineering*. eng. 9th ed., SI Version. Hoboken, N.J: Wiley, 2015. ISBN: 978-1-118-31922-2.

[26] Michal Ksiazek, Merete Tangstad, and Eli Ringdalen. "The thermophysical properties of raw materials for ferromanganese production". In: *Southern African Pyrometallurgy 2011* (2011).

[27] Gahan Lawrence and Allan G. Blackman. *Aylward and Findlay's SI chemical data*. 7th edition. New York, Wiley, 2014.

[28] Geraldo Lúcio de Faria et al. "Decrepitation of Brazilian manganese lump ores." In: *INFACON XII* (2010), pp. 641–660.

[29] RL Coble and WD Kingery. "Effect of porosity on thermal stress fracture". In: *Journal of the American Ceramic Society* 38.1 (1955). Publisher: Wiley Online Library, pp. 33–37.

[30] Larryn W. Diamond, Alexandre Tarantola, and Holger Stünitz. "Modification of fluid inclusions in quartz by deviatoric stress. II: experimentally induced changes in inclusion volume and composition". In: *Contributions to Mineralogy and Petrology* 160.6 (Dec. 2010), pp. 845–864.

[31] A. Tarantola et al. "Modification of fluid inclusions in quartz by deviatoric stress. III: Influence of principal stresses on inclusion density and orientation". In: *Contributions to Mineralogy and Petrology* 164.3 (Sept. 2012), pp. 537–550.

[32] James D Blacic. "Plastic-deformati on mechanisms in quartz: the effect of water". In: *Tectonophysics* 27.3 (1975), pp. 271–294.

[33] Volker Lueders, Jens Gutzmer, and Nicolas J. Beukes. "Fluid inclusion studies in cogenetic hematite, hausmannite, and gangue minerals from high-grade manganese ores in the Kalahari manganese field, South Africa". In: *Economic Geology* 94.4 (1999), pp. 589–595.

[34] Geraldo Lúcio de Faria et al. "Disintegration on heating of a Brazilian manganese lump ore". In: *International Journal of Mineral Processing* 124 (2013), pp. 132–137.

[35] Sarina Bao and Eli Ringdalen. *WP 3.1 Characterisation of Mn sources*. Presentation. NTNU, Feb. 2019.
[36] M. Visser et al. "Properties of Nchwaning and Gloria ore in the production of Mn ferroalloys". In: *Proceedings of INFACONXII* (2013), pp. 553–566.
[37] Merete Tangstad. *Private communication, Theoretical weight loss*. Dec. 2019.
[38] Jarle Hjelen. *Scanning elektron-mikroskopi*. 1986.

A Appendix

A.1 Heating curves

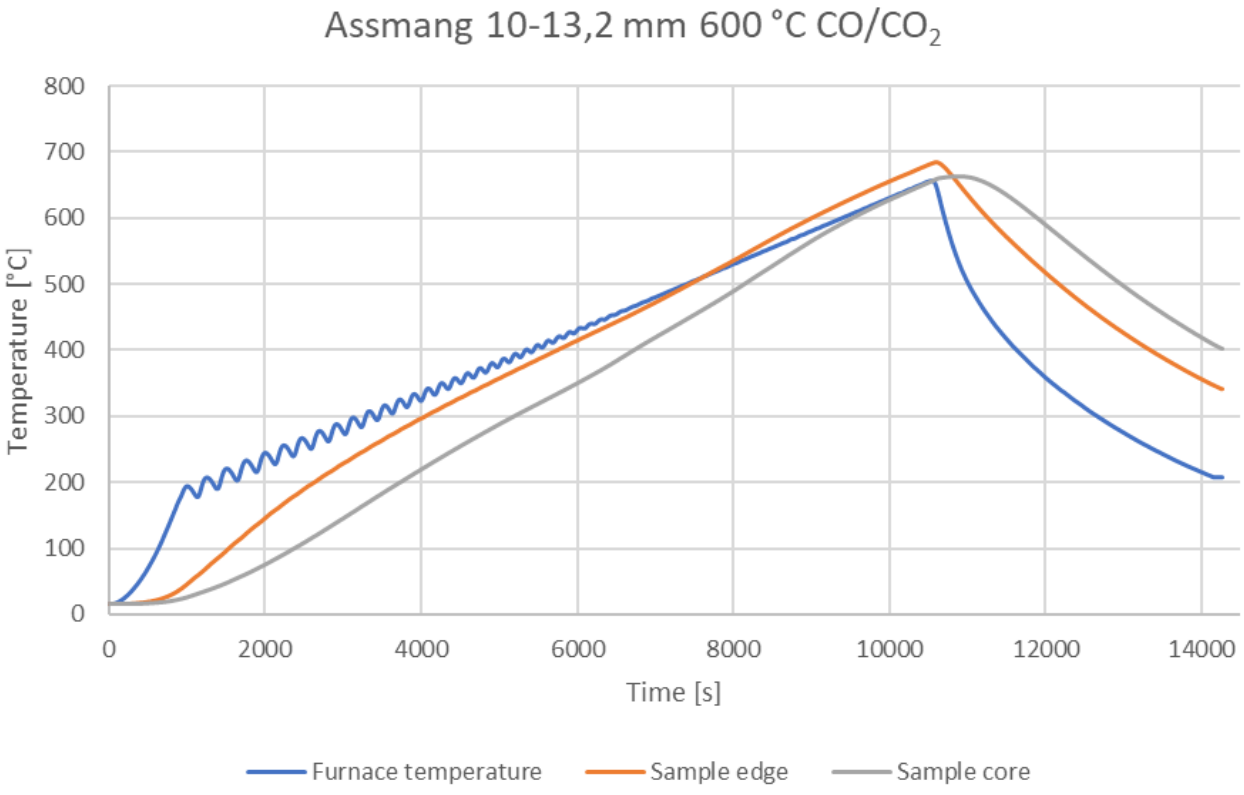

Figure 60: Heating curve for Assmang heated to 600°in CO/CO_2

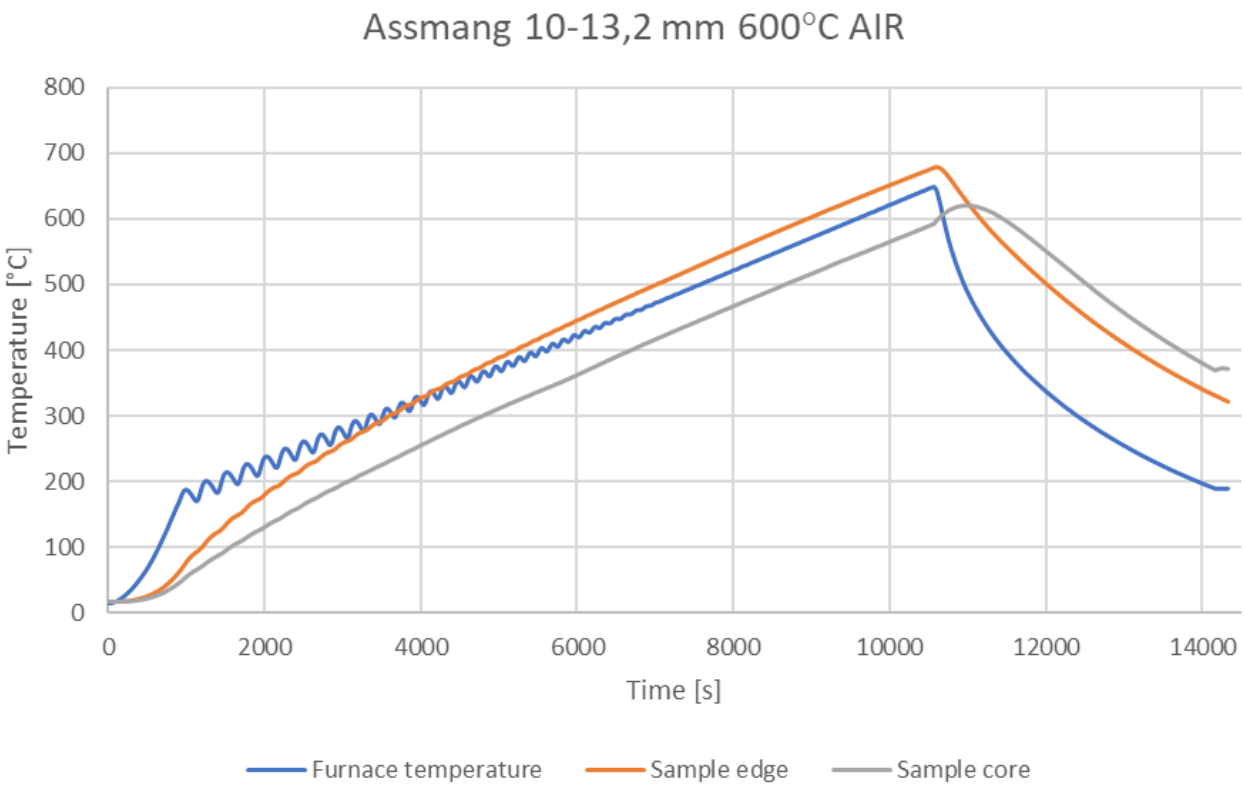

Figure 61: Heating curve for Assmang heated to 600°in synthetic air

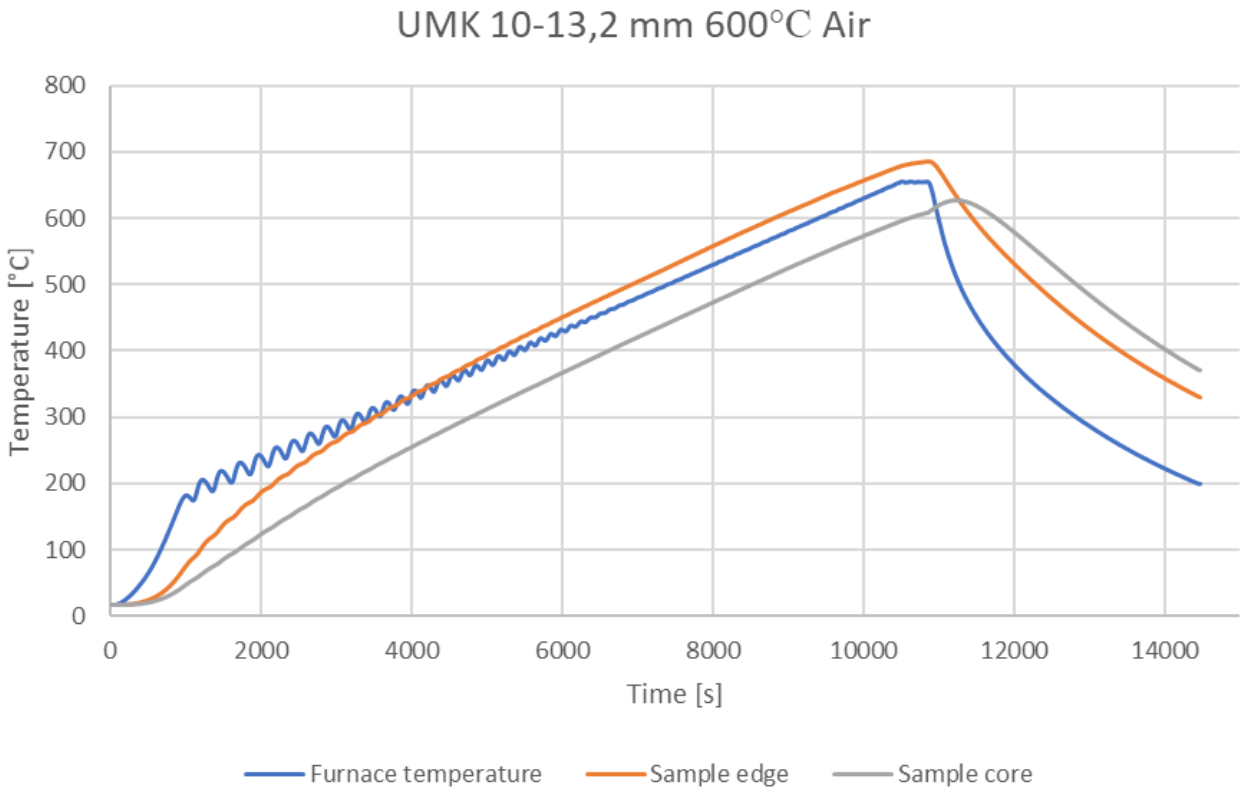

Figure 62: Heating curve for UMK heated to 600°in synthetic air

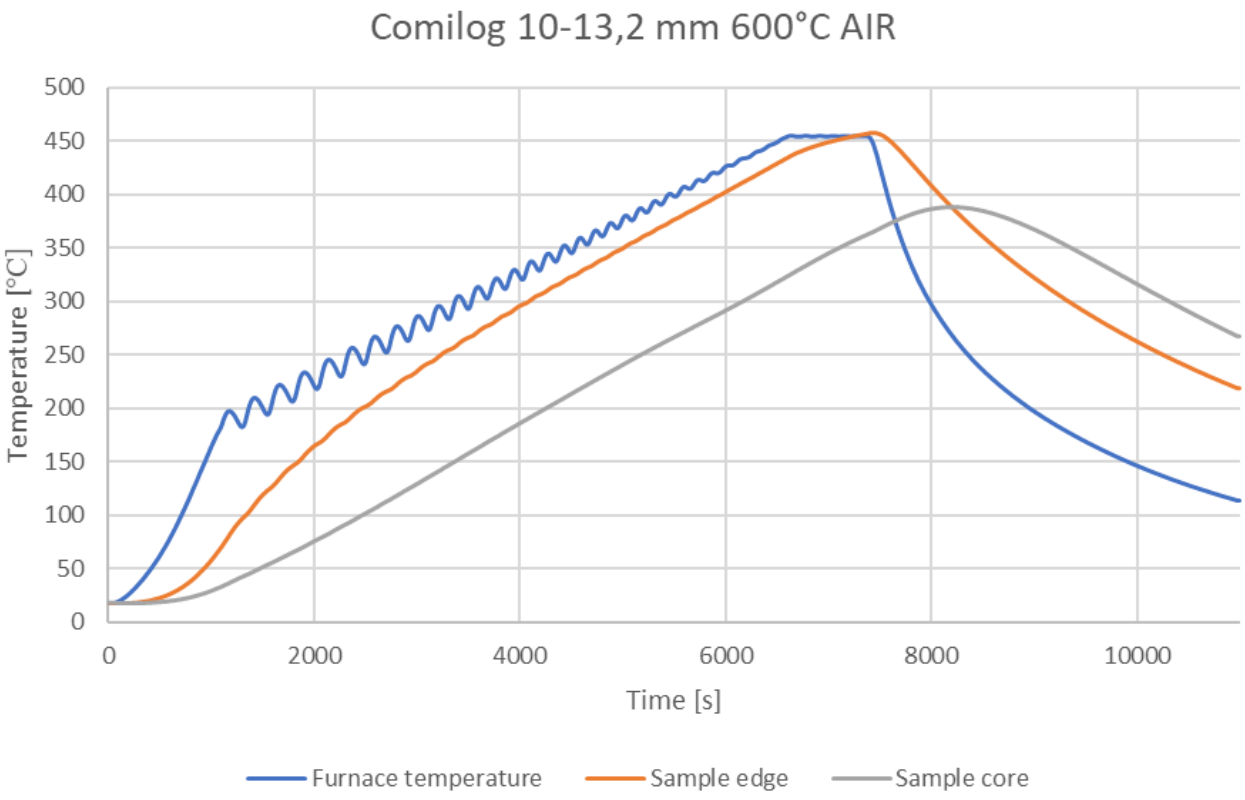

Figure 63: Heating curve for Comilog heated to 600°in synthetic air

A.2 Chemical analysis

SINTEF NORLAB

SINTEF AS
Olav Biornstad
SINTEF Industri
Alfred Getz' vei 2
7034 Trondheim

SINTEF

SINTEF Norlab AS
Org. nr.: NO 953 018 144 MVA
Postboks 611
NO-8607 Mo i Rana
www.sintefnorlab.no

Tlf: (+47) 404 84 100

Ordrenr:	83352
Sted:	Mo i Rana
Antall prøver:	7
Bestillingsnr:	PreMa

ANALYSERAPPORT

Analyse av Mn-malm

Prøvenr.:	Prøvetype:	Prøvemerking:				Prøvetaker:	Mottaksdato:
83352-001		Assmang 10-13,2 mm 800 °C CO/CO2 Prøve 1				Oppdragsgiver	21.02.2020
Analyse/Parameter		Resultat	Enhet	Usikkerhet	Analysedato	Metodbeskrivelse	
*) LOI 950		-3.37	%	5.5 %	03.03.20	Thermogravimetric	
*) Mn		51.91	%	0.2 %	03.03.20	XRF - Fused bead	
*) Fe		9.69	%	1.5 %	03.03.20	XRF - Fused bead	
*) SiO2		4.28	%	10 %	03.03.20	XRF - Fused bead	
*) Al2O3		0.55	%	9 %	03.03.20	XRF - Fused bead	
*) CaO		7.80	%	1 %	03.03.20	XRF - Fused bead	
*) MgO		1.47	%	40 %	03.03.20	XRF - Fused bead	
*) P		0.030	%	4 %	03.03.20	XRF - Fused bead	
*) S		0.101	%	10 %	03.03.20	XRF - Fused bead	
*) TiO2		<0.01	%	3 %	03.03.20	XRF - Fused bead	
*) K2O		0.03	%	3 %	03.03.20	XRF - Fused bead	
*) BaO		0.35	%	5 %	03.03.20	XRF - Fused bead	
*) MnO2		<0.05	%	10 %	03.03.20	Titrimetric	

Prøvenr.:	Prøvetype:	Prøvemerking:				Prøvetaker:	Mottaksdato:
83352-002		Assmang 10-13,2 mm 600 °C CO/CO2 Prøve 2				Oppdragsgiver	21.02.2020
Analyse/Parameter		Resultat	Enhet	Usikkerhet	Analysedato	Metodbeskrivelse	
*) LOI 950		2.11	%	5.5 %	03.03.20	Thermogravimetric	
*) Mn		48.54	%	0.2 %	03.03.20	XRF - Fused bead	
*) Fe		9.36	%	1.5 %	03.03.20	XRF - Fused bead	
*) SiO2		4.01	%	10 %	03.03.20	XRF - Fused bead	
*) Al2O3		0.52	%	9 %	03.03.20	XRF - Fused bead	
*) CaO		7.37	%	1 %	03.03.20	XRF - Fused bead	
*) MgO		1.48	%	40 %	03.03.20	XRF - Fused bead	
*) P		0.029	%	4 %	03.03.20	XRF - Fused bead	
*) S		0.110	%	10 %	03.03.20	XRF - Fused bead	
*) TiO2		<0.01	%	3 %	03.03.20	XRF - Fused bead	
*) K2O		0.02	%	3 %	03.03.20	XRF - Fused bead	
*) BaO		0.35	%	5 %	03.03.20	XRF - Fused bead	
*) MnO2		19.59	%	10 %	03.03.20	Titrimetric	

Rapportert av:
Faglaborant
Ann-Heidi Andreassen

03.03.20 kl 12.10

Prøvenr.:	Prøvetype:	Prøvemerking:				Prøvetaker:	Mottaksdato:
83352-003		Assmang 10-13,2 mm 400 °C CO/CO2 Prøve 3				Oppdragsgiver	21.02.2020
Analyse/Parameter		Resultat	Enhet	Usikkerhet	Analysedato	Metodbeskrivelse	
*) LOI 950		3.99	%	5.5 %	03.03.20	Thermogravimetric	
*) Mn		48.61	%	0.2 %	03.03.20	XRF - Fused bead	
*) Fe		8.60	%	1.5 %	03.03.20	XRF - Fused bead	
*) SiO2		3.89	%	10 %	03.03.20	XRF - Fused bead	
*) Al2O3		0.42	%	9 %	03.03.20	XRF - Fused bead	
*) CaO		7.05	%	1 %	03.03.20	XRF - Fused bead	
*) MgO		1.10	%	40 %	03.03.20	XRF - Fused bead	
*) P		0.030	%	4 %	03.03.20	XRF - Fused bead	
*) S		0.088	%	10 %	03.03.20	XRF - Fused bead	
*) TiO2		<0.01	%	3 %	03.03.20	XRF - Fused bead	
*) K2O		0.02	%	3 %	03.03.20	XRF - Fused bead	
*) BaO		0.25	%	5 %	03.03.20	XRF - Fused bead	
*) MnO2		35.41	%	10 %	03.03.20	Titrimetric	

Prøvenr.:	Prøvetype:	Prøvemerking:				Prøvetaker:	Mottaksdato:
83352-004		Assmang 800 °C AFT Fines				Oppdragsgiver	21.02.2020
Analyse/Parameter		Resultat	Enhet	Usikkerhet	Analysedato	Metodbeskrivelse	
*) LOI 950		-4.10	%	5.5 %	03.03.20	Thermogravimetric	
*) Mn		55.53	%	0.2 %	03.03.20	XRF - Fused bead	
*) Fe		8.68	%	1.5 %	03.03.20	XRF - Fused bead	
*) SiO2		3.04	%	10 %	03.03.20	XRF - Fused bead	
*) Al2O3		0.40	%	9 %	03.03.20	XRF - Fused bead	
*) CaO		7.19	%	1 %	03.03.20	XRF - Fused bead	
*) MgO		1.09	%	40 %	03.03.20	XRF - Fused bead	
*) P		0.031	%	4 %	03.03.20	XRF - Fused bead	
*) S		0.197	%	10 %	03.03.20	XRF - Fused bead	
*) TiO2		<0.01	%	3 %	03.03.20	XRF - Fused bead	
*) K2O		0.01	%	3 %	03.03.20	XRF - Fused bead	
*) BaO		0.63	%	5 %	03.03.20	XRF - Fused bead	
*) MnO2		<0.05	%	10 %	03.03.20	Titrimetric	

Prøvenr.:	Prøvetype:	Prøvemerking:				Prøvetaker:	Mottaksdato:
83352-005		Assmang 600 °C AFT Fines				Oppdragsgiver	21.02.2020
Analyse/Parameter		Resultat	Enhet	Usikkerhet	Analysedato	Metodbeskrivelse	
*) LOI 950		-0.56	%	5.5 %	03.03.20	Thermogravimetric	
*) Mn		53.04	%	0.2 %	03.03.20	XRF - Fused bead	
*) Fe		8.86	%	1.5 %	03.03.20	XRF - Fused bead	
*) SiO2		1.68	%	10 %	03.03.20	XRF - Fused bead	
*) Al2O3		0.56	%	9 %	03.03.20	XRF - Fused bead	
*) CaO		6.33	%	1 %	03.03.20	XRF - Fused bead	
*) MgO		1.04	%	40 %	03.03.20	XRF - Fused bead	
*) P		0.033	%	4 %	03.03.20	XRF - Fused bead	
*) S		0.233	%	10 %	03.03.20	XRF - Fused bead	
*) TiO2		<0.01	%	3 %	03.03.20	XRF - Fused bead	
*) K2O		0.02	%	3 %	03.03.20	XRF - Fused bead	
*) BaO		0.83	%	5 %	03.03.20	XRF - Fused bead	

Rapportert av:
Faglaborant
Ann-Heidi Andreassen

Prøvenr.:	Prøvetype:	Prøvemerking:				Prøvetaker:	Mottaksdato:
83352-005		Assmang 600 °C AFT Fines				Oppdragsgiver	21.02.2020
Analyse/Parameter		Resultat	Enhet	Usikkerhet	Analysedato	Metodbeskrivelse	
*) MnO2		3.95	%	10 %	03.03.20	Titrimetric	

Prøvenr.:	Prøvetype:	Prøvemerking:				Prøvetaker:	Mottaksdato:
83352-006		Assmang fines 800 °C BFT				Oppdragsgiver	21.02.2020
Analyse/Parameter		Resultat	Enhet	Usikkerhet	Analysedato	Metodbeskrivelse	
*) LOI 950		-4.01	%	5.5 %	03.03.20	Thermogravimetric	
*) Mn		54.10	%	0.2 %	03.03.20	XRF - Fused bead	
*) Fe		8.52	%	1.5 %	03.03.20	XRF - Fused bead	
*) SiO2		3.57	%	10 %	03.03.20	XRF - Fused bead	
*) Al2O3		0.40	%	9 %	03.03.20	XRF - Fused bead	
*) CaO		7.39	%	1 %	03.03.20	XRF - Fused bead	
*) MgO		1.01	%	40 %	03.03.20	XRF - Fused bead	
*) P		0.032	%	4 %	03.03.20	XRF - Fused bead	
*) S		0.296	%	10 %	03.03.20	XRF - Fused bead	
*) TiO2		0.01	%	3 %	03.03.20	XRF - Fused bead	
*) K2O		0.01	%	3 %	03.03.20	XRF - Fused bead	
*) BaO		1.03	%	5 %	03.03.20	XRF - Fused bead	
*) MnO2		<0.05	%	10 %	03.03.20	Titrimetric	

Prøvenr.:	Prøvetype:	Prøvemerking:				Prøvetaker:	Mottaksdato:
83352-007		Assmang fines 600 °C BFT				Oppdragsgiver	21.02.2020
Analyse/Parameter		Resultat	Enhet	Usikkerhet	Analysedato	Metodbeskrivelse	
*) LOI 950		0.86	%	5.5 %	03.03.20	Thermogravimetric	
*) Mn		51.77	%	0.2 %	03.03.20	XRF - Fused bead	
*) Fe		8.65	%	1.5 %	03.03.20	XRF - Fused bead	
*) SiO2		2.26	%	10 %	03.03.20	XRF - Fused bead	
*) Al2O3		0.26	%	9 %	03.03.20	XRF - Fused bead	
*) CaO		6.22	%	1 %	03.03.20	XRF - Fused bead	
*) MgO		0.87	%	40 %	03.03.20	XRF - Fused bead	
*) P		0.032	%	4 %	03.03.20	XRF - Fused bead	
*) S		0.328	%	10 %	03.03.20	XRF - Fused bead	
*) TiO2		<0.01	%	3 %	03.03.20	XRF - Fused bead	
*) K2O		0.01	%	3 %	03.03.20	XRF - Fused bead	
*) BaO		1.22	%	5 %	03.03.20	XRF - Fused bead	
*) MnO2		7.01	%	10 %	03.03.20	Titrimetric	

Angitt måleusikkerhet er beregnet med dekningsfaktor k=2. Ved intervallangivelse viser det høyeste tallet usikkerheten nært rapporteringsgrensen. For nærmere informasjon gjeldende usikkerhet, vennligst ta kontakt. SINTEF Norlab er akkreditert med test nr. 032. Hvilke analyser som inngår i akkrediteringen fremkommer i rapporten, *) = Ikke akkreditert, mod = modifisert standard.

Rapportert av:
Faglaborant
Ann-Heidi Andreassen

03.03.20 kl 12.10

SINTEF NORLAB

NTNU Regnskapsseksjonen
Olav Bjørnstad
Alfred Getz vei 2B

7034 Trondheim

SINTEF Norlab AS
Org. nr.: NO 953 018 144 MVA
Postboks 611
NO-8607 Mo i Rana
www.sintefnorlab.no

Tlf: (+47) 404 84 100

Ordrenr:	86546
Sted:	Mo i Rana
Antall prøver:	6
Bestillingsnr:	

ANALYSERAPPORT

Kjemisk analyse

Prøvenr.:	Prøvetype:	Prøvemerking:				Prøvetaker:	Mottaksdato:
86546-001	Manganese Ore	Comilog 800 AIR 10-13,2 mm				Oppdragsgiver	13.05.2020
Analyse/Parameter		Resultat	Enhet	Usikkerhet	Analysedato	Metodbeskrivelse	
*) LOI 950		0.76	%	5.5 %	19.05.20	Thermogravimetric	
*) Mn		58.86	%	0.2 %	29.05.20	XRF - Fused bead	
*) Fe		4.15	%	1.5 %	29.05.20	XRF - Fused bead	
*) SiO2		2.66	%	10 %	29.05.20	XRF - Fused bead	
*) Al2O3		4.67	%	9 %	29.05.20	XRF - Fused bead	
*) CaO		0.05	%	1 %	29.05.20	XRF - Fused bead	
*) MgO		<0.03	%	40 %	29.05.20	XRF - Fused bead	
*) P		0.134	%	4 %	29.05.20	XRF - Fused bead	
*) S		<0.010	%	10 %	29.05.20	XRF - Fused bead	
*) TiO2		0.10	%	3 %	29.05.20	XRF - Fused bead	
*) K2O		0.81	%	3 %	29.05.20	XRF - Fused bead	
*) BaO		0.18	%	5 %	29.05.20	XRF - Fused bead	
*) MnO2		45.91	%	10 %	25.05.20	Titrimetric	

Prøvenr.:	Prøvetype:	Prøvemerking:				Prøvetaker:	Mottaksdato:
86546-002	Manganese Ore	Comilog 800 AIR Fines				Oppdragsgiver	13.05.2020
Analyse/Parameter		Resultat	Enhet	Usikkerhet	Analysedato	Metodbeskrivelse	
*) LOI 950		1.49	%	5.5 %	19.05.20	Thermogravimetric	
*) Mn		49.58	%	0.2 %	29.05.20	XRF - Fused bead	
*) Fe		6.48	%	1.5 %	29.05.20	XRF - Fused bead	
*) SiO2		6.73	%	10 %	29.05.20	XRF - Fused bead	
*) Al2O3		9.89	%	9 %	29.05.20	XRF - Fused bead	
*) CaO		0.08	%	1 %	29.05.20	XRF - Fused bead	
*) MgO		0.14	%	40 %	29.05.20	XRF - Fused bead	
*) P		0.151	%	4 %	29.05.20	XRF - Fused bead	
*) S		0.028	%	10 %	29.05.20	XRF - Fused bead	
*) TiO2		0.23	%	3 %	29.05.20	XRF - Fused bead	
*) K2O		1.05	%	3 %	29.05.20	XRF - Fused bead	
*) BaO		0.26	%	5 %	29.05.20	XRF - Fused bead	
*) MnO2		37.53	%	10 %	25.05.20	Titrimetric	

Rapportert av:
Faglaborant
Ann-Heidi Andreassen

29.05.20 kl 11.42

Prøvenr.:	Prøvetype:	Prøvemerking:				Prøvetaker:	Mottaksdato:
86546-003	Manganese Ore	Comilog 600 AIR Fines				Oppdragsgiver	13.05.2020
Analyse/Parameter		Resultat	Enhet	Usikkerhet	Analysedato	Metodbeskrivelse	
*) LOI 950		4.04	%	5.5 %	19.05.20	Thermogravimetric	
*) Mn		49.33	%	0.2 %	29.05.20	XRF - Fused bead	
*) Fe		5.91	%	1.5 %	29.05.20	XRF - Fused bead	
*) SiO2		6.03	%	10 %	29.05.20	XRF - Fused bead	
*) Al2O3		9.40	%	9 %	29.05.20	XRF - Fused bead	
*) CaO		0.15	%	1 %	29.05.20	XRF - Fused bead	
*) MgO		0.04	%	40 %	29.05.20	XRF - Fused bead	
*) P		0.137	%	4 %	29.05.20	XRF - Fused bead	
*) S		0.013	%	10 %	29.05.20	XRF - Fused bead	
*) TiO2		0.22	%	3 %	29.05.20	XRF - Fused bead	
*) K2O		0.86	%	3 %	29.05.20	XRF - Fused bead	
*) BaO		0.21	%	5 %	29.05.20	XRF - Fused bead	
*) MnO2		45.30	%	10 %	25.05.20	Titrimetric	

Prøvenr.:	Prøvetype:	Prøvemerking:				Prøvetaker:	Mottaksdato:
86546-004	Manganese Ore	Comilog 600 AIR 10-13,2 mm				Oppdragsgiver	13.05.2020
Analyse/Parameter		Resultat	Enhet	Usikkerhet	Analysedato	Metodbeskrivelse	
*) LOI 950		3.86	%	5.5 %	19.05.20	Thermogravimetric	
*) Mn		55.41	%	0.2 %	29.05.20	XRF - Fused bead	
*) Fe		4.71	%	1.5 %	29.05.20	XRF - Fused bead	
*) SiO2		2.97	%	10 %	29.05.20	XRF - Fused bead	
*) Al2O3		5.12	%	9 %	29.05.20	XRF - Fused bead	
*) CaO		0.04	%	1 %	29.05.20	XRF - Fused bead	
*) MgO		0.06	%	40 %	29.05.20	XRF - Fused bead	
*) P		0.131	%	4 %	29.05.20	XRF - Fused bead	
*) S		0.016	%	10 %	29.05.20	XRF - Fused bead	
*) TiO2		0.11	%	3 %	29.05.20	XRF - Fused bead	
*) K2O		0.84	%	3 %	29.05.20	XRF - Fused bead	
*) BaO		0.23	%	5 %	29.05.20	XRF - Fused bead	
*) MnO2		55.83	%	10 %	25.05.20	Titrimetric	

Prøvenr.:	Prøvetype:	Prøvemerking:				Prøvetaker:	Mottaksdato:
86546-005	Manganese Ore	Comilog 400 AIR 10-13,2 mm				Oppdragsgiver	13.05.2020
Analyse/Parameter		Resultat	Enhet	Usikkerhet	Analysedato	Metodbeskrivelse	
*) LOI 950		8.44	%	5.5 %	19.05.20	Thermogravimetric	
*) Mn		54.13	%	0.2 %	29.05.20	XRF - Fused bead	
*) Fe		3.59	%	1.5 %	29.05.20	XRF - Fused bead	
*) SiO2		3.04	%	10 %	29.05.20	XRF - Fused bead	
*) Al2O3		4.92	%	9 %	29.05.20	XRF - Fused bead	
*) CaO		0.05	%	1 %	29.05.20	XRF - Fused bead	
*) MgO		0.07	%	40 %	29.05.20	XRF - Fused bead	
*) P		0.120	%	4 %	29.05.20	XRF - Fused bead	
*) S		0.010	%	10 %	29.05.20	XRF - Fused bead	
*) TiO2		0.11	%	3 %	29.05.20	XRF - Fused bead	
*) K2O		0.75	%	3 %	29.05.20	XRF - Fused bead	
*) BaO		0.18	%	5 %	29.05.20	XRF - Fused bead	

Rapportert av:
Faglaborant
Ann-Heidi Andreassen

Prøvenr.:	Prøvetype:	Prøvemerking:				Prøvetaker:	Mottaksdato:
86546-005	Manganese Ore	Comilog 400 AIR 10-13,2 mm				Oppdragsgiver	13.05.2020
Analyse/Parameter		Resultat	Enhet	Usikkerhet	Analysedato	Metodbeskrivelse	
*) MnO2		75.22	%	10 %	25.05.20	Titrimetric	

Prøvenr.:	Prøvetype:	Prøvemerking:				Prøvetaker:	Mottaksdato:
86546-006	Manganese Ore	Comilog 400 AIR Fines				Oppdragsgiver	13.05.2020
Analyse/Parameter		Resultat	Enhet	Usikkerhet	Analysedato	Metodbeskrivelse	
*) LOI 950		8.80	%	5.5 %	19.05.20	Thermogravimetric	
*) Mn		43.02	%	0.2 %	29.05.20	XRF - Fused bead	
*) Fe		7.13	%	1.5 %	29.05.20	XRF - Fused bead	
*) SiO2		7.36	%	10 %	29.05.20	XRF - Fused bead	
*) Al2O3		9.73	%	9 %	29.05.20	XRF - Fused bead	
*) CaO		0.54	%	1 %	29.05.20	XRF - Fused bead	
*) MgO		0.30	%	40 %	29.05.20	XRF - Fused bead	
*) P		0.141	%	4 %	29.05.20	XRF - Fused bead	
*) S		0.040	%	10 %	29.05.20	XRF - Fused bead	
*) TiO2		0.23	%	3 %	29.05.20	XRF - Fused bead	
*) K2O		0.80	%	3 %	29.05.20	XRF - Fused bead	
*) BaO		0.24	%	5 %	29.05.20	XRF - Fused bead	
*) MnO2		60.43	%	10 %	25.05.20	Titrimetric	

Angitt måleusikkerhet er beregnet med dekningsfaktor k=2. Ved intervallangivelse viser det høyeste tallet usikkerheten nært rapporteringsgrensen. For nærmere informasjon gjeldende usikkerhet, vennligst ta kontakt. SINTEF Norlab er akkreditert med test nr. 032. Hvilke analyser som inngår i akkrediteringen fremkommer i rapporten, *) = Ikke akkreditert, mod = modifisert standard.

Rapportert av:
Faglaborant
Ann-Heidi Andreassen

SINTEF NORLAB

NTNU Regnskapsseksjonen
Olav Biørnstad

SINTEF

SINTEF Norlab AS
Org. nr.: NO 953 018 144 MVA
Postboks 611
NO-8607 Mo i Rana
www.sintefnorlab.no

Tlf: (+47) 404 84 100

Ordrenr:	87152
Sted:	Mo i Rana
Antall prøver:	7
Bestillingsnr:	PreMa

ANALYSERAPPORT

Kjemisk analyse

Prøvenr.:	Prøvetype:	Prøvemerking:				Prøvetaker:	Mottaksdato:
87152-001	Manganese Ore	Comilog Q1 Fines				Oppdragsgiver	27.05.2020
Analyse/Parameter		Resultat	Enhet	Usikkerhet	Analysedato	Metodbeskrivelse	
*) LOI 950		-3.82	%	5.5 %	28.05.20	Thermogravimetric	
*) Mn		60.27	%	0.2 %	02.06.20	XRF - Fused bead	
*) Fe		3.95	%	1.5 %	02.06.20	XRF - Fused bead	
*) SiO2		5.99	%	10 %	02.06.20	XRF - Fused bead	
*) Al2O3		6.13	%	9 %	02.06.20	XRF - Fused bead	
*) CaO		0.09	%	1 %	02.06.20	XRF - Fused bead	
*) MgO		0.06	%	40 %	02.06.20	XRF - Fused bead	
*) P		0.161	%	4 %	02.06.20	XRF - Fused bead	
*) S		<0.010	%	10 %	02.06.20	XRF - Fused bead	
*) TiO2		0.14	%	3 %	02.06.20	XRF - Fused bead	
*) K2O		0.91	%	3 %	02.06.20	XRF - Fused bead	
*) BaO		0.21	%	5 %	02.06.20	XRF - Fused bead	
*) MnO2		7.13	%	10 %	04.06.20	Titrimetric	

Prøvenr.:	Prøvetype:	Prøvemerking:				Prøvetaker:	Mottaksdato:
87152-002	Manganese Ore	Comilog Q2 Fines				Oppdragsgiver	27.05.2020
Analyse/Parameter		Resultat	Enhet	Usikkerhet	Analysedato	Metodbeskrivelse	
*) LOI 950		-3.91	%	5.5 %	28.05.20	Thermogravimetric	
*) Mn		62.59	%	0.2 %	04.06.20	XRF - Fused bead	
*) Fe		3.47	%	1.5 %	04.06.20	XRF - Fused bead	
*) SiO2		5.01	%	10 %	04.06.20	XRF - Fused bead	
*) Al2O3		5.21	%	9 %	04.06.20	XRF - Fused bead	
*) CaO		0.07	%	1 %	04.06.20	XRF - Fused bead	
*) MgO		<0.03	%	40 %	04.06.20	XRF - Fused bead	
*) P		0.148	%	4 %	04.06.20	XRF - Fused bead	
*) S		<0.010	%	10 %	04.06.20	XRF - Fused bead	
*) TiO2		0.12	%	3 %	04.06.20	XRF - Fused bead	
*) K2O		0.90	%	3 %	04.06.20	XRF - Fused bead	
*) BaO		0.18	%	5 %	04.06.20	XRF - Fused bead	
*) MnO2		6.43	%	10 %	04.06.20	Titrimetric	

Rapportert av:
Faglaborant
Ann-Heidi Andreassen

05.06.20 kl 10.22

Prøvenr.:	Prøvetype:	Prøvemerking:				Prøvetaker:	Mottaksdato:
87152-003	Manganese Ore	Comilog Q1 10-13,2 mm (800)				Oppdragsgiver	27.05.2020
Analyse/Parameter		Resultat	Enhet	Usikkerhet	Analysedato	Metodbeskrivelse	
*) LOI 950		-4.33	%	5.5 %	29.05.20	Thermogravimetric	
*) Mn		61.81	%	0.2 %	04.06.20	XRF - Fused bead	
*) Fe		4.03	%	1.5 %	04.06.20	XRF - Fused bead	
*) SiO2		4.11	%	10 %	04.06.20	XRF - Fused bead	
*) Al2O3		5.86	%	9 %	04.06.20	XRF - Fused bead	
*) CaO		0.22	%	1 %	04.06.20	XRF - Fused bead	
*) MgO		0.15	%	40 %	04.06.20	XRF - Fused bead	
*) P		0.132	%	4 %	04.06.20	XRF - Fused bead	
*) S		0.019	%	10 %	04.06.20	XRF - Fused bead	
*) TiO2		0.13	%	3 %	04.06.20	XRF - Fused bead	
*) K2O		0.90	%	3 %	04.06.20	XRF - Fused bead	
*) BaO		0.24	%	5 %	04.06.20	XRF - Fused bead	
*) MnO2		6.08	%	10 %	04.06.20	Titrimetric	

Prøvenr.:	Prøvetype:	Prøvemerking:				Prøvetaker:	Mottaksdato:
87152-004	Manganese Ore	Comilog Q2 10-13,2 mm (800)				Oppdragsgiver	27.05.2020
Analyse/Parameter		Resultat	Enhet	Usikkerhet	Analysedato	Metodbeskrivelse	
*) LOI 950		-3.86	%	5.5 %	29.05.20	Thermogravimetric	
*) Mn		61.89	%	0.2 %	04.06.20	XRF - Fused bead	
*) Fe		3.68	%	1.5 %	04.06.20	XRF - Fused bead	
*) SiO2		4.41	%	10 %	04.06.20	XRF - Fused bead	
*) Al2O3		5.61	%	9 %	04.06.20	XRF - Fused bead	
*) CaO		0.19	%	1 %	04.06.20	XRF - Fused bead	
*) MgO		0.10	%	40 %	04.06.20	XRF - Fused bead	
*) P		0.125	%	4 %	04.06.20	XRF - Fused bead	
*) S		0.017	%	10 %	04.06.20	XRF - Fused bead	
*) TiO2		0.14	%	3 %	04.06.20	XRF - Fused bead	
*) K2O		0.98	%	3 %	04.06.20	XRF - Fused bead	
*) BaO		0.23	%	5 %	04.06.20	XRF - Fused bead	
*) MnO2		7.93	%	10 %	04.06.20	Titrimetric	

Prøvenr.:	Prøvetype:	Prøvemerking:				Prøvetaker:	Mottaksdato:
87152-005	Manganese Ore	Asssang 3,35-6,7 mm (600)				Oppdragsgiver	27.05.2020
Analyse/Parameter		Resultat	Enhet	Usikkerhet	Analysedato	Metodbeskrivelse	
*) LOI 950		1.05	%	5.5 %	29.05.20	Thermogravimetric	
*) Mn		49.52	%	0.2 %	04.06.20	XRF - Fused bead	
*) Fe		9.30	%	1.5 %	04.06.20	XRF - Fused bead	
*) SiO2		3.78	%	10 %	04.06.20	XRF - Fused bead	
*) Al2O3		0.41	%	9 %	04.06.20	XRF - Fused bead	
*) CaO		7.36	%	1 %	04.06.20	XRF - Fused bead	
*) MgO		1.31	%	40 %	04.06.20	XRF - Fused bead	
*) P		0.027	%	4 %	04.06.20	XRF - Fused bead	
*) S		0.143	%	10 %	04.06.20	XRF - Fused bead	
*) TiO2		<0.03	%	3 %	04.06.20	XRF - Fused bead	
*) K2O		<0.03	%	3 %	04.06.20	XRF - Fused bead	
*) BaO		0.49	%	5 %	04.06.20	XRF - Fused bead	

Rapportert av:
Faglaborant
Ann-Heidi Andreassen

Prøvenr.:	Prøvetype:	Prøvemerking:				Prøvetaker:	Mottaksdato:
87152-005	Manganese Ore	Asssang 3,35-6,7 mm (600)				Oppdragsgiver	27.05.2020
Analyse/Parameter		Resultat	Enhet	Usikkerhet	Analysedato	Metodbeskrivelse	
*) MnO2		13.49	%	10 %	04.06.20	Titrimetric	

Prøvenr.:	Prøvetype:	Prøvemerking:				Prøvetaker:	Mottaksdato:
87152-006	Manganese Ore	Assang 3,35-6,7 mm (400)				Oppdragsgiver	27.05.2020
Analyse/Parameter		Resultat	Enhet	Usikkerhet	Analysedato	Metodbeskrivelse	
*) LOI 950		4.22	%	5.5 %	29.05.20	Thermogravimetric	
*) Mn		47.80	%	0.2 %	04.06.20	XRF - Fused bead	
*) Fe		8.60	%	1.5 %	04.06.20	XRF - Fused bead	
*) SiO2		3.81	%	10 %	04.06.20	XRF - Fused bead	
*) Al2O3		0.48	%	9 %	04.06.20	XRF - Fused bead	
*) CaO		7.01	%	1 %	04.06.20	XRF - Fused bead	
*) MgO		1.18	%	40 %	04.06.20	XRF - Fused bead	
*) P		0.028	%	4 %	04.06.20	XRF - Fused bead	
*) S		0.128	%	10 %	04.06.20	XRF - Fused bead	
*) TiO2		<0.03	%	3 %	04.06.20	XRF - Fused bead	
*) K2O		0.04	%	3 %	04.06.20	XRF - Fused bead	
*) BaO		0.41	%	5 %	04.06.20	XRF - Fused bead	
*) MnO2		34.80	%	10 %	04.06.20	Titrimetric	

Prøvenr.:	Prøvetype:	Prøvemerking:				Prøvetaker:	Mottaksdato:
87152-007	Manganese Ore	Assang 3,35-6,7 mm (800)				Oppdragsgiver	27.05.2020
Analyse/Parameter		Resultat	Enhet	Usikkerhet	Analysedato	Metodbeskrivelse	
*) LOI 950		-3.21	%	5.5 %	29.05.20	Thermogravimetric	
*) Mn		51.34	%	0.2 %	04.06.20	XRF - Fused bead	
*) Fe		9.97	%	1.5 %	04.06.20	XRF - Fused bead	
*) SiO2		3.84	%	10 %	04.06.20	XRF - Fused bead	
*) Al2O3		0.47	%	9 %	04.06.20	XRF - Fused bead	
*) CaO		8.05	%	1 %	04.06.20	XRF - Fused bead	
*) MgO		1.48	%	40 %	04.06.20	XRF - Fused bead	
*) P		0.031	%	4 %	04.06.20	XRF - Fused bead	
*) S		0.138	%	10 %	04.06.20	XRF - Fused bead	
*) TiO2		<0.03	%	3 %	04.06.20	XRF - Fused bead	
*) K2O		<0.03	%	3 %	04.06.20	XRF - Fused bead	
*) BaO		0.46	%	5 %	04.06.20	XRF - Fused bead	
*) MnO2		<0.05	%	10 %	04.06.20	Titrimetric	

Angitt måleusikkerhet er beregnet med dekningsfaktor k=2. Ved intervallangivelse viser det høyeste tallet usikkerheten nært rapporteringsgrensen. For nærmere informasjon gjeldende usikkerhet, vennligst ta kontakt. SINTEF Norlab er akkreditert med test nr. 032. Hvilke analyser som inngår i akkrediteringen fremkommer i rapporten, *) = Ikke akkreditert, mod = modifisert standard.

Rapportert av:
Faglaborant
Ann-Heidi Andreassen

SINTEF NORLAB

SINTEF AS
Olav Biørnstad
SINTEF Industri
Alfred Getz vei 2 B
7034 Trondheim

SINTEF

SINTEF Norlab AS
Org. nr.: NO 953 018 144 MVA
Postboks 611
NO-8607 Mo i Rana
www.sintefnorlab.no

Tlf: (+47) 404 84 100

Ordrenr:	85689
Sted:	Mo i Rana
Antall prøver:	9
Bestillingsnr:	

ANALYSERAPPORT

Analyse av Mn-malm

Kommentar: På grunn av mange prøver i forbindelse med PreMa og utfordringer med Corona-situasjonen må det beregnes noe lengre leveringstid for oppdraget.

Prøvenr.:	Prøvetype:	Prøvemerking:				Prøvetaker:	Mottaksdato:
85689-001		UMK 10-13.2 400 °C Air				Oppdragsgiver	20.04.2020
Analyse/Parameter		Resultat	Enhet	Usikkerhet	Analysedato	Metodbeskrivelse	
*) LOI 950		15.26	%	5.5 %	28.04.20	Thermogravimetric	
*) Mn		36.27	%	0.2 %	30.04.20	XRF - Fused bead	
*) Fe		5.37	%	1.5 %	30.04.20	XRF - Fused bead	
*) SiO2		5.32	%	10 %	30.04.20	XRF - Fused bead	
*) Al2O3		0.42	%	9 %	30.04.20	XRF - Fused bead	
*) CaO		15.52	%	1 %	30.04.20	XRF - Fused bead	
*) MgO		2.62	%	40 %	30.04.20	XRF - Fused bead	
*) P		0.018	%	4 %	30.04.20	XRF - Fused bead	
*) S		<0.010	%	10 %	30.04.20	XRF - Fused bead	
*) TiO2		<0.03	%	3 %	30.04.20	XRF - Fused bead	
*) K2O		0.20	%	3 %	30.04.20	XRF - Fused bead	
*) BaO		0.07	%	5 %	30.04.20	XRF - Fused bead	
*) MnO2		26.67	%	10 %	24.04.20	Titrimetric	

Prøvenr.:	Prøvetype:	Prøvemerking:				Prøvetaker:	Mottaksdato:
85689-002		UMK 10-13.2 600 °C Air				Oppdragsgiver	20.04.2020
Analyse/Parameter		Resultat	Enhet	Usikkerhet	Analysedato	Metodbeskrivelse	
*) LOI 950		14.92	%	5.5 %	28.04.20	Thermogravimetric	
*) Mn		36.83	%	0.2 %	30.04.20	XRF - Fused bead	
*) Fe		5.31	%	1.5 %	30.04.20	XRF - Fused bead	
*) SiO2		5.63	%	10 %	30.04.20	XRF - Fused bead	
*) Al2O3		0.55	%	9 %	30.04.20	XRF - Fused bead	
*) CaO		15.33	%	1 %	30.04.20	XRF - Fused bead	
*) MgO		3.02	%	40 %	30.04.20	XRF - Fused bead	
*) P		0.019	%	4 %	30.04.20	XRF - Fused bead	
*) S		<0.010	%	10 %	30.04.20	XRF - Fused bead	
*) TiO2		<0.03	%	3 %	30.04.20	XRF - Fused bead	
*) K2O		0.26	%	3 %	30.04.20	XRF - Fused bead	

Rapportert av:
Faglaborant
Ann-Heidi Andreassen

30.04.20 kl 12.08

Prøvenr.:	Prøvetype:	Prøvemerking:				Prøvetaker:	Mottaksdato:
85689-002		UMK 10-13.2 600 °C Air				Oppdragsgiver	20.04.2020
Analyse/Parameter		Resultat	Enhet	Usikkerhet	Analysedato	Metodbeskrivelse	
*) BaO		0.09	%	5 %	30.04.20	XRF - Fused bead	
*) MnO2		26.55	%	10 %	24.04.20	Titrimetric	

Prøvenr.:	Prøvetype:	Prøvemerking:				Prøvetaker:	Mottaksdato:
85689-003		UMK 10-13.2 800 °C Air				Oppdragsgiver	20.04.2020
Analyse/Parameter		Resultat	Enhet	Usikkerhet	Analysedato	Metodbeskrivelse	
*) LOI 950		7.01	%	5.5 %	28.04.20	Thermogravimetric	
*) Mn		40.10	%	0.2 %	30.04.20	XRF - Fused bead	
*) Fe		5.99	%	1.5 %	30.04.20	XRF - Fused bead	
*) SiO2		6.24	%	10 %	30.04.20	XRF - Fused bead	
*) Al2O3		0.53	%	9 %	30.04.20	XRF - Fused bead	
*) CaO		16.70	%	1 %	30.04.20	XRF - Fused bead	
*) MgO		3.25	%	40 %	30.04.20	XRF - Fused bead	
*) P		0.021	%	4 %	30.04.20	XRF - Fused bead	
*) S		<0.010	%	10 %	30.04.20	XRF - Fused bead	
*) TiO2		<0.03	%	3 %	30.04.20	XRF - Fused bead	
*) K2O		0.24	%	3 %	30.04.20	XRF - Fused bead	
*) BaO		0.10	%	5 %	30.04.20	XRF - Fused bead	
*) MnO2		32.37	%	10 %	24.04.20	Titrimetric	

Prøvenr.:	Prøvetype:	Prøvemerking:				Prøvetaker:	Mottaksdato:
85689-004		Assmang 10-13.2 400 °C Air				Oppdragsgiver	20.04.2020
Analyse/Parameter		Resultat	Enhet	Usikkerhet	Analysedato	Metodbeskrivelse	
*) LOI 950		5.36	%	5.5 %	28.04.20	Thermogravimetric	
*) Mn		47.75	%	0.2 %	30.04.20	XRF - Fused bead	
*) Fe		8.12	%	1.5 %	30.04.20	XRF - Fused bead	
*) SiO2		3.94	%	10 %	30.04.20	XRF - Fused bead	
*) Al2O3		0.42	%	9 %	30.04.20	XRF - Fused bead	
*) CaO		7.48	%	1 %	30.04.20	XRF - Fused bead	
*) MgO		1.33	%	40 %	30.04.20	XRF - Fused bead	
*) P		0.026	%	4 %	30.04.20	XRF - Fused bead	
*) S		0.127	%	10 %	30.04.20	XRF - Fused bead	
*) TiO2		<0.03	%	3 %	30.04.20	XRF - Fused bead	
*) K2O		<0.03	%	3 %	30.04.20	XRF - Fused bead	
*) BaO		0.35	%	5 %	30.04.20	XRF - Fused bead	
*) MnO2		37.05	%	10 %	28.04.20	Titrimetric	

Prøvenr.:	Prøvetype:	Prøvemerking:				Prøvetaker:	Mottaksdato:
85689-005		Assmang 10-13.2 600 °C Air				Oppdragsgiver	20.04.2020
Analyse/Parameter		Resultat	Enhet	Usikkerhet	Analysedato	Metodbeskrivelse	
*) LOI 950		5.00	%	5.5 %	28.04.20	Thermogravimetric	
*) Mn		46.81	%	0.2 %	30.04.20	XRF - Fused bead	
*) Fe		8.28	%	1.5 %	30.04.20	XRF - Fused bead	
*) SiO2		4.23	%	10 %	30.04.20	XRF - Fused bead	
*) Al2O3		0.56	%	9 %	30.04.20	XRF - Fused bead	
*) CaO		7.92	%	1 %	30.04.20	XRF - Fused bead	

Rapportert av:
Faglaborant
Ann-Heidi Andreassen

Prøvenr.:	Prøvetype:	Prøvemerking:				Prøvetaker:	Mottaksdato:
85689-005		Assmang 10-13.2 600 °C Air				Oppdragsgiver	20.04.2020
Analyse/Parameter		Resultat	Enhet	Usikkerhet	Analysedato	Metodbeskrivelse	
*) MgO		1.59	%	40 %	30.04.20	XRF - Fused bead	
*) P		0.026	%	4 %	30.04.20	XRF - Fused bead	
*) S		0.107	%	10 %	30.04.20	XRF - Fused bead	
*) TiO2		<0.03	%	3 %	30.04.20	XRF - Fused bead	
*) K2O		<0.03	%	3 %	30.04.20	XRF - Fused bead	
*) BaO		0.43	%	5 %	30.04.20	XRF - Fused bead	
*) MnO2		36.84	%	10 %	28.04.20	Titrimetric	

Prøvenr.:	Prøvetype:	Prøvemerking:				Prøvetaker:	Mottaksdato:
85689-006		Assmang 10-13.2 800 °C Air				Oppdragsgiver	20.04.2020
Analyse/Parameter		Resultat	Enhet	Usikkerhet	Analysedato	Metodbeskrivelse	
*) LOI 950		2.90	%	5.5 %	28.04.20	Thermogravimetric	
*) Mn		47.09	%	0.2 %	30.04.20	XRF - Fused bead	
*) Fe		9.18	%	1.5 %	30.04.20	XRF - Fused bead	
*) SiO2		5.00	%	10 %	30.04.20	XRF - Fused bead	
*) Al2O3		0.68	%	9 %	30.04.20	XRF - Fused bead	
*) CaO		7.66	%	1 %	30.04.20	XRF - Fused bead	
*) MgO		1.63	%	40 %	30.04.20	XRF - Fused bead	
*) P		0.028	%	4 %	30.04.20	XRF - Fused bead	
*) S		0.099	%	10 %	30.04.20	XRF - Fused bead	
*) TiO2		<0.03	%	3 %	30.04.20	XRF - Fused bead	
*) K2O		<0.03	%	3 %	30.04.20	XRF - Fused bead	
*) BaO		0.36	%	5 %	30.04.20	XRF - Fused bead	
*) MnO2		37.03	%	10 %	28.04.20	Titrimetric	

Prøvenr.:	Prøvetype:	Prøvemerking:				Prøvetaker:	Mottaksdato:
85689-007		Assmang 10-13.2 600 °C Air Etter tømbling				Oppdragsgiver	20.04.2020
Analyse/Parameter		Resultat	Enhet	Usikkerhet	Analysedato	Metodbeskrivelse	
*) LOI 950		4.23	%	5.5 %	28.04.20	Thermogravimetric	
*) Mn		48.61	%	0.2 %	30.04.20	XRF - Fused bead	
*) Fe		7.56	%	1.5 %	30.04.20	XRF - Fused bead	
*) SiO2		2.87	%	10 %	30.04.20	XRF - Fused bead	
*) Al2O3		0.33	%	9 %	30.04.20	XRF - Fused bead	
*) CaO		8.65	%	1 %	30.04.20	XRF - Fused bead	
*) MgO		0.95	%	40 %	30.04.20	XRF - Fused bead	
*) P		0.022	%	4 %	30.04.20	XRF - Fused bead	
*) S		0.191	%	10 %	30.04.20	XRF - Fused bead	
*) TiO2		<0.03	%	3 %	30.04.20	XRF - Fused bead	
*) K2O		0.03	%	3 %	30.04.20	XRF - Fused bead	
*) BaO		0.72	%	5 %	30.04.20	XRF - Fused bead	
*) MnO2		41.46	%	10 %	28.04.20	Titrimetric	

Prøvenr.:	Prøvetype:	Prøvemerking:				Prøvetaker:	Mottaksdato:
85689-008		Assmang 10-13.2 800 °C Air Før tømbling				Oppdragsgiver	20.04.2020
Analyse/Parameter		Resultat	Enhet	Usikkerhet	Analysedato	Metodbeskrivelse	
*) LOI 950		1.61	%	5.5 %	28.04.20	Thermogravimetric	

Rapportert av:
Faglaborant
Ann-Heidi Andreassen

Prøvenr.:	Prøvetype:	Prøvemerking:				Prøvetaker:	Mottaksdato:
85689-008		Assmang 10-13.2 800 °C Air Før tømbling				Oppdragsgiver	20.04.2020
Analyse/Parameter		Resultat	Enhet	Usikkerhet	Analysedato	Metodbeskrivelse	
*) Mn		50.27	%	0.2 %	30.04.20	XRF - Fused bead	
*) Fe		8.04	%	1.5 %	30.04.20	XRF - Fused bead	
*) SiO2		3.49	%	10 %	30.04.20	XRF - Fused bead	
*) Al2O3		0.48	%	9 %	30.04.20	XRF - Fused bead	
*) CaO		7.61	%	1 %	30.04.20	XRF - Fused bead	
*) MgO		0.92	%	40 %	30.04.20	XRF - Fused bead	
*) P		0.030	%	4 %	30.04.20	XRF - Fused bead	
*) S		0.146	%	10 %	30.04.20	XRF - Fused bead	
*) TiO2		<0.03	%	3 %	30.04.20	XRF - Fused bead	
*) K2O		<0.03	%	3 %	30.04.20	XRF - Fused bead	
*) BaO		0.52	%	5 %	30.04.20	XRF - Fused bead	
*) MnO2		40.29	%	10 %	28.04.20	Titrimetric	

Prøvenr.:	Prøvetype:	Prøvemerking:				Prøvetaker:	Mottaksdato:
85689-009		Assmang 10-13.2 800 °C Air Etter tumbletest				Oppdragsgiver	20.04.2020
Analyse/Parameter		Resultat	Enhet	Usikkerhet	Analysedato	Metodbeskrivelse	
*) LOI 950		2.90	%	5.5 %	28.04.20	Thermogravimetric	
*) Mn		45.52	%	0.2 %	30.04.20	XRF - Fused bead	
*) Fe		9.00	%	1.5 %	30.04.20	XRF - Fused bead	
*) SiO2		3.68	%	10 %	30.04.20	XRF - Fused bead	
*) Al2O3		0.49	%	9 %	30.04.20	XRF - Fused bead	
*) CaO		10.67	%	1 %	30.04.20	XRF - Fused bead	
*) MgO		1.74	%	40 %	30.04.20	XRF - Fused bead	
*) P		0.028	%	4 %	30.04.20	XRF - Fused bead	
*) S		0.158	%	10 %	30.04.20	XRF - Fused bead	
*) TiO2		<0.03	%	3 %	30.04.20	XRF - Fused bead	
*) K2O		<0.03	%	3 %	30.04.20	XRF - Fused bead	
*) BaO		0.53	%	5 %	30.04.20	XRF - Fused bead	
*) MnO2		37.40	%	10 %	28.04.20	Titrimetric	

Angitt måleusikkerhet er beregnet med dekningsfaktor k=2. Ved intervallangivelse viser det høyeste tallet usikkerheten nært rapporteringsgrensen. For nærmere informasjon gjeldende usikkerhet, vennligst ta kontakt. SINTEF Norlab er akkreditert med test nr. 032. Hvilke analyser som inngår i akkrediteringen fremkommer i rapporten, *) = Ikke akkreditert, mod = modifisert standard.

Rapportert av:
Faglaborant
Ann-Heidi Andreassen

A.3 Porosity measurements

SINTEF

POROSITET

Prøver fra: **Olav Bjørnstad** **Dato:** 2020-05-22

Prøve	Innvekt (g)	Absolutt tetthet (g/cm^3)	Tilsynelatende tetthet (g/cm^3)	Porøsitet (%)
Assmang Ubehandlet	6,258	4,21		
1.	3,611		4,21	0,1
2	2,649		4,21	0,1
400 °C	8,455	4,33		
1.	3,848		4,33	0,1
2.	4,600		4,33	0,1
800 °C	6,970	4,47		
1.	3,420		3,50	21,8
2.	3,537		4,42	1,0

SINTEF Industri

SINTEF

POROSITET

Prøver fra: **Olav Bjørnstad** **Dato:** 2020-05-22

Prøve	Innvekt (g)	Absolutt tetthet (g/cm^3)	Tilsynelatende tetthet (g/cm^3)	Porøsitet (%)
UMK Ubehandlet	4,909	3,70		
1.	2,020		3,09	16,4
2	2,888		3,60	2,6
400 °C	4,288	3,45		
1.	2,168		3,44	0,4
2.	2,115		3,45	0,1
800 °C	2,649	3,25		
1.	1,340	3,45	3,35	2,8
2.	1,311	2,91	2,69	7,5

SINTEF Industri

PORØSITET

Prøver fra: **Olav Bjørnstad** **Dato:** 2020-05-22

Prøve	Innvekt (g)	Absolutt tetthet (g/cm^3)	Tilsynelatende tetthet (g/cm^3)	Porøsitet (%)
Comilog Ubehandlet	**4,525**	**4,56**		
1.	**2,576**		**4,40**	**3,6**
2	**1,961**		**3,97**	**12,9**
400 ºC	**2,134**	**4,61**		
1.	**1,355**		**3,21**	**30,4**
2.	**0,782**		**2,14**	**53,6**
800 ºC	**2,314**	**5,00**		
1.	**1,084**		**3,03**	**39,4**
2.	**1,234**		**3,28**	**34,5**

SINTEF Industri

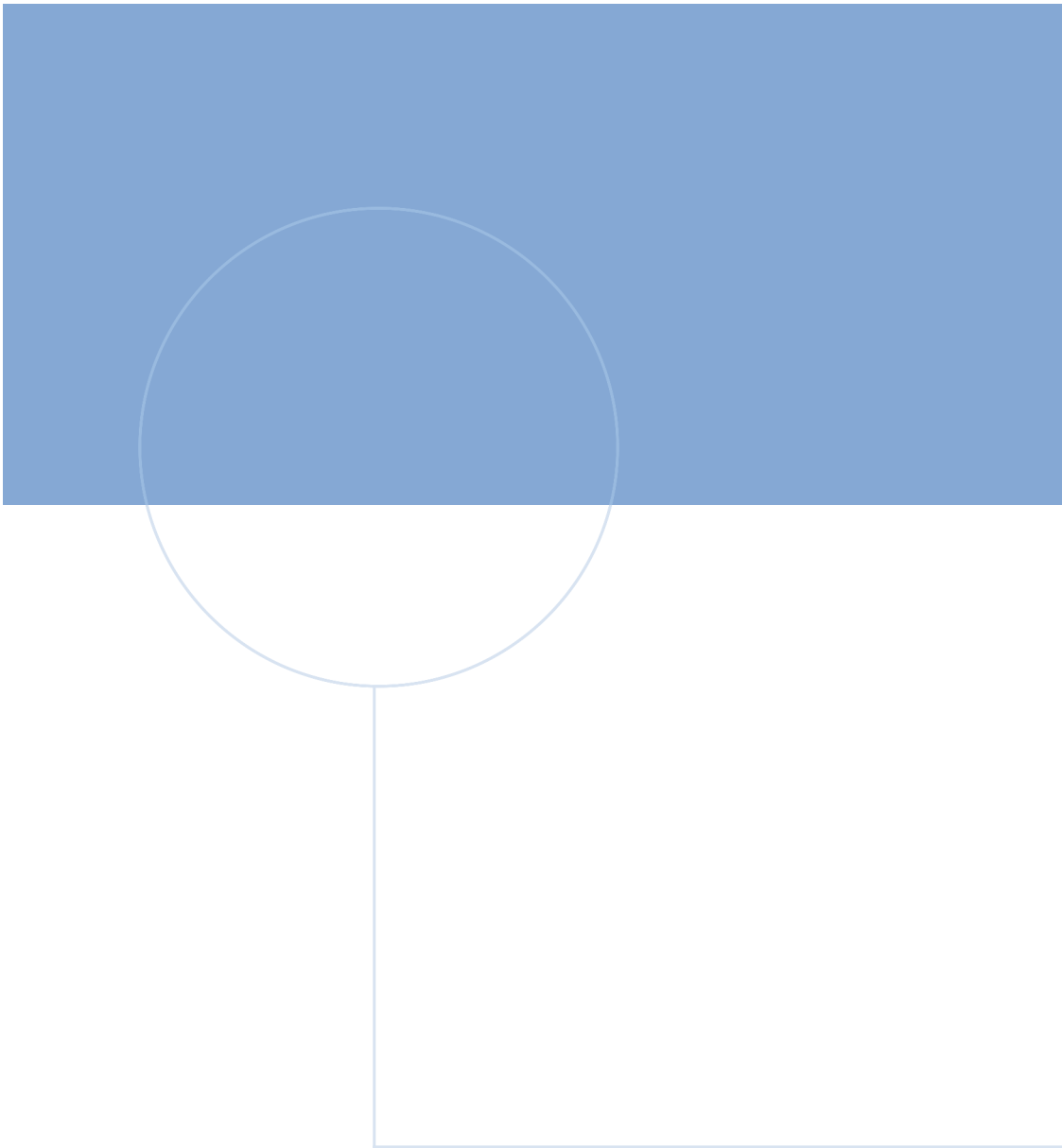

NTNU

Norwegian University of
Science and Technology